

RECEIVED

AUG 21 1978

Patents and TU Office

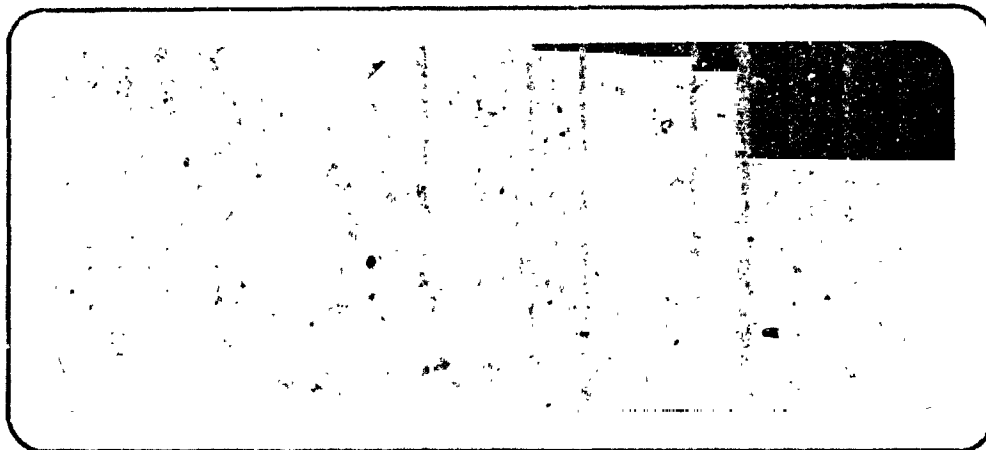
(NASA-CR-157942) A CONCEPT STUDY OF A
REMOTELY PILOTED VEHICLE FOR MARS
EXPLORATION Final Technical Report
(Development Sciences, Inc.) 139 p HC
A07/MF A01

N79-12128

Unclas

CSCL 22A G3/15 38117

15757 EAST VALLEY BOULEVARD
P. O. BOX 1264
CITY OF INDUSTRY, CALIF. 91749
(213) 330-6865



JET PROPULSION LABORATORY

CONTRACT NO. 955012

FINAL TECHNICAL REPORT

SOW - TASK 4

A CONCEPT STUDY OF A REMOTELY PILOTED
VEHICLE FOR MARS EXPLORATION

AUGUST 1, 1978

TABLE OF CONTENTS

PREFACE

PERSPECTIVE

1.	INTRODUCTION	1
1.1	Mission Description	1
1.2	Mars Environment	5
1.3	The Scientific Payload	8
1.4	The Descent System	11
1.5	System Limitations & Design Approach	16
2.	CANDIDATE CONFIGURATIONS	20
2.1	Basic Configuration	20
2.2	Hydrazine Powered Airplane	21
2.3	Electric Powered Airplane	28
2.4	Lander Airplane	30
3.	TECHNICAL ANALYSIS AND TECHNOLOGY ASSESSMENT	34
3.1	Aerodynamics	34
3.2	Powerplant	50
3.3	Structure and Materials	54
3.4	Deployment and Descent System Interface	55
3.5	Payload	58
3.6	Lander Version	60
3.7	Secondary Power	63
3.8	Thermal Control	66

3.9	Navigation, Guidance and Control	67
3.10	Communications	67
3.11	Weight and Center of Gravity	70
3.12	Performance	72
3.13	Flight Testing	75
4.	RECOMMENDED CONFIGURATION	78
APPENDIX A	- PROPELLER DESIGN & BLOWOVER CALCULATIONS FOR THE MARS AIRPLANE	A-1 - A-15
APPENDIX B	- INITIAL CONCEPT STUDY NAVIGATION, GUIDANCE & CONTROL FOR THE MARS AIRPLANE	B-1 - B-28

LIST OF FIGURES

FIGURE (1)	AIRPLANE/COMSAT LAUNCH CONFIGURATION	2
FIGURE (2)	AIRPLANE/COMSAT ORBIT INSERTION	3
FIGURE (3)	AIRPLANE/COMSAT GROSS WEIGHT BREAKDOWN	4
FIGURE (4)	MARS ATMOSPHERIC PARAMETERS	6
FIGURE (5)	PRELIMINARY AIRPLANE PAYLOAD PACKAGE	9
FIGURE (6)	FORWARD FUSELAGE & PAYLOAD MOCK-UP	10
FIGURE (7)	STOWING CONTAINER - PREVIOUS DESIGN - NOV 77	12
FIGURE (8)	WING DEPLOYMENT - PREVIOUS DESIGN - NOV 77	13
FIGURE (9)	DEPLOYED CONFIGURATION - PREVIOUS DESIGN NOV 77	14
FIGURE (10)	AEROSHELL GEOMETRY	15
FIGURE (11)	DEORBIT AND DEPLOYMENT SEQUENCE	17
FIGURE (12)	ATMOSPHERIC ENTRY PROFILE	18
FIGURE (13)	BASIC AIRPLANE CONFIGURATION	22
FIGURE (14)	STOWED GEOMETRY	23
FIGURE (15a)	1/10 SCALE DISPLAY MODEL	24
FIGURE (15b)	1/10 SCALE DISPLAY MODEL	25
FIGURE (16)	HYDRAZINE POWERED CRUISER	26
FIGURE (17)	ELECTRIC POWERED CRUISER	31
FIGURE (18)	HYDRAZINE POWERED LANDER	32
FIGURE (19)	CRUISE AIRSPEED	35
FIGURE (20)	CRUISE REYNOLD'S NUMBER	36
FIGURE (21)	LIFT COEFFICIENT CHANGES WITH REYNOLDS NOs.	38
FIGURE (22)	LIFT/DRAG RATIO CHANGES WITH REYNOLDS Nos.	39
FIGURE (23)	LIFT/DRAG RATIO OF VARIOUS AIRFOILS	41
FIGURE (24a)	DRAG OF THE PPFENINGER .048 AIRFOIL	42
FIGURE (24b)	THEORETICAL PERFORMANCE OF THE EPPLER 385 AND 387 AIRFOILS	43

FIGURE (25)	MEASURED PERFORMANCE OF THE EPPLER 385 AIRFOIL	45
FIGURE (26)	MEASURED PERFORMANCE OF THE EPPLER 387 AIRFOIL	46
FIGURE (27)	THEORETICAL PERFORMANCE OF THE EPPLER 61 AND 62 AIRFOIL	47
FIGURE (28)	CRUISE MACH NUMBER	48
FIGURE (29)	CRUISE LIFT/DRAG RATIO	49
FIGURE (30)	THE HYDRAZINE ENGINE INSTALLATION IN THE MINI-SNIFFER	51
FIGURE (31)	TYPICAL WING STRUCTURE	56
FIGURE (32)	DIVE RECOVERY FROM 7.5 KM DEPLOYMENT	57
FIGURE (33)	DIVE RECOVERY FROM 11 KM DEPLOYMENT	59
FIGURE (34)	VERTICAL LANDING	62
FIGURE (35)	VERTICAL TAKEOFF	64
FIGURE (36)	SURFACE WIND SPEED FOR BLOW OVER OF 150 KG LANDER	65
FIGURE (37)	AIRPLANE/COMSAT COMMUNICATION SYSTEM	68
FIGURE (38)	WEIGHT BREAKDOWN	71
FIGURE (39)	CRUISE PERFORMANCE	73
FIGURE (40)	CLIMB PERFORMANCE - HYDRAZINE POWERED	74
FIGURE (41)	GLIDE RANGE	76

PREFACE

For the record, it is appropriate to give a brief background as to the chronological evolution of the MARS airplane concept*.

The concept for a Mars airplane evolved from a January 1977 meeting between David Scott, former director of NASA Dryden FRC, and Dr. Bruce Murray, director of Jet Propulsion Laboratory (JPL).

Basically, Dryden had developed a mini-remotely piloted vehicle called the Mini-Sniffer which was designed to fly at 70,000 to 100,000 feet over the earth. The major driver for this plane was a low cost alternative to the U-2 for atmospheric research. Dr. Jose Chirivella of JPL recognized the potential of the Mini-Sniffer as a precursor for a Mars airplane. In essence, he had the good sense to realize that the technology of aeronautics had substantially advanced to the point where Mars airplane flight should be seriously considered. A major factor in his thinking was that the Mini-Sniffer's power plant, a new invention by James Akkerman of JSC, was an airless hydrazine engine with low dry weight and reasonable specific fuel consumption. In July 1977, Dr. Chirivella enlisted Mr. Vic Clarke's active support for advancing the Mars airplane. After the Mars 84 program failed to gain NASA acceptance, it was decided to open up the options for Mars exploration. Dr. Lou Friedman, the new Manager, gave Mr. Vic Clarke \$5,000 for a small Mars Airplane Study Contract to industry in early October 1977. Dr. Chirivella and Mr. Clarke visited several companies including Developmental Sciences (DSI), and Lear Siegler Astronics (LSI). Eventually they chose the DSI/LSI combination as being well qualified by reason of their experience in superlight weight mini-RPV's and military

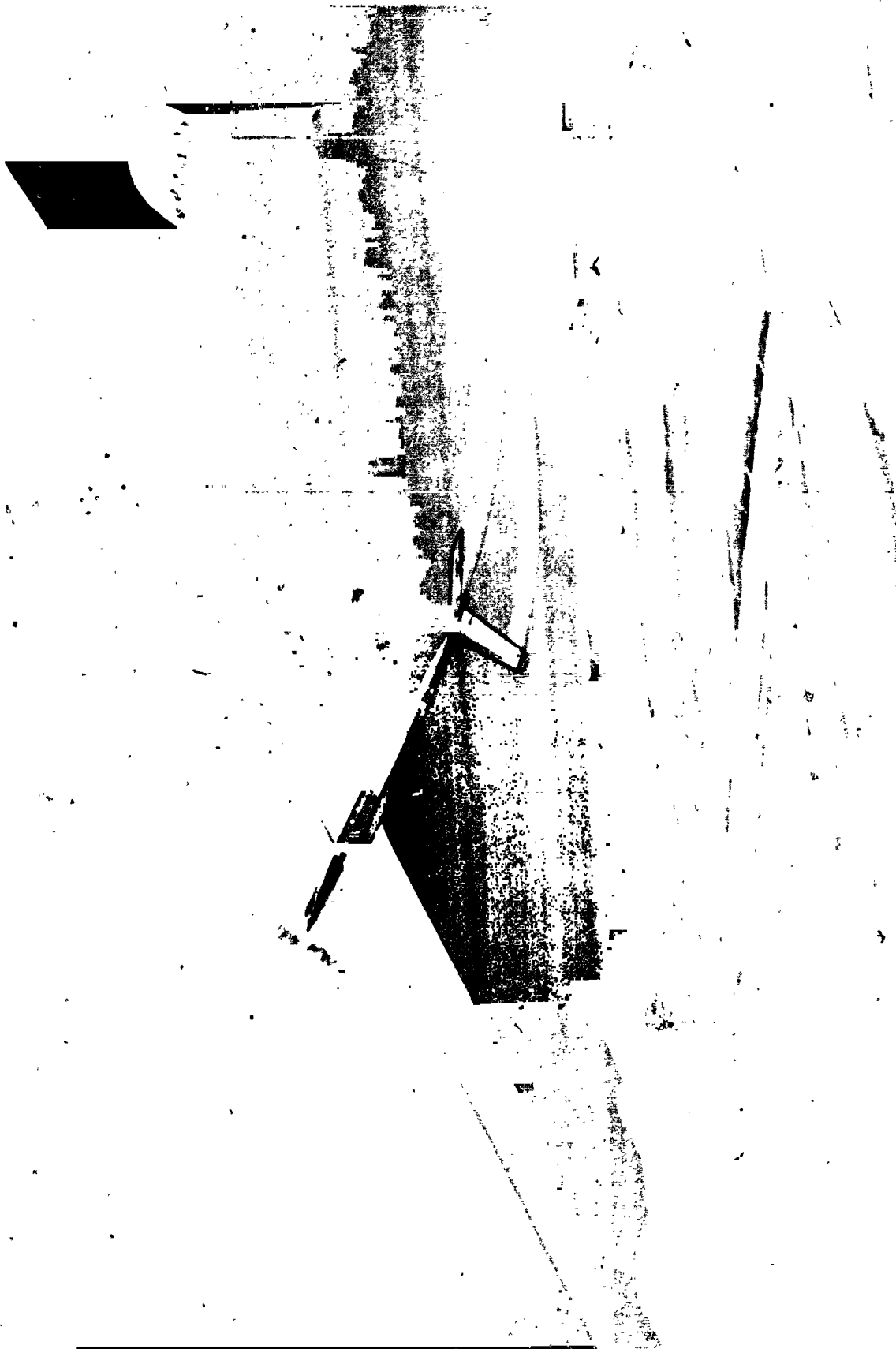
*In accomplishing this I draw heavily upon Mr. Victor Clarke Jr.'s (JPL) historical account prior to DSI's chronological involvement.

RPV flight control and navigation systems. DSI designed and developed the Army's Aquila Mini-RPV. LSI supplies the flight control and navigation systems for Ryan's family of drones. They also build the FC&N system for the L-1011. DSI also was currently flight testing their design of an unfolding airplane for the Navy, called NOPEC, which fully deploys in a fraction of a second. (DSI's background, see Jane's "All the World's Aircraft.") Dr. Gordon Harris, Mr. Abraham Kerem and myself worked on this study.

The results of this small study were reported in JPL Document 760-198, Part I, on November 28, 1977. Basically, DSI designed a plane which had the characteristics of a competition glider, an airframe of 58 lbs., a total dry weight of 142 lbs., payload of 100 lbs., and an all up weight of 450 lbs. It had a tip-to-tip wing span of 15 meters and was 5.25 m nose-to-tail. The airfoil used was a thin, low Re (40,000 - 70,000 range) Eppler type. At the same time, Vic Clarke developed the concept of flying multiple airplanes (16) with mil-spec or commercial hardware to achieve major cost savings, while maintaining overall mission reliability.

Encouraged by the positive results, Dr. Friedman granted Mr. Clarke \$120,000 to delve deeper into the Mars Airplane. From this sum, he gave DSI a \$60,000 contract. DSI, in turn, subcontracted to Lear Siegler for flight control and navigation work, and to Dr. Peter Lissaman of AeroVironment, Inc. for design of the propellor. (Dr. Lissaman is the aerodynamics designer of the Gossamer-Condor, the world's first human powered airplane). This second contract started February 15, 1978, and Mr. Kerem was made the DSI project leader. On March 9, JPL and DSI/LSI went to NASA OAST to give a presentation on the Mars airplane for purposes of soliciting \$10 million from OAST to develop and flight test two pre-production prototypes by mid-1981. This presentation is documented in JPL Publication 760-198, Part II. For this presentation DSI had enlarged the plane to 300 kg all-up weight with 40-100 kg payload, depending on range desired.

ORIGINAL PAGE IS
OF POOR QUALITY



For 40 kg, range is 6700 km. For 100 kg, range is 4800 km. Wing span was increased to 21m. The most significant factor, however, was Mr. Kerem's ingenious design for stowing the folded airplane into a Viking-like aeroshell only 1 foot greater in diameter than Viking's. Essentially the Viking aeroshell/parachute entry method was adopted. A major difference is that the total entry weight of the airplane system is only 960 lbs as compared to Viking's 2160 lbs. Another of Mr. Kerem's ingenious designs was to stack 7 airplane capsules clustered around a pole mounted on the carrier spacecraft. We then assumed direct entry of the capsules. We have since backed off to four capsules carried into a 500 km x 4 sol orbit and deorbited like Viking. Three such sets of four capsules are envisioned to give 12 airplanes total. The carrier spacecrafts kick into 1 sol synchronous orbits to become comsats.

An unexpected result of the March 9, 1978 NASA Headquarters meeting was that OAST thought funds should be solicited from OSS because the technology of the airplane's design was well established. An airplane science working group headed by Dr. John Minear, NASA-JSC was formed to review science missions for the airplane. DSI prepared payload preliminary interface specifications dated March 20, 1978. Vic Clarke proposed dividing science into four-plane squadrons with identical instruments for reliability, and to overcome the obvious conflict between geochemistry and biology as was expressed at the MSWG meeting. Each scientific discipline can have their own set of four planes to do with as they please.

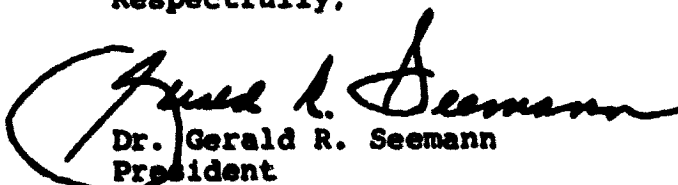
The airplane science working group met May 8 and 9, 1978 at JPL followed by a Mars Science Advisory group meeting May 11 - 13, 1978 at JPL to which Dr. Minear presented his group's findings. These showed the airplane to have unique advantages for Mars exploration as an aerial survey platform.

for sample retrieval, and deployment of science packages. Of particular importance was obtaining high resolution (30 cm/pixel) oblique images over large tracts of rugged land. A full scale forward section of the fuselage was fabricated by DSI to demonstrate science instrument packaging in the payload compartments. Shortly thereafter data on a new lithium primary battery become available that made electric propulsion potentially very attractive for the airplane. DSI and JPL worked hard to prepare the effect of this new technology on the Mars airplane system and its performance for the NASA Headquarters review. The Mars Mission review was in Reston, VA, June 22 and 23, 1978. A 1/10 scale model of the plane was built by DSI for this meeting.

While the Mars airplane (named Astroplane by DSI) was given good marks, the NASA Headquarters initial position was to go for a sample return mission which excluded auxiliary vehicles, i.e., penetrators, airplanes, large rover, balls, and hard landers. There was a vocal minority opinion at the meeting which advocated a more modest initial mission including the Mars airplane and orbiter.

The DSI contract terminated August 15, 1978 with the preparation of this final report. It is our hope that the Mars airplane technology is continued by NASA in order that its benefits can be utilized on a mission to MARS in the 1980s.

Respectfully,


Dr. Gerald R. Seemann
President
Developmental Sciences, Inc.

PERSPECTIVE

MARS MISSION SCENARIO

One day in the mid 1980's, a strange group of objects will be taken from the sterilization chambers at NASA-JSC. The MARS AIRPLANES (Astroplanes) each multiply folded in its own Viking-like aeroshell is encased in a bioshield. Twelve Astroplanes and three Comsats will then be transported to a space transportation system - Shuttle plus interim upper stage. The three Shuttles will be launched a week apart. Each spacecraft will consist of an orbiter (Comsat) and four Astroplanes. The Shuttle will put the spacecraft into a parking orbit. A two-stage, solid/liquid propellant IUS rocket will be used to insert the spacecraft into Mars orbit. Slightly over 9 months later the units will arrive at Mars.

The three spacecrafts would deorbit the 12 Astroplanes from a 500 km altitude periapsis by 1 sol orbit, similar to Viking. If deorbited near the equator and at selected longitudes, they will be able to go anywhere on Mars. It is expected that the Astroplanes will be deorbited one at a time sequenced or at will. The spacecraft will be maneuvered into a 4 sol synchronous circular orbit, 120° apart in longitude, 28° inclination and form a MARS COMSAT network with 100% global coverage. These long life Comsats would serve as high capacity communication relay satellites to earth for all Mars vehicles.

Each Astroplane will penetrate the Mars upper atmosphere inside its aeroshell until it reaches an altitude of 7.5 km above the Mars surface. At this time a parachute entry system deploys, slowing the aeroshell to 60 m/s, the plane unfolds, engine starts, detaches from the parachute, and flies off. Two options for the Astroplane are currently

envisioned, (1) a powered cruiser which could carry up to 100 kg of payload and fly for 18 hours and 5700 km or (2) an Astroplane equipped with a Viking lander variable thrust rocket so that it may soft land and later take-off which could carry 50 kg of payload, make two stops and travel over 3000 km. The Astroplane cruiser could be used to (a) perform high resolution photo, magnetic, gravity and geochemical aerial surveys, (b) perform aerial search for subsurface water, geothermal fields and active volcanos, (c) perform atmospheric sounding for meteorology or constituent analyses up to 15 km above the Martian surface, (d) deploying navigation aids and/or soft landing experiment packages at distributed points on the surface, and (e) exploration of the vast canyon network of Mars. The Astroplane soft lander could be used for (a) gathering widely dispersed samples and delivering them to a selected site where a Mars sample return (MSR) vehicle will pick them up, (b) deploy network science (e.g. seismometers, meteorology stations, etc.), (c) performing site selection surveys for Mars sample return spacecraft, and (d) perform in situ elemental and mineral phase analysis or biological exploration at preferred sites. With twelve Astroplanes, it seems clear that an enormous amount of relevant scientific data could be gathered from all sectors of the Martian planet. The data would be transmitted to earth via the Comsat network. An Astroplane mission would make an excellent precursor to a MSR mission or could complement and play a formidable role during a MSR mission.

1. INTRODUCTION

1.1 Mission Description

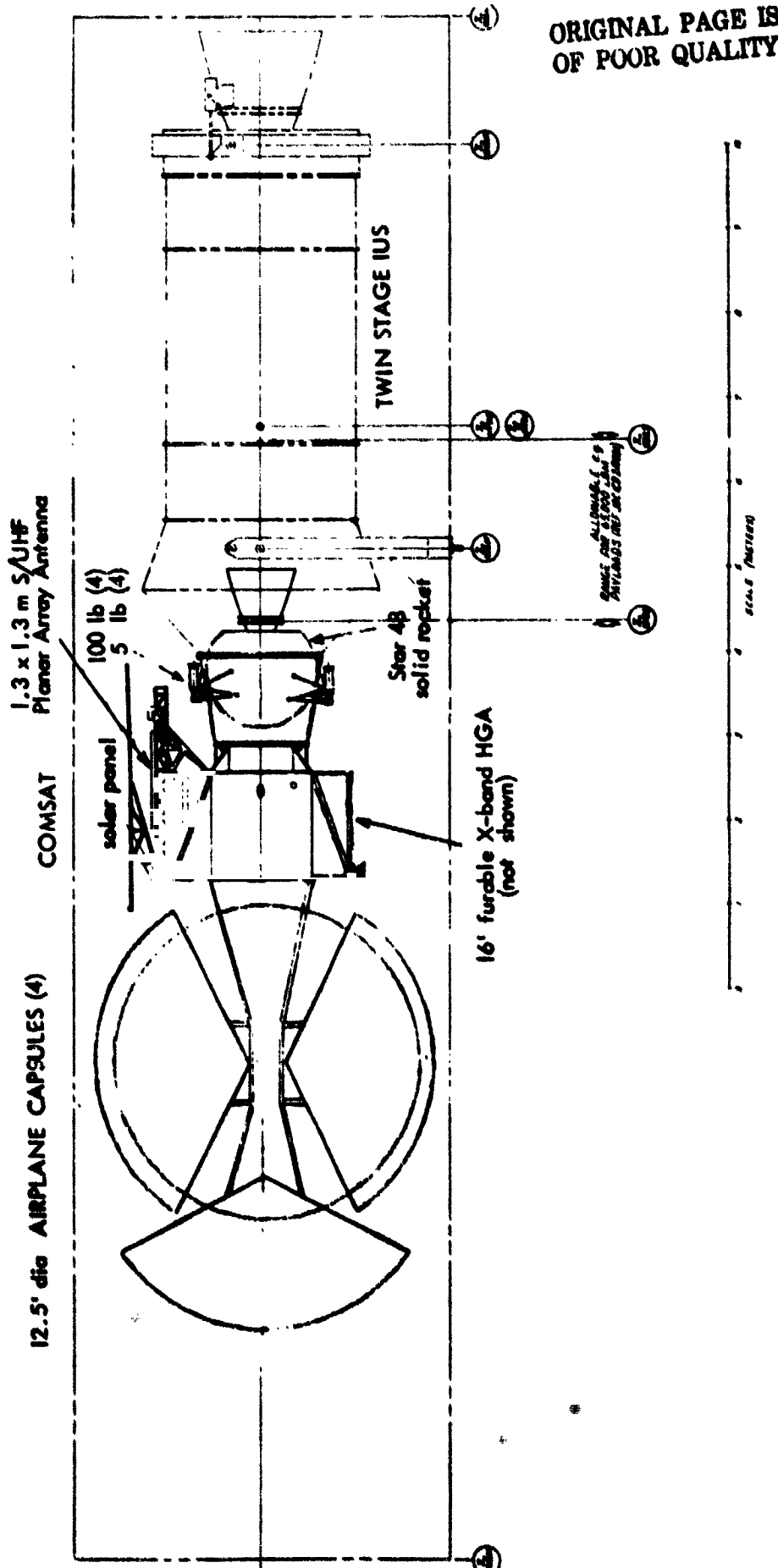
The mission concept for the Mars airplane has evolved during this study from the basic idea of simultaneous direct entry of 12 - 14 airplanes from the two planned spacecraft, to the concept of using three spacecraft, each carrying one comsat and four airplane capsules (Figure 1). In this scenario, the spacecraft are inserted into a 500 km 4 sol elliptical orbit (Figure 2). The comsats are separated and maneuvered into a 1 sol circular orbit, 120° apart in longitude, 28° inclination, and form a Mars Comsat Network with 100% global coverage. These comsats would have very long life, typical of earth comsats. They would serve as high capacity communication relay satellites to earth for all Mars vehicles, including sample return, geochemical orbiter, rovers, etc.

Each airplane has its own Viking-like aeroshell and parachute entry system. The airplane attachment to the central structure makes possible the deorbit of the airplanes in any order (see Figure 1). This fact and the fact that being in orbit (able to deorbit an airplane at almost any point on Mars at anytime - at 4 sol intervals) give a very high mission flexibility. The airplane payload capability (up to 100 kg) may be used for different scientific instrument packages, and the decision as to what airplane (with what payload) to deploy when and where on Mars is made during the mission as more data from airplane missions is accumulated and processed.

Figure 3 shows the weight breakdown of the spacecraft. The 300. kg airplane weight is detailed in section 3.12. The 190 kg for the entry system and deorbit fuel is based on a study of the Mars airplane descent system done by Martin Marietta dated June 1978 (report no. MCR-78-570). 29 kg are allocated for the addition of a sun-tracker and solar cells to one airplane capsule to give it a full orbiter capability. This capsule (possibly the one mounted on the end of the superstructure) will be deorbited the last of all four airplane capsules. All other weight statements are based on various studies performed by JPL.

AIRPLANE/COMSAT LAUNCH CONFIGURATION

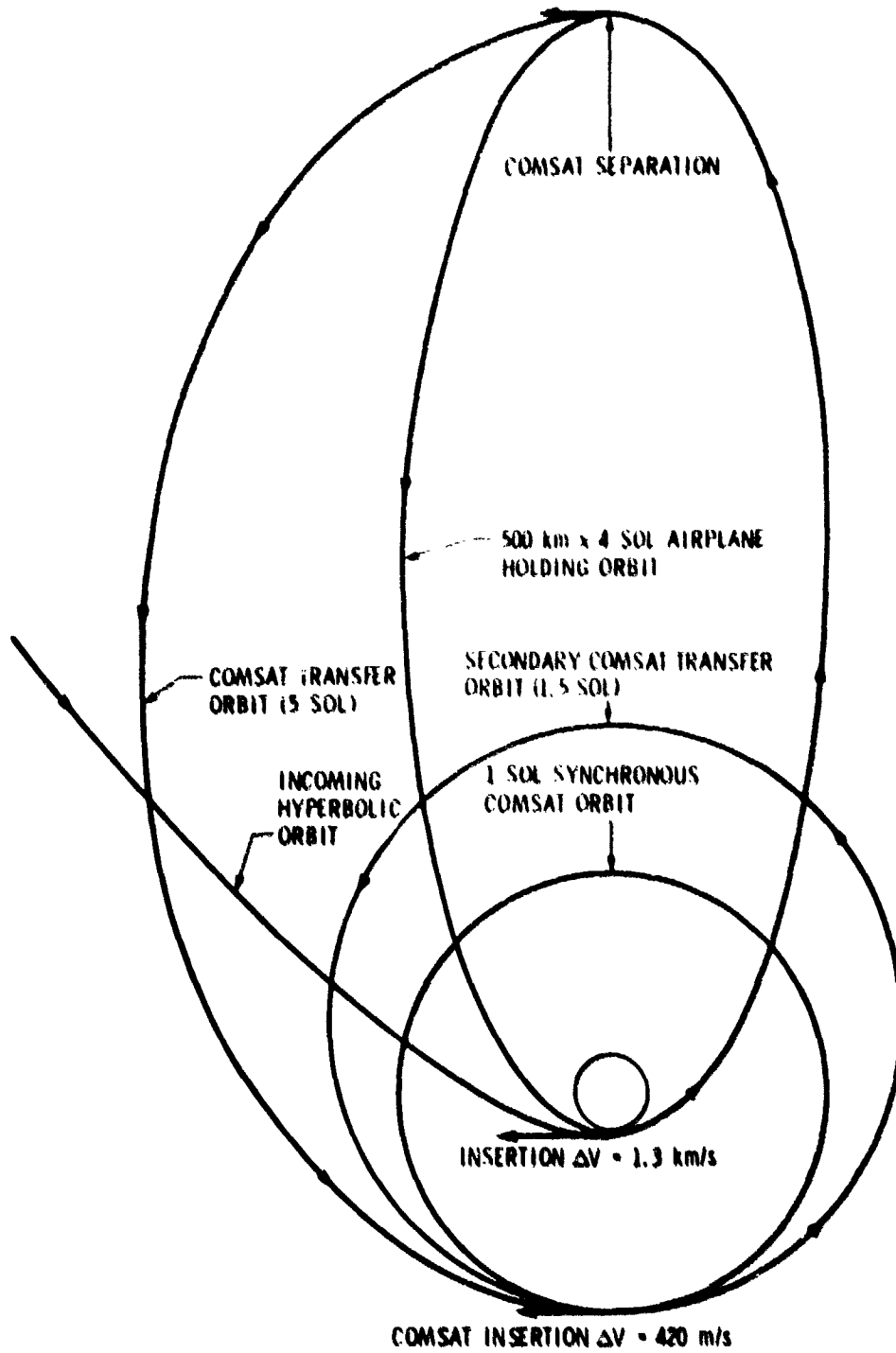
FIGURE (1)



AIRPLANE/COMSAT ORBIT INSERTION

FIGURE (2)

TRANSFER COMSAT $\Delta V = 204 \text{ m/s}$



AIRPLANE/COMSAT
GROSS WEIGHT BREAKDOWN

FIGURE (3)

4 PLANES

CAPSULES		
AIRPLANE, EA.	300	
ENTRY SYSTEM, EA.	178	
HYDRAZINE, EA.	12	
		490 KG
AUGMENTATION	29	
SUPERSTRUCTURE	70	
COMSAT		
DRY	630	
HYDRAZINE	371	
		1001
SOLID ROCKET		
CASE	98	
PROPELLANT	1700	
ADAPTER	88	
CONTINGENCY		
		1960 KG
		29
		70
		1001
		98
		1733
		<u>88</u>
		4979
		<u>245</u>
		5224*

* IUS CAPABILITY = 5224 KG @ $C_3 = 13.6 \text{ km}^2/\text{Sec}^2$ ON 12-19-84

The entry system is very similar to the Viking lander entry system (similar orbit, entry profile, controlled lift entry and using similar entry rockets), but the aeroshell diameter is increased from 11.5 ft (3.5 m) on Viking to 12.5 ft (3.8 m) to best utilize the available volume in the Space Shuttle payload bay. Since the Airplane weighs only 300 kg compared to 660 kg of the Viking lander, it was possible to make a reduction in entry system weight using the same technology of the Viking system. An additional reduction (estimated at 50 kg per system) is achievable if up-to-date aeroshell structural and parachute materials are used. The big difference between the airplane and Viking descent systems is that the airplane capsule is an integral unit; the descent system has no communication, attitude sensors, radar altimeter, computer or electrical power source. All of these functions are performed by the airplane systems; the descent system includes only the aeroshell and basecover structures, the rocket system and the parachute.

The entry system brings the airplane to a 60 m/sec descend speed at 7.5 km altitude. The aeroshell is separated, the airplane deploys its wings, tail, and propeller, then detaches from the parachute and flies off.

1.2 Mars Environment

Of all Mars environmental parameters, the most important for the Mars airplane mission is the Mars atmosphere. Figure 4 shows density and temperature (based on Viking Lander I measurements) and calculated speed of sound. The density of Mars atmosphere at ground level is about 1% of its value at sea level on earth (corresponding to 100,000 ft density altitude on earth). This low density required the use of large wing area airplane (low wing loading) to be able to fly at subsonic speeds and limit the power required to fly to an acceptable level. The fact that the speed of sound is lower than on earth (about 70% of its value on sea level earth) severely limits the propeller rpm if the limiting tip Mach number for efficient operation is not to be exceeded.

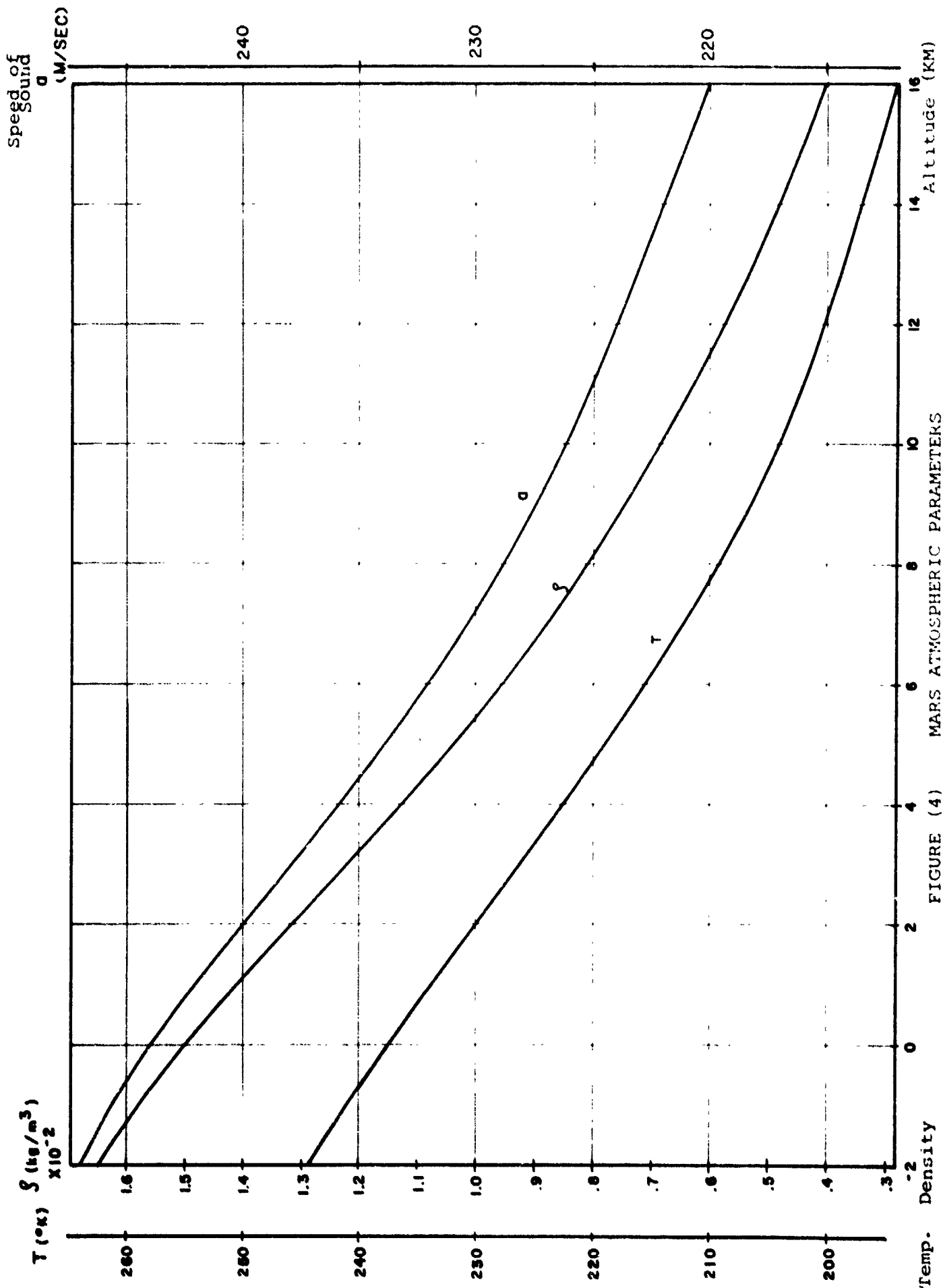


FIGURE (4) MARS ATMOSPHERIC PARAMETERS

Mars atmosphere is mainly CO₂, requiring the powerplant to be non-airbreathing. If we compare the fuel consumption of an airbreathing piston engine to a Hydrazine monofuel piston engine (which, for example, powers the NASA Dryden FRC Mini-Sniffer high altitude RPV) we find that the specific fuel consumption of the latter is almost 10 times higher. This fact puts a severe range and endurance limits on the Mars airplane.

Mars gravity is only .377 of earth gravity. This fact offsets some of the performance degradation due to the thin atmosphere. The reduced gravity gives the Mars lower effective wing loading and for the same ratio of lift to drag a 2.65 time longer range.

The temperature at ground level on Mars varies between 0 and -120°C. These low temperatures have an impact on the payload, avionics, fuel and batteries environmental control especially in case of a soft landing airplane that has to survive the surface environment for a long time with limited power sources.

The average surface wind velocity measured by the Viking Landers was quite low (typically below 10 m/sec). But, surface wind velocity of 30 and even 40 m/sec must be anticipated at certain landing sites. However, because of the very low density, these winds would still correspond to relatively low dynamic pressures. With the landing gear configuration designed for the Lander Airplane, the airplane takes up to 50 m/sec wind at minimum mass of 150 kg (70 m/sec at 300 kg) before it is blown-over (see paragraph 3.6). The airplane being optimized for cruise has a relatively low rate of climb (5 - 12 m/sec or 1000 - 2400 ft/min which is typical for turboprop powered airplanes on earth) may encounter problems of keeping altitude in a strong downdraft when flying along the wall of a canyon with a strong side wind. The airplane computer requires sufficient logic to keep the airplane out of downdrafts stronger than a certain limit.

The Mars atmosphere being very thin, will offer reduced protection against ultra-violet radiation. This may require the

use of special coating to protect the structure and system of the Lander Airplane which is required to survive this radiation for several months (possibly years).

1.3 The Scientific Payload

During this study phase a major effort was the study of the airplane role in the future exploration of Mars and the design of the airplane to be best suited to this role. This was done in several steps:

1. Optimize the airplane/descent system to maximize payload-range capability.
2. Configure the fuselage to provide a payload volume of 200 liters for the Hydrazine powered lander and more than 300 liters on the cruiser airplane.
3. Issue preliminary payload interface specifications to be used by scientists on the Mars project (DSI technical paper 14134, March 20, 1978).
4. Integrate the scientists first reactions and define a possible payload package of 100 kg (see Figure 5) including a 100 liters deployable payload (performed by JPL during April 1978).
5. Design and build a full scale forward fuselage with mock-up of the payload package (Figure 6).
6. Discuss the airplane role and payload in a three day meeting of the Mars Airplane Science working group (JPL May 8 - 11, 1978).

The Mars Airplane was studied as a transport vehicle for scientific payloads in three possible missions:

1. Flight surveillance.
2. Deployment of scientific payloads (either in flight or after landing).
3. Transportation of samples to a central site.

FIGURE (5) PRELIMINARY AIRPLANE PAYLOAD PACKAGE (April '78)

INSTRUMENT	MEASUREMENT	PROTOTYPE	RESOLUTION PER ELEMENT AT 1 Km ALTITUDE	MASS (Kg)	POWER (WATTS)	VOLUME	DATA RATE KILOBITS/SEC	BER MAXIMUM	COMMENT
GAMMA RAY SPECTROMETER (w/COOLING)	LOW RESOLUTION ELEMENT COMPOSITION Th, K, U, Fe, Mg, Ti, Al, Ca, Na, Si, O H-RICH COMPOUNDS	APOLLO, LPO	1 Km	8	10	1650 cm ³	4	5x10 ⁻⁵	LOCATED ON LEFT WING 4 m FROM FUSELAGE OPT TEMP ~120°K
REFLECTANCE SPECTROMETER	MINERALOGY, COMPOSITION, SOIL MATURITY (AGGLUTINATES)	EARTH TELESCOPES, LPO	5 m	13	10	31x19x24 cm	10.4	10 ⁻⁴	400 CHANNELS 0.35-4μ OPT TEMP ~-50°C ~4 SAMPLES/SEC/CHANNEL
ELECTROMAGNETIC SOUNDER	UNDERGROUND WATER	TERRESTRIAL APPLICATIONS	100 m air	9	10	13x13x40 cm	0.5	10 ⁻²	20 m ANTENNA ON UNDERSIDE OF WINGS. 10 - 7.5 mhz
GRAVITY GRADIENTER	GRAVITY ANOMALIES	MILITARY, LPO	2.5-25 km	21	18	25 cm LONG x 22 cm DIA CYL ELEC-TRONICS 6x15x63 cm	0.1	5x10 ⁻³	QUOTED RESOLUTION IS FOR 1 MILLIGAL FEATURES AND 1 EU SENSITIVITY
MAGNETOMETER (DUAL)	REMANENT MAGNETIZISM	PIONEER VENUS, LPO, VOYAGER	NA	4.5	2	28x25x8 cm	0.3	10 ⁻⁴	LOCATED ON RIGHT WING- ONE 2/3 DISTANCE FROM FUSELAGE, ONE AT TIP. WEIGHT INCLUDES SENSOR AND CABLES
INFRARED RADIOMETER	HOT SPOTS	MVM 73	9 m	4	2.5 AVG 7.5 PEAK	15x15x25 cm	.016	1.25x10 ⁻³	TEMPERATURE RANGE -120° TO 100°C
GAS CHROMATOGRAPHY/MASS SPECTROMETER	AIR CONSTITUENT ANALYSIS	VIKING	NA	20	33 AVG 88 PEAK	28x26x36 cm	16 OR 4	5x10 ⁻⁴	MASS RATIO m/e = 12-200 RESOLUTION 1:200 AT m/e = 200.
IMAGING 10xZOOM 14.8-150 mm F.1.8	SURFACE FEATURES	GALILEO	33 cm PIXEL RES.	12	10	33 cm DIA SPHERE ELEC-TRONICS 15x15x15 cm		10 ⁻³	800x800 CCD MULTI SPECTRAL IMAGER 0.3 - 1.1μ OPT. TEMP -50°C
TOTALS				91.5	95.5				
DEPLOYABLE PACKAGE	SEISMOMETER/METEOROLOGY	VIKING, SURVEYOR		9.5		46x46x46 cm			

ORIGINAL PAGE IS OF POOR QUALITY

ORIGINAL PAGE IS
OF POOR QUALITY

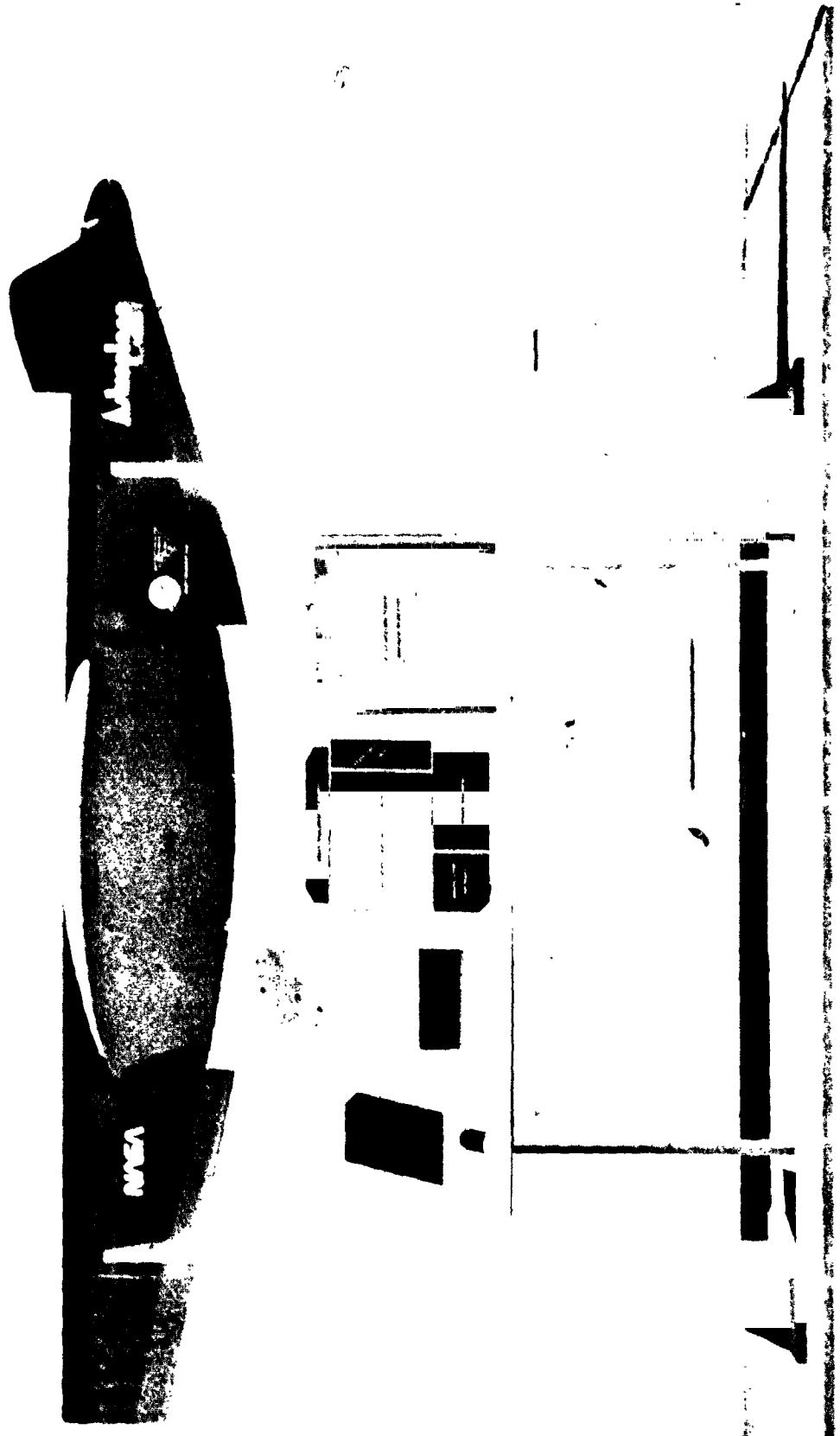


FIGURE (6) FORWARD FUSELAGE & PAYLOAD MOCK-UP

For all three missions, the main design effort was to maximize the payload-range capability of the airplane. The maximum payload was increased from 45 kg on the first version presented on November 1977 to 100 kg on all airplane versions studied during this phase. Even with the heavier payload and the heavier avionics package needed to perform the terrain following mission (50 kg compared to 6 kg on the first version) the range of some new versions was almost doubled. This increase in payload-range capability is the result of two major advances made during this study.

1. An increase of the airplane, wing area from 10 m² to 20 m² and of the airplane weight from 204 kg to 300 kg made possible by an in-depth study of the Space Shuttle, spacecraft and descent system and changing the stowed airplane package size from the 1 m diameter 3 m long cylinder (see Figures 7 - 9) specified by JPL on the previous study to a Viking-like aeroshell of 3.8 m diameter (see paragraph 1.4).
2. The study of a very high energy-density Lithium batteries (300 Wh/lb) and an advanced lightweight packaging for these batteries to boost the energy density to an estimated 550 Wh/lb. These batteries give better airplane performance than the non-air-breathing Hydrazine engine (see paragraph 3.12).

For the flight surveillance mission, the larger wing area results in a reduction in cruise speed and therefore increased resolution per available data rate. The reduced minimum speed also resulted in decreased fuel consumed during landing and take-off of the Lander Airplane.

1.4 The Descent System

From a study of the Space Shuttle payload capability it was found that a 3.8 m diameter Viking-like aeroshell with a cone angle of 63° and spherical base cover (Figure 10) will best utilize

ORIGINAL PAGE IS
OF POOR QUALITY



FIGURE (7) STOWING CONTAINER - PREVIOUS DESIGN - NOV. 77

ORIGINAL PAGE IS
OF POOR QUALITY

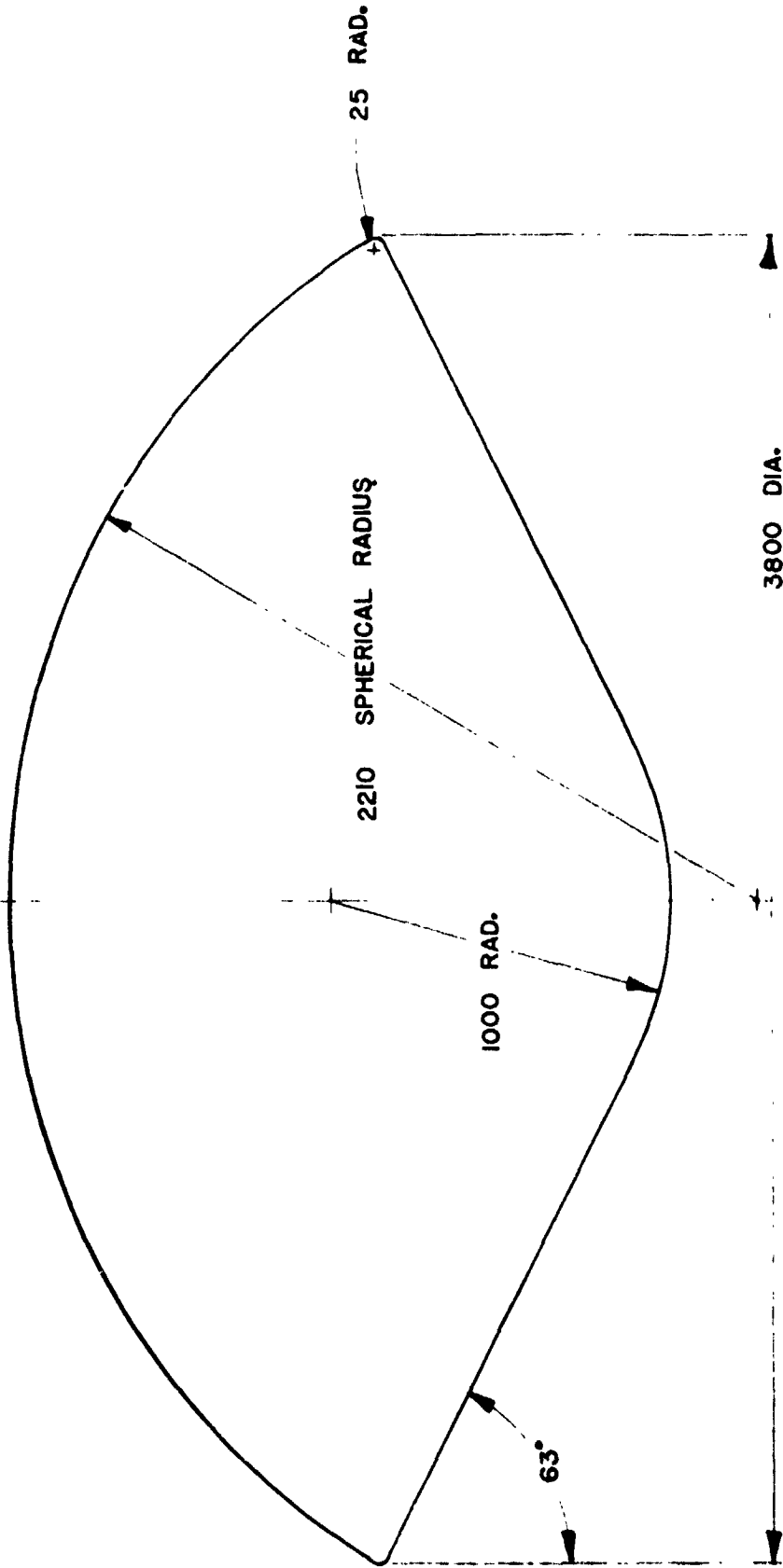


FIGURE (8) WING DEPLOYMENT - PREVIOUS DESIGN - NOV. 77

ORIGINAL PAGE IS
OF POOR QUALITY



FIGURE (9) DEPLOYED CONFIGURATION - PREVIOUS DESIGN - NOV. 77



ALL DIMENSIONS IN MM.

FIGURE (10) AEROSHELL GEOMETRY

the volume of the Space Shuttle payload bay assuming the carriage of twin stage IUS, a Comsat, and 4-7 airplane capsules (the higher figure is beyond the Space Shuttle weight limitations on the Mars Mission).

The requirement of the descent system was to decelerate the airplane to 60 m/sec speed at 7.5 km altitude (Figure 11). This requirement was chosen to assure a flutter-free deployment of the large lightweight wing and ample height to assure recovery after deployment (recovery requires 3 km and the pull-up is a 3 g maneuver, see paragraph 3.4).

After separation the deorbit velocity of 60 m/sec will get the aeroshell into the required entry angle (Figure 12), the parachute deploys at 165 m/sec and 9 km altitude and brings the airplane capsule to the required deployment conditions.

1.5 System Limitations and Design Approach

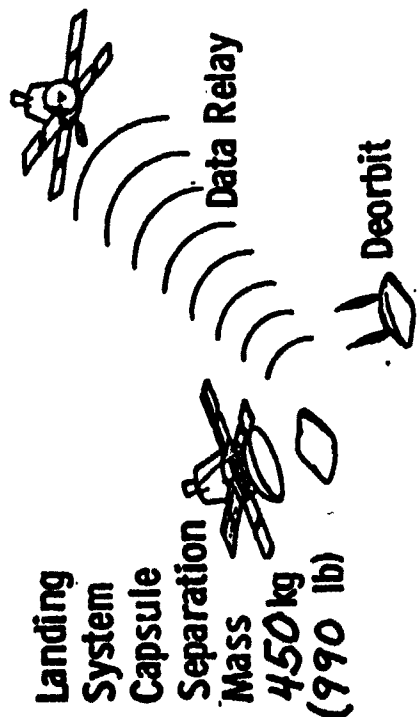
The first consideration that led the design approach in this study was that the airplane mission involves a complex system (Space Shuttle, Spacecraft, Comsat, descent system, airplane and payload). In order to be able to achieve a good airplane design it was essential to work with JPL, Lear Siegler, Inc. (subcontracted to perform the study of the avionics), Martin-Marietta, and the Airplane Science Working Group to define the interfaces between the subsystems so that the airplane design will not get into a state of "constantly changing" due to changes in the interface with other subsystems. It is felt that system definition has been achieved so that the airplane can proceed into the detail design phase and prototype phase with relatively minor changes due to changes in other subsystems.

When approaching the design of a Mars Airplane system we faced some major problems:

1. Low density atmosphere (requiring a low wing loading and giving decreased performance due to low Reynolds numbers).

MARS AIRPLANE

FIGURE (1.1) DEORBIT AND DEPLOYMENT SEQUENCE

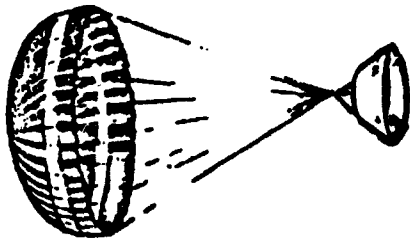


Landing System Capsule Separation & Mass 450 kg (990 lb)

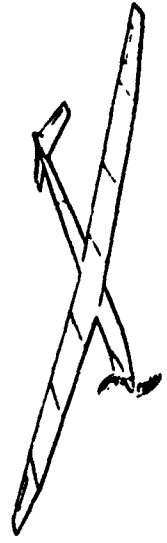
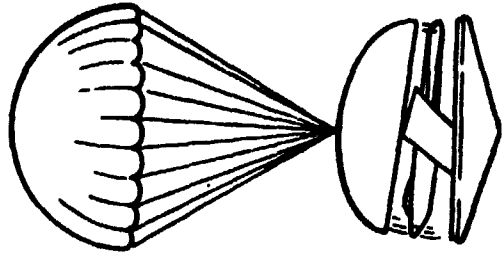
Entry Mass 435 kg (960 lb) Velocity 4650 mps (15,275 fps)

Note: Entire entry-to-DEPLOYMENT sequence takes about 10 minutes.

Parachute Deceleration Altitude 9.0 km (30,000 ft) Mass 425 kg (935 lb)



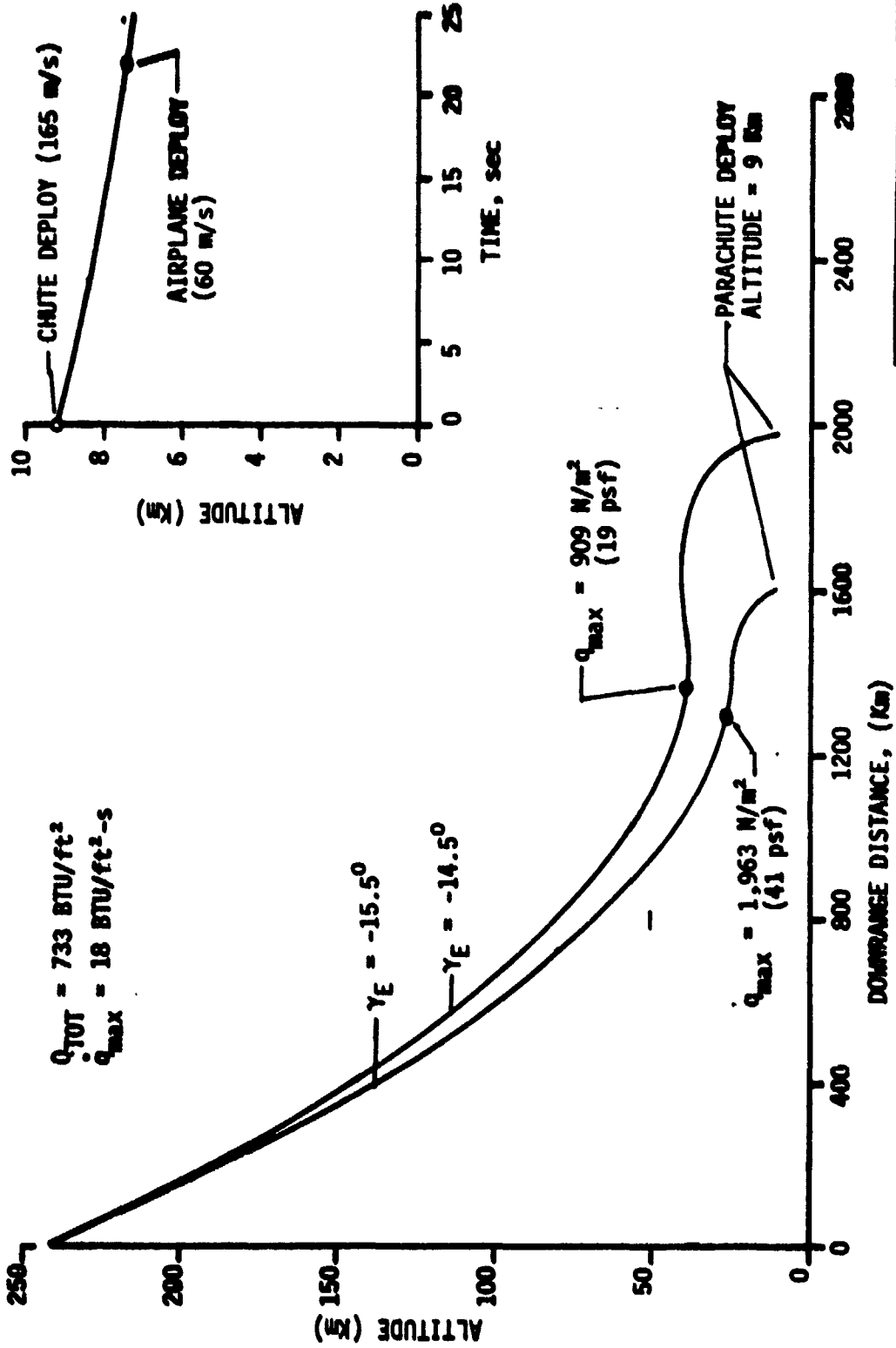
Aeroshell Jettison



RPV DEPLOYMENT AT 7.5 KM ALTITUDE Velocity 60 mps MASS 300 Kg (660 lb)

ORIGINAL PAGE IS OF POOR QUALITY

FIGURE (12) ATMOSPHERIC ENTRY PROFILE



MARTIN MARIETTA

ORIGINAL PAGE IS OF POOR QUALITY

2. Limited aeroshell volume (requiring a deployable structure to achieve the large wing area).
3. The atmosphere contains no oxidizer (non-airbreathing engine - about 10 times higher fuel consumption).
4. Airplane weight must be low (for performance and to satisfy the multiple airplane per spacecraft approach).
5. Mapping accuracy of Mars is 5 - 10 km (the airplane is required to navigate to a point whose location is not accurately known).
6. Communication delay (no real-time communication and earth aided visual navigation and no real-time decision-making).

In face of these problems (and tens of other smaller difficulties) the design approach in this study was to try to solve the problems in a "direct" way without compromising the mission performance we felt is needed for the Mars Airplane (deploying 4 airplanes per spacecraft, each carrying a "good size" payload for a range of several thousands kilometers flying at a relatively low speed to obtain good resolution imaging with the limited data rate, accurately navigating to pin-point targets on Mars, accurately following the surface contours and, possibly, making a soft landing and take-off to bring a sample to a central site).

2. CANDIDATE CONFIGURATIONS

2.1 Basic Configuration

As mentioned previously, both data rate limitations and flight energy efficiency consideration required a relatively low flying speed. A study of the Space Shuttle/IUS/Comsat/descent system/airplane resulted in the weight breakdown given in Figure 3, which for a 4 airplane per spacecraft mission allocates 300 kg per airplane. Designing the aeroshell to best use the Space-Shuttle payload bay cross-section, designing the airplane fuselage as a "flat-top" to fit into the cone of the aeroshell and using the thin wing section, it was possible to stow a 20 m² area 21 m span wing in the maximum diameter part of the base cover using only 6 wing breaks. The wing loading achieved (55.5 N/m² with the 3.7 m/sec² Mars gravity), the high cruise lift coefficient airfoil and the high aspect ratio (22.05) give a cruise speed of 90 m/sec (175 kts) at 300 kg airplane mass at 1 km altitude (Mach number of .37).

Several different configurations were studied including pusher engine configurations and canard configurations. It was found that the conventional tailed design with the wing near the center of gravity has important advantages from stowage and aeroshell center of gravity considerations.

Other considerations which influenced the choice of the airplane configuration:

1. The big tail volume to tolerate the possible large shifts in center of gravity (due to payload deployment).
2. The large propeller required for efficient high altitude (up to 15 km) flight in the Mars thin atmosphere.
3. The preference of a configuration that gives the maximum possible volume in the aeroshell around the fuselage center section for protrusions of sensors (the imaging system for example), and possible future requirements for more payload volume.

All of these mission related considerations (volume limits, performance, aerodynamics, etc.) are the same for all three configurations studied (electric powered cruiser, Hydrazine powered cruiser and lander airplane. Therefore, the basic configuration was the same for all candidate airplane configurations studied.

The possible use of a glider was briefly studied and discontinued because the performance was too low to achieve most of the science goals of the mission (even if we assume a deployment altitude of 20 km and a glide ratio of 30, the range will be only 600 km and most of the distance traveled will be at a high altitude resulting in unsatisfactory sensor performance).

Figure 13 shows the basic airplane configuration and Figure 14 shows the stowed geometry. Stowed geometry and deployment may be easier to visualize with the 1/10 scale model (Figure 15). The fuselage has 3 structural breaks and the tail is of an inverted V configuration (included angle of 140°) and is turned 360° and rolled 180° during stowage to stow in the "deepest" point of the aeroshell under the central wing panel. The propeller blades are hinged near the spinner and stow in a way which makes possible the stowage of propellers of increased diameter (if required).

The control surfaces include one aileron on the left wing outer panel (the two sets of Magnetometer sensors in the right wing make the proximity of electromagnetic servo actuators undesirable and the single aileron is adequate for control and lighter than two smaller ailerons).

The two-piece elevator may be used also as a rudder (but if active yaw control proves to be necessary, a small spoiler in the wing outer panel may prove to be more effective).

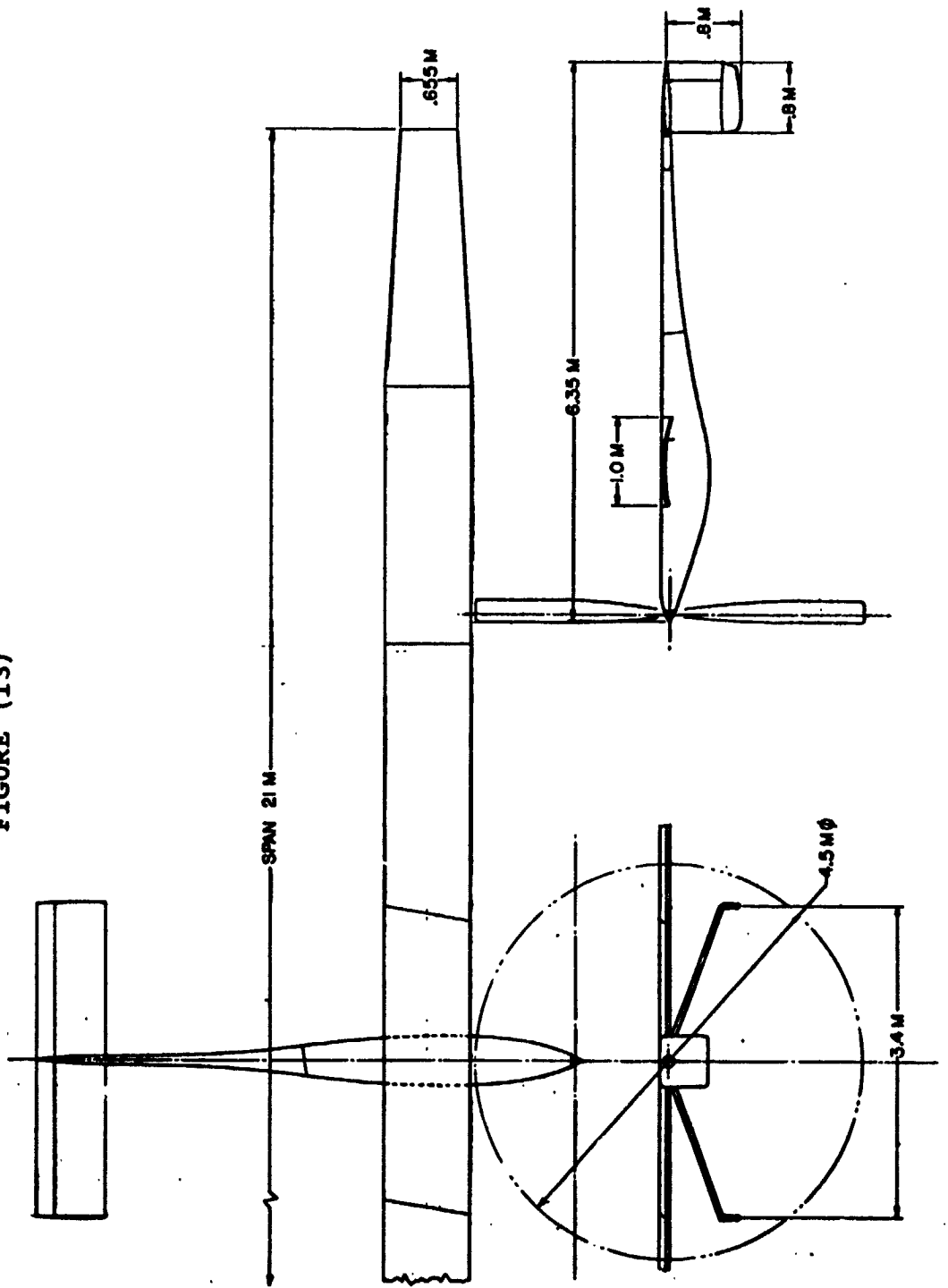
2.2 Hydrazine Powered Airplane

The Hydrazine powered airplane was the configuration examined in most detail during this study phase. Figure 16 shows an inboard profile of the Hydrazine powered cruiser.

The 200 liters payload bay is placed near the center of gravity with the 100 liters deployable package on the center of

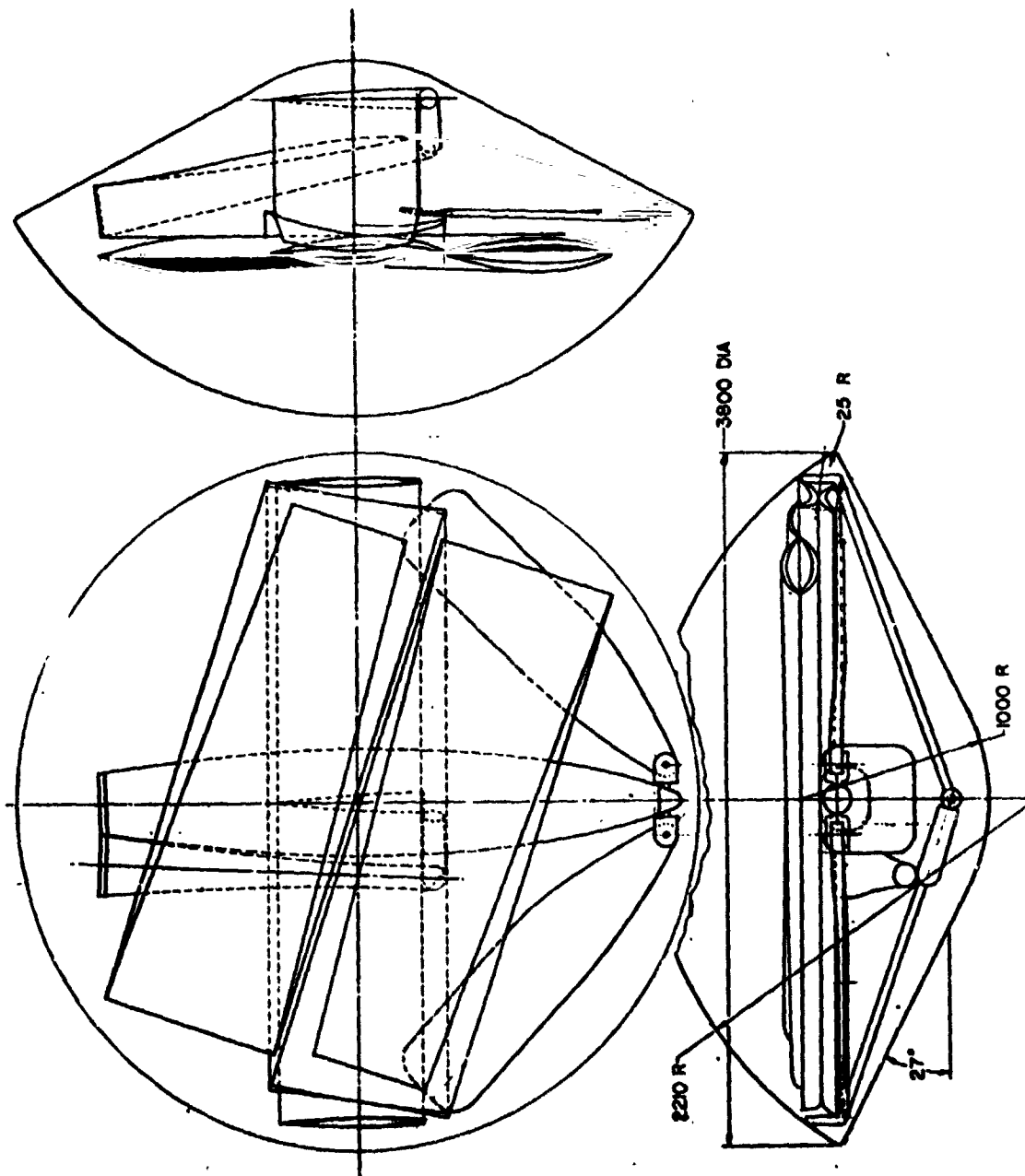
BASIC AIRPLANE CONFIGURATION

FIGURE (13)



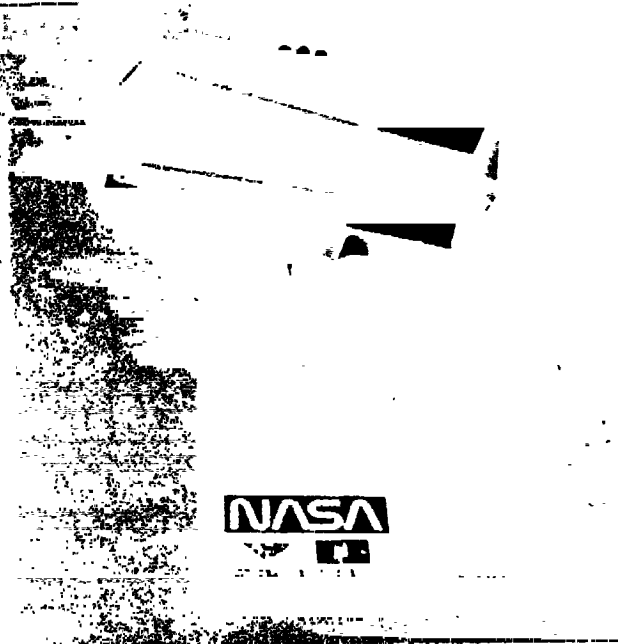
STOWED GEOMETRY

FIGURE (14)





AIRPLANE IN AEROSHELL



BASECOVER REMOVED

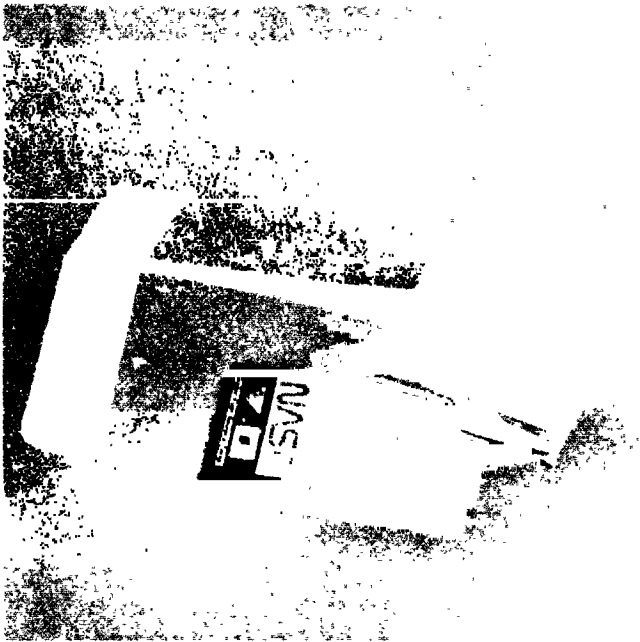


AEROSHELL REMOVED

TAIL DEPLOYMENT

ORIGINAL PAGE IS
OF POOR QUALITY

FIGURE (15a) 1/10 SCALE DISPLAY MODEL

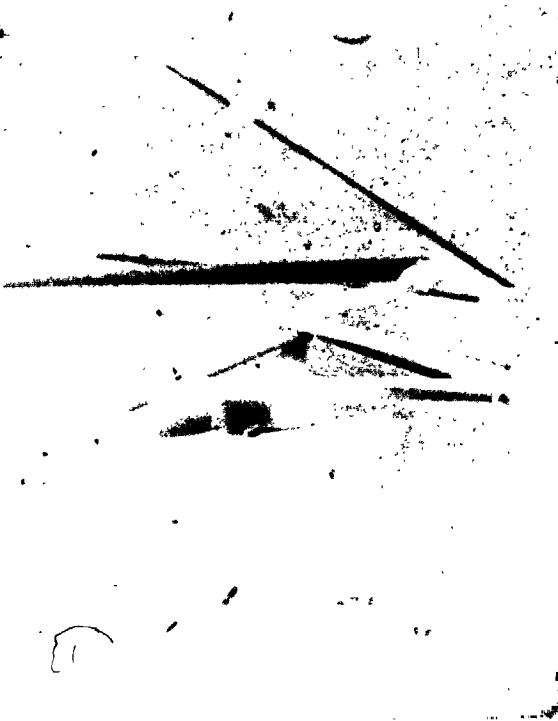


TAIL DEPLOYED

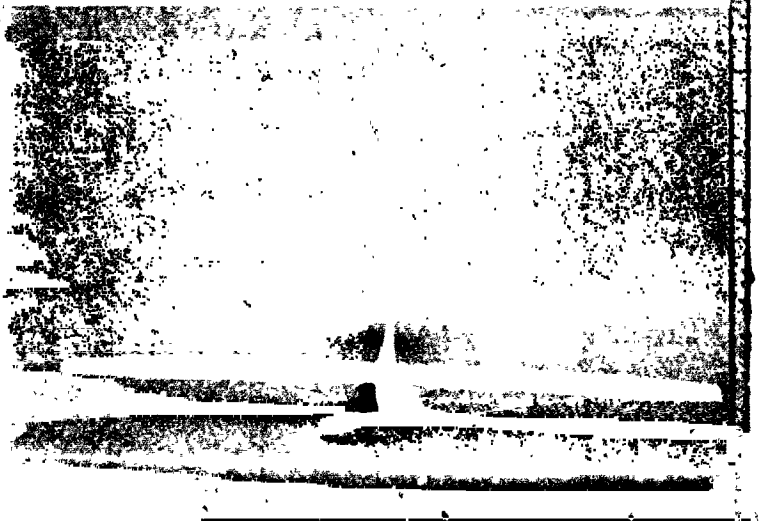


WING DEPLOYMENT

**ORIGINAL PAGE IS
OF POOR QUALITY**



WING DEPLOYMENT

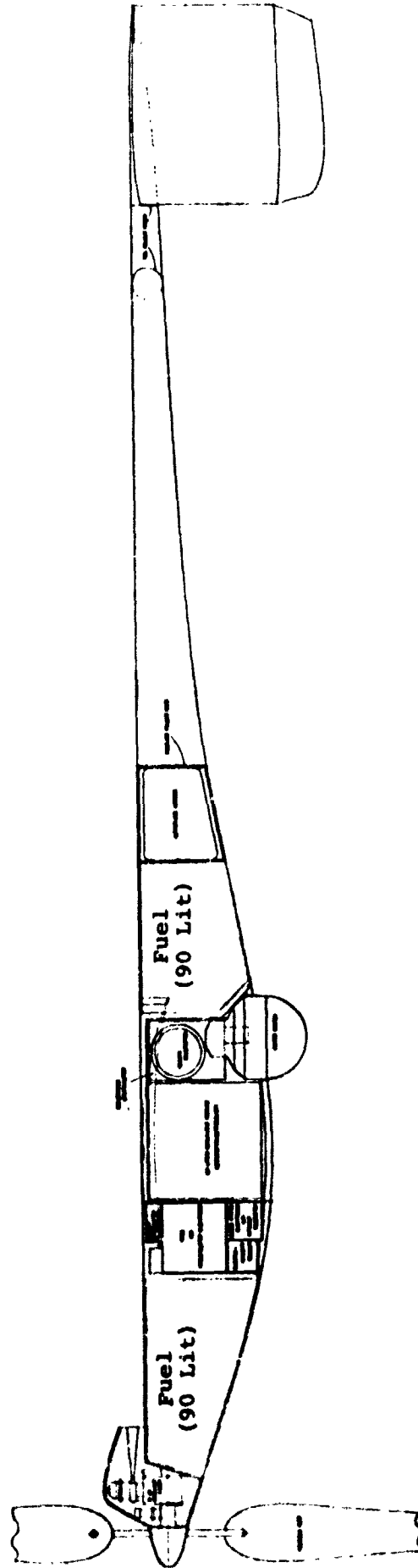


**WING AND PROPELLER
DEPLOYED**

FIGURE (15b) 1/10 SCALE DISPLAY MODEL

HYDRAZINE POWERED CRUISER

FIGURE (16)



gravity and the "fixed" payload installed forward and aft of it. Two Hydrazine fuel tanks are placed symmetrically forward and aft of the payload bay. The basic design is such that maximum fuel load of 180 kg can be carried with 200 liters of payload. This design feature results in a small drag increase but makes the fuselage structure identical for all payload/range options, so that the airplane production is not affected by a late decision to trade some fuel for payload or a change in Space Shuttle/IUS/spacecraft weights or carrying capabilities which may allow an airplane weight increase (section 2.4 will also show that this design makes the structure of the Hydrazine powered lander identical to that of the cruiser). The Hydrazine feed from the two tanks to the engine is proportioned to keep the center of gravity of the airplane between well controlled limits. This feature is necessary because of the high fuel fraction (up to 50% of the all-up-weight) and widely spaced fuel tanks.

The airplane avionics bay is in the aft part of the main fuselage section. As mentioned in paragraph 1.3, the avionics package was increased during this study to 50 kg to expand the mission capability to include terrain following and high data rate communication with comsats at ranges up to 25,000 km. This new package may require the addition of a forward avionics bay to increase the available volume and balance the airplane.

The powerplant installation is fairly straightforward with engine-mounted fuel pump, variable pitch propeller, engine shock-mounting and oil-Hydrazine heat exchanger like the proven installation on the NASA Dryden Mini-Sniffer.

The engine is a scaled-down version of the Akkerman engine on the Mini-Sniffer (15 HP compared to a design power of 30 HP on the Mini-Sniffer). The spinner and engine fairing are of very "clean" aerodynamic shape and add very little drag to the basic "competition-glider" configuration.

One of the design concepts was to keep most of airplane systems in the main part of the fuselage and the central wing panel attached to it, so that the systems flexible connections through

the deployment breaks are kept to a minimum. This was almost totally achieved, the exceptions being:

1. The elevator and aileron servos
2. The two magnetometer sets of sensors in the right wing
3. The Gamma Ray Spectrometer in the left wing
4. The antenna of the Electromagnetic Sounder on the underside of the wing
5. The Solar Cell Array on the upper surface of the two inboard wing panels (Lander airplane only)

The exhaust of the Hydrazine engine is on the top of the fuselage so that the sensors in the payload bay are practically shielded (the sensors are facing down and the propeller spiral flow is almost negligible on this airplane with high cruise speed to power ratio and big slow turning propeller).

Only the three wing spar-caps are carried through the fuselage, the wing skins are not, so that maximum usable volume is made for payload.

2.3 Electric Powered Airplane

As stated previously, the basic airplane configuration is common to all candidate airplane configurations studied.

The electric powered Mars airplane idea was considered several times during this study and the short term previous study (November 77). The achievable energy density of the advanced Lithium batteries was always quoted as 100-150 Wh/lb. Even if we assume 85% total motor efficiency (motor, electronics, and transmission) this energy density is equivalent to 8.8 - 5.9 lb/HP h. This gives only about half the range with the Hydrazine engine (which achieves 4.5 lb/HP h fuel consumption including transmission); this, taking into account that the electric powered airplane weight is constant and the weight of the Hydrazine powered airplane decreases with fuel consumption (requiring

less energy to fly a certain range) and also that the average airplane weight being higher with the electrical power requires a higher powered engine to achieve a reasonable average climb performance (20 HP compared to 15 HP), so that the electric powerplant weight is estimated at 20 kg compared to 13 kg for the Hydrazine powerplant giving reduced battery weight (compared to fuel weight).

Because of this reduced performance the electric power was considered as a back-up candidate in the event that insurmountable problems arose in qualifying the Hydrazine engine for operation in Mars environment.

It was not until early May 78 that a survey of batteries and a calculation of Mars airplane performance with electric power, performed by Harvey H. Frank of JPL, refocused the attention on the new 150-300 Wh/lb Lithium battery being developed for the U.S. Navy by Altus Company, Palo Alto, California. Performance calculations showed that with a 300 Wh/lb battery (equivalent to 2.9 lb/HP h specific "fuel" consumption) the range was 10% - 30% higher than that of the Hydrazine powered cruiser. But, the most promising fact was not the 300 Wh/lb figure but the fact that the increase of the energy density from 150 to 300 Wh/lb was achieved by reduction of the packaging weight with the same basic cell. A discussion of the subject with Altus clarified that the basic "internal" cell energy density is approximately 600 Wh/lb. After obtaining the design requirements of the packaging from Altus, an ultra lightweight packaging technique was designed which promises a total of 550 Wh/lb. With this battery the performance of the Mars cruiser airplane is more than doubled compared to the Hydrazine powered cruiser.

Contacts were made with Delco Electronics, Gould, and Sunstrand for a high power to weight high efficiency electric motor of the Samarium-Cobalt rotor magnet type. These contacts gave the estimated volume, weight and performance of the powerplant (motor, inverter and gearbox - see paragraph 3.2 for details).

Design iterations with Altus and Sunstrand narrowed to a 245 volt 72 cell package. The basic cell will be cylindrical of 9" (23 cm) diameter, the cell thickness (and total energy capacity) will vary with the payload/range trade-off to give a constant 245 volt system for variable battery total weights. The airplane fuselage was widened to accommodate the batteries in a two-cell side-by-side configuration. The payload bay volume of the electrical powered cruiser may be shaped as a 2.1 m (7 ft) long bay of 300 liters volume (Figure 17).

2.4 Lander Airplane

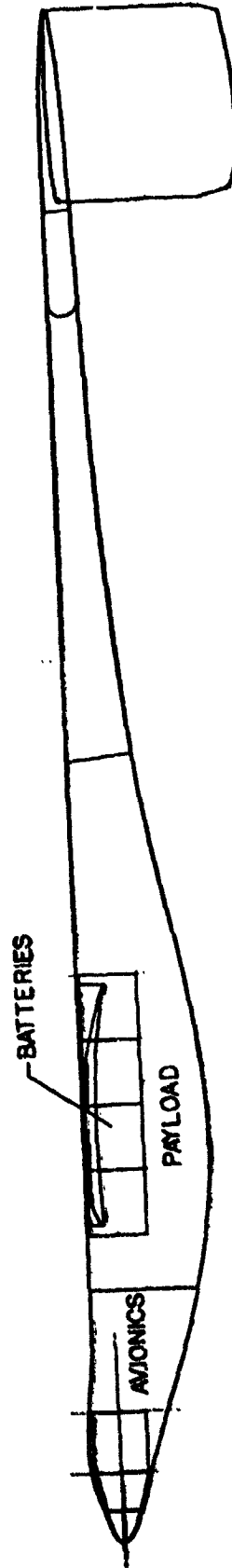
The Lander Mars Airplane makes use of two main Viking Lander Terminal Descent rockets (each with 18 nozzles to reduce surface erosion during landing) mounted vertically in the fuselage (Figure 18) and four Viking Lander Terminal Descent roll rockets mounted in the wing near the inboard hinge point (two for roll control and two for yaw control) to perform a soft landing on the surface of Mars. The airplane flight control system having the sensors and computation capability to perform accurate navigation and terrain following missions (using radar altimeter, radar doppler and strapped-down inertial system) needs only a small added capability (automatic site selection system) to perform the soft landing maneuvers.

The Hydrazine is fed to the rockets from two 22 liter Titanium spherical tanks having internal bladders and pressurized to 500 psi. The main rockets and the spherical tanks are installed inside the cruise fuel tanks.

The landing gear includes 4 deployable lightweight tapered tubular struts with tilting landing pads. Two struts are attached to the wing leading edge at the inboard hinge points, and two attached to the tail underfins. This configuration is chosen because of the good airplane stability it offers both against wind blow-over (see paragraph 3.6), and in the use as a drilling platform.

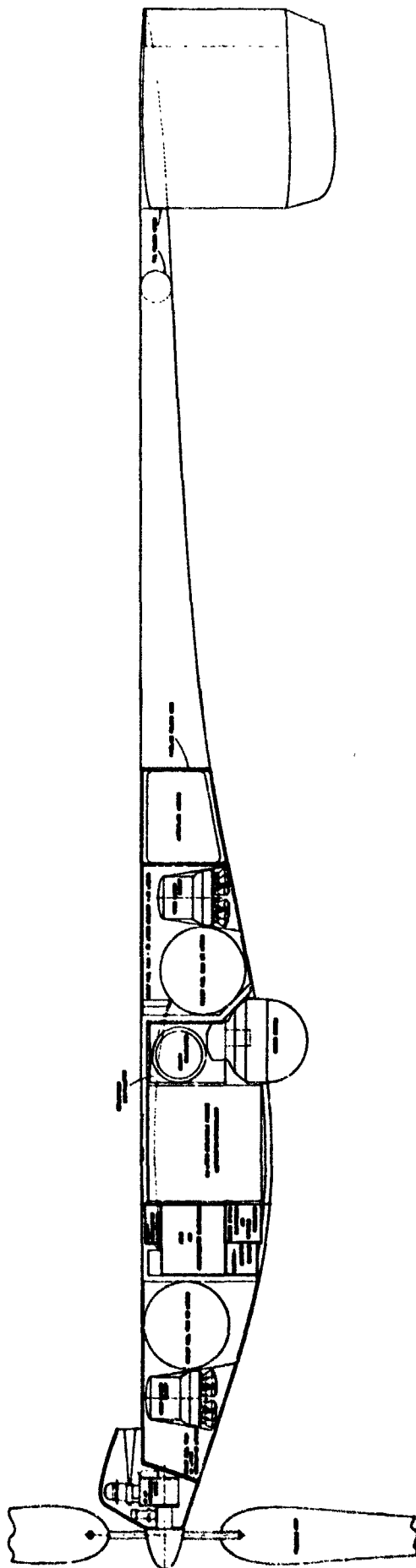
ELECTRIC POWERED CRUISER

FIGURE (17)



HYDRAZINE POWERED LANDER

FIGURE (18)



The empty weight of the Lander airplane is estimated at 35 kg higher than the cruiser, this includes the rocket system, fuel tanks, rocket controls, landing gear, solar cells, rechargeable battery and extra environmental control to survive the extremely low temperatures it may encounter on the surface of Mars.

3. TECHNICAL ANALYSIS AND TECHNOLOGY ASSESSMENT

3.1 Aerodynamics

Flight in the thin Mars atmosphere (see Figure 4 for atmospheric parameters) using a relatively low speed surveillance airplane presents some special aerodynamic difficulties which may be called the "Lift Coefficient - Reynolds Number - Mach Number Problem".

The low density of the Mars atmosphere (approximately 1% of its value on sea level earth) and the moderate flying speed (mandated by the limited data rate from the airplane) result in very low Reynolds numbers. Figure 19 shows the true airspeed versus flight altitude at different airplane mass. The wing area (20 m^2) and the speed range of the airplane are typical for a propeller driven executive airplane on earth. But, whereas the latter usually cruises at Reynolds numbers higher than 10^7 , the Mars airplane cruises at Reynolds numbers lower than 10^5 (Figure 20). These low Reynolds numbers are typical for model aircraft and birds on earth.

The airflow over flying bodies create a boundary layer (the flow layer adjacent to the surface) where the airstream slows (due to viscosity) to zero speed on the surface of flying body. The performance and stability of flying vehicles depends heavily on the behavior of the airflow in the boundary layer. The flow in the boundary layer may be laminar or turbulent. A turbulent boundary layer has better flow stability in the pressure gradients characteristic of flow over lifting bodies, whereas the laminar boundary layer tends to easily separate in positive pressure gradients. The separated flow decreases the lift and increases the drag of the flying body.

The flow characteristics in the boundary layer depends on the flow speed, the streamwise length of the body, and the density and viscosity of the fluid. The "ruling parameter" is called Reynolds number:

FIGURE (19) CRUISE AIRSPEED

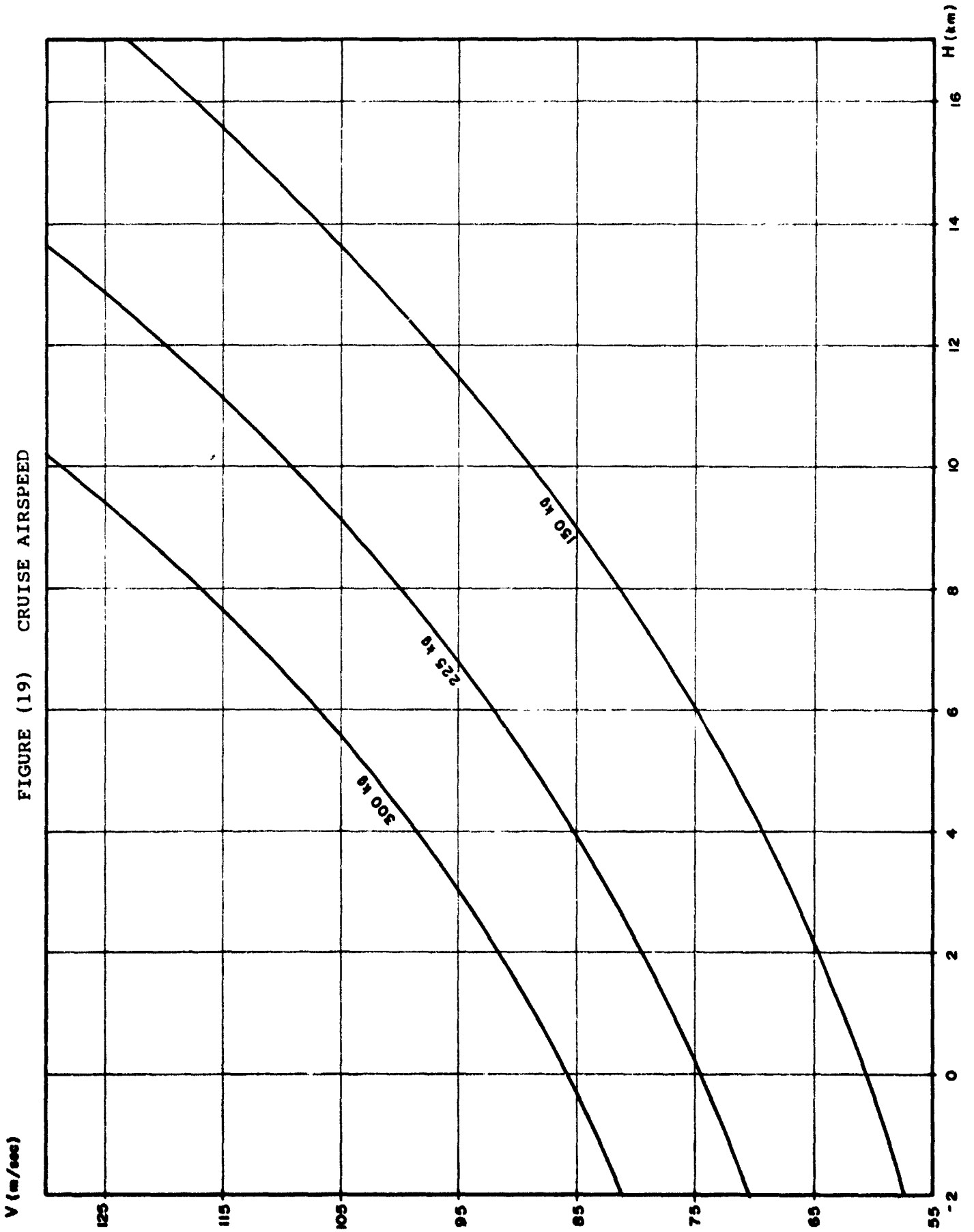
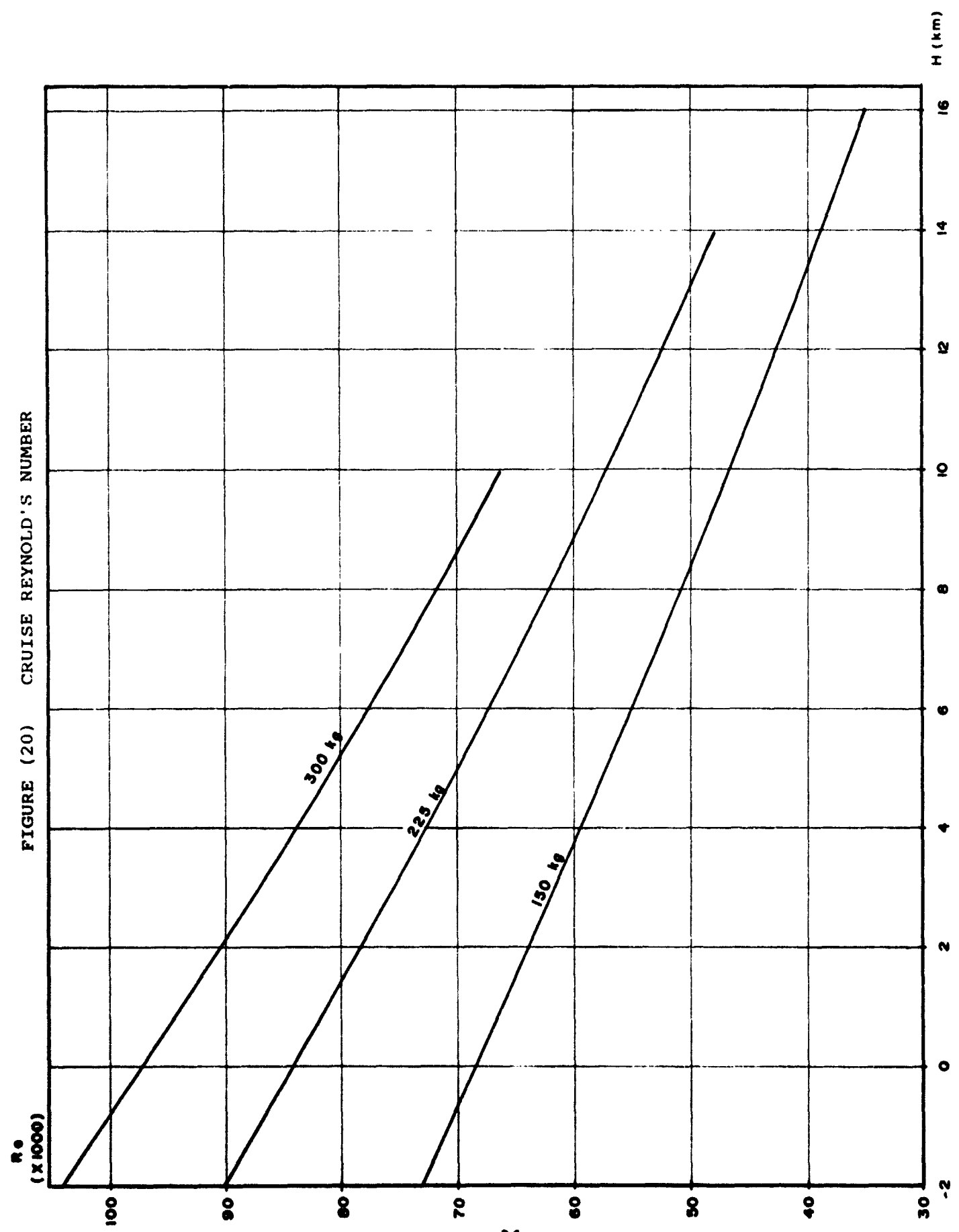


FIGURE (20) CRUISE REYNOLD'S NUMBER



$$\text{Re} \propto \frac{\rho V L}{\mu}$$

ρ - fluid density L - streamwise length
V - flow velocity μ - fluid viscosity

At relatively high Reynolds Numbers (say above 10^6), the flow drag associated with laminar flow is usually lower than that with a turbulent boundary layer. Therefore, competition sailplanes, operating in the $1 - 3 \times 10^6$ Reynolds number range use specially designed airfoils to keep the boundary layer laminar on a large part of their surfaces.

Flow at low Reynolds numbers tend to be inherently laminar in the boundary layer, but the drag increases sharply at low Reynolds numbers and the maximum generated lift drops sharply (due to flow detachment as discussed above).

Figure 21 shows the sharp decrease in lift generated by a typical airfoil with the decrease in Reynolds number. Figure 22 shows the increase in drag of the same airfoil. The ratio of lift to drag of an airplane is the aerodynamic parameter which governs the range capability of the airplane. It is easily seen that the lift/drag ratio of this wing airfoil dropped from 140 at a typical light airplane cruise Reynolds number of 3×10^6 to 7 at a Reynolds number of 45,000 which is typical to Mars airplane flight at 10 km altitude above the surface of Mars. This would practically translate into 10 times reduction in maximum range of the airplane, which is unacceptable if reasonable mission performance is to be achieved.

Very little research has been done in the aerodynamic domain of low Reynolds numbers. Most of the experiments were done by aeromodellers with only few valid wind-tunnel tests done by careful aerodynamicists usually kept within very low budgets. The available data is scattered and hard to find because this domain is of no interest to aerospace industry for earth applications.

DSI has (mostly on company funding) carefully researched the literature and contacted a large number of the "small low Reynolds number aerodynamics community" to come with the data required to substantiate the Mars Airplane feasibility and performance.

NACA 4412

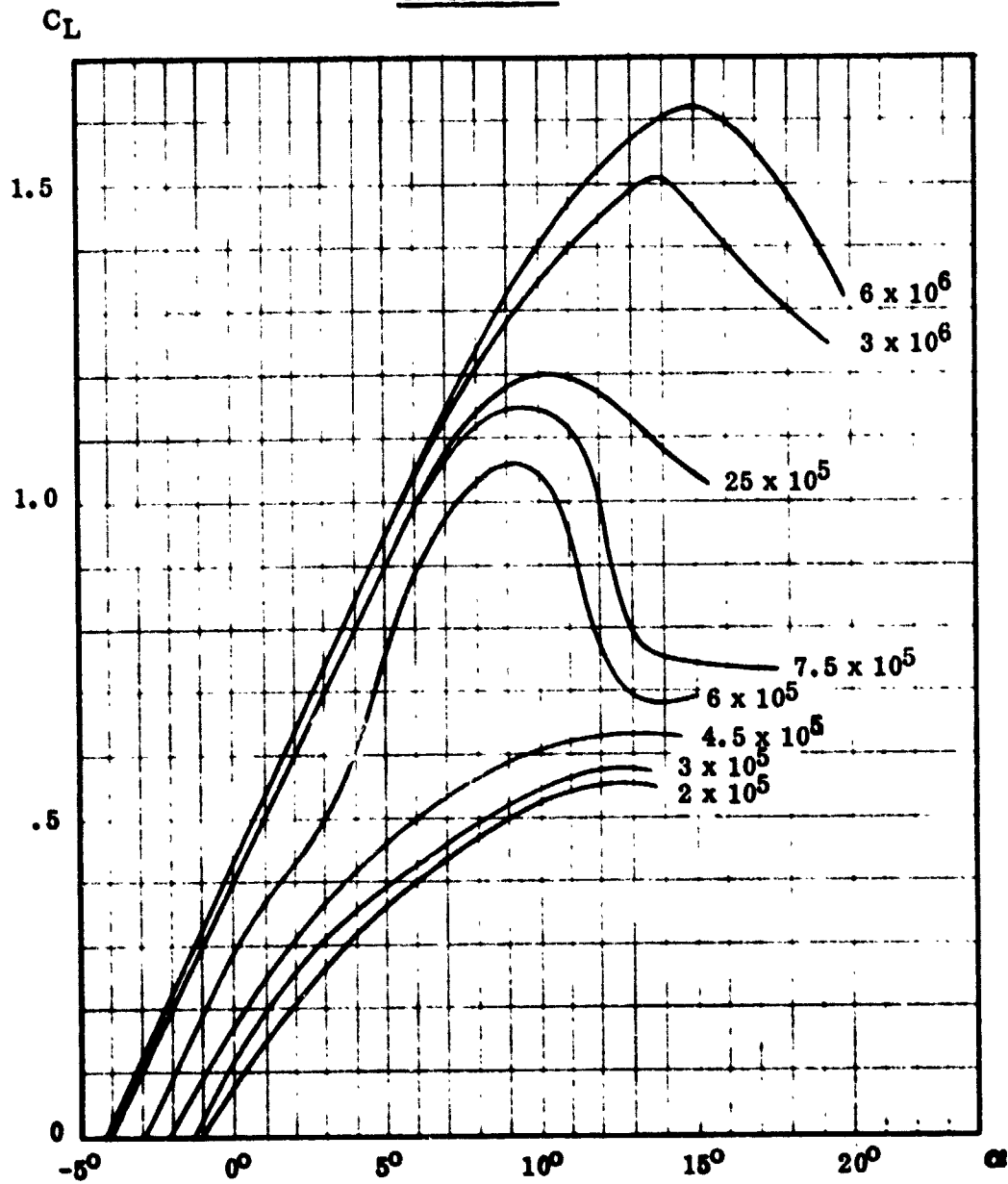


FIGURE (21) LIFT COEFFICIENT CHANGES WITH REYNOLD'S NUMBERS

ORIGINAL PAGE IS
OF POOR QUALITY

NACA 4412

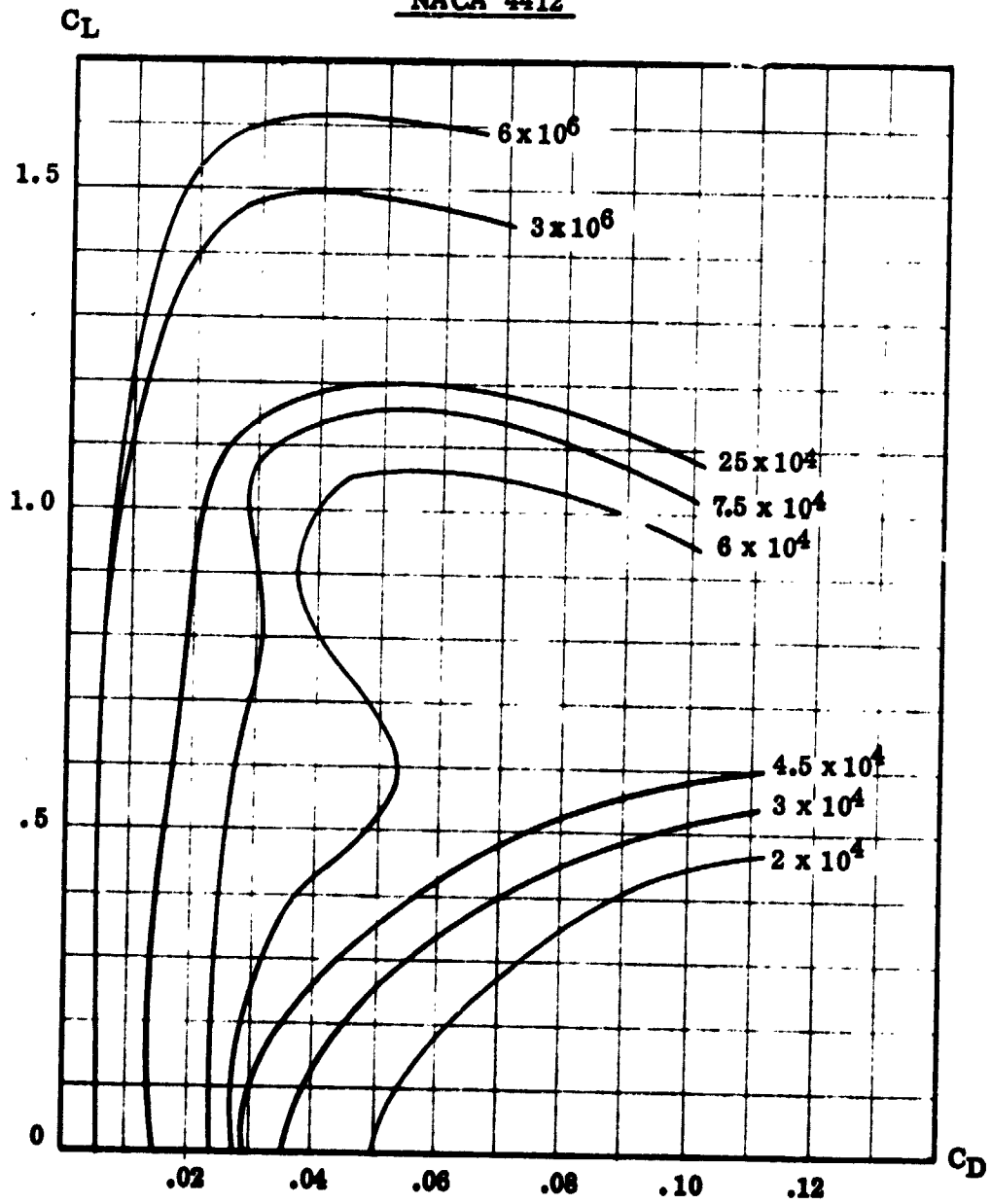


FIGURE (22) LIFT/DRAG RATIO CHANGES WITH REYNOLD'S NUMBERS

Figure 23 illustrates the performance gain possible below Reynolds number of 10^5 through the use of special airfoils and flow tripping techniques. The curves for the 12% thick NACA 4412 and 12.5% thick N60 airfoils demonstrate the big drop in performance below a critical Reynolds number. This drop is a result of flow detachment on the upper surface of the wing due to the positive pressure gradients associated with generating lift on the upper surface with these airfoils designed for higher Reynolds numbers. The other curves demonstrate the improved performance of the thin airfoils widely used on small low speed aeromodels. These thin airfoils generate a big part of their lift on the highly undercambered lower surface where the separation is most unprobable. The upper surface is moderately cambered and the lift coefficient for best lift to drag ratio is attained at relatively low angle of attack, these two facts prevent the flow separation on the upper surface. Figure 23 also illustrates the gain in performance through the use of tripping devices to force the boundary layer on the upper surface to change from laminar to turbulent (the experiments were done with a 7.5% thick airfoil with and without forced turbulation).

Figure 24a shows the wind-tunnel measurement of drag of a 4.8% thick Pffeningen airfoil with several tripping strips. These test results are probably the most valuable low Reynolds data available in the Free World. They clearly show the advantage of the use of trippers below Reynolds number of 10^5 , and the need to trip the flow more upstream (to stabilize the flow at a given lift coefficient) as Reynolds number is decreased.

Figure 24b shows two Eppler airfoils designed for Reynolds numbers of $1 - 2 \times 10^5$ using special computer programs and their calculated performance. Richard Eppler of the University of Stuttgart is well known for his aerodynamic expertise in the low Reynolds number regime and his computer program for airfoil design has proven to be successful and efficient (it is adopted now by NASA Langley and will be distributed by NASA).

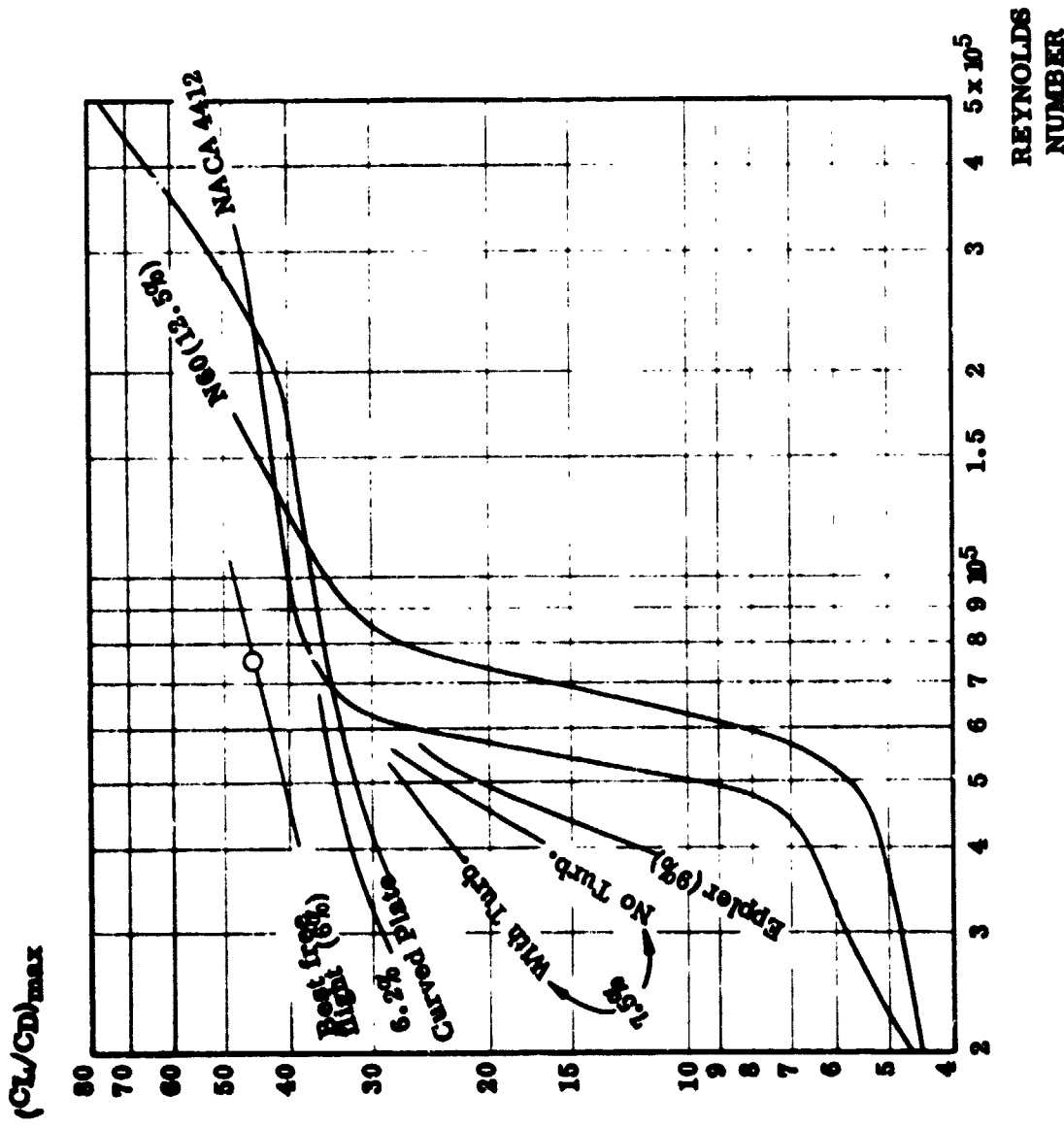
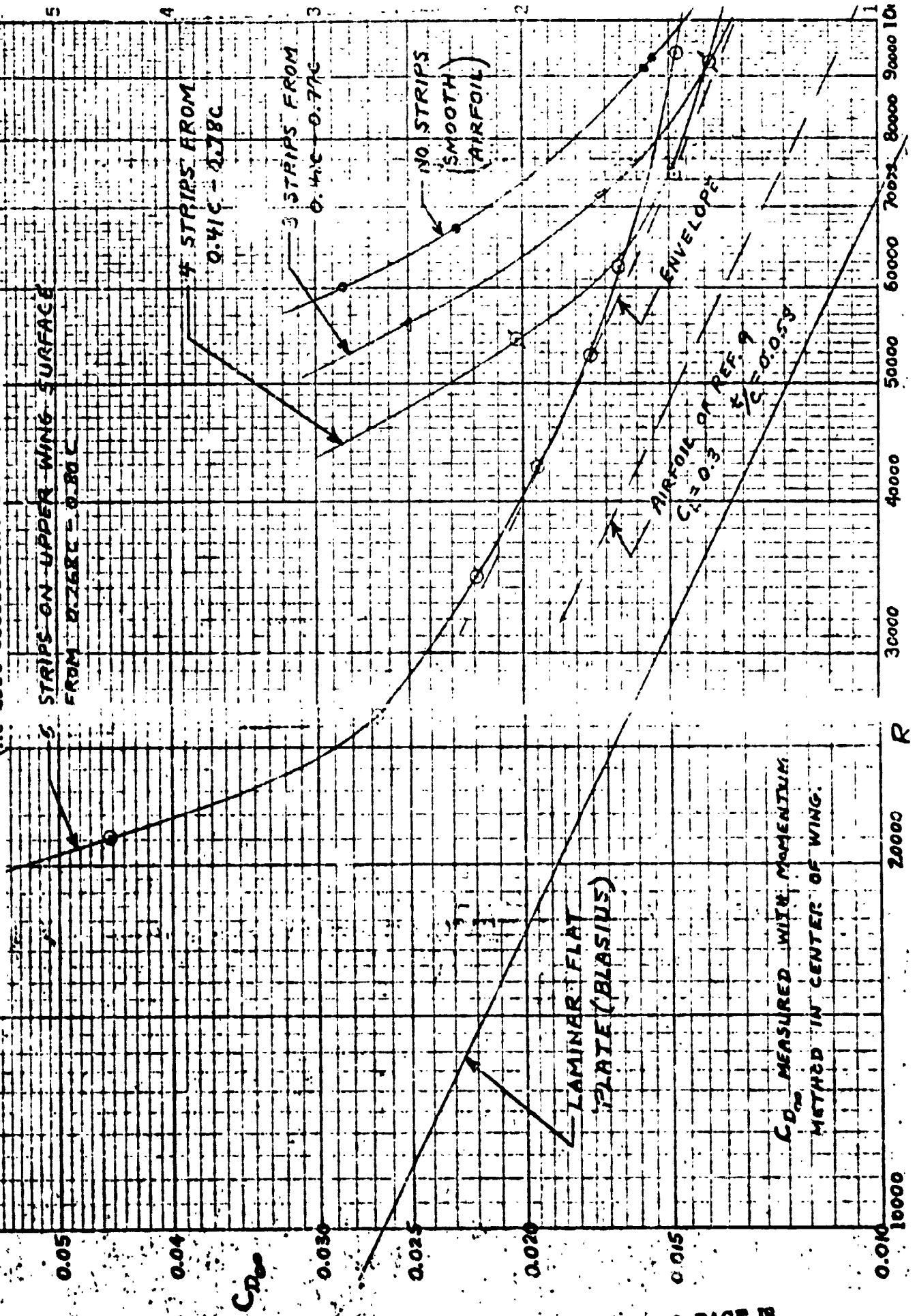


FIGURE (23) LIFT/DRAG RATIO OF VARIOUS AIRFOILS

FIGURE (24g) DRAG OF THE PFENNIGER .048 AIRFOIL
(At Lift Coefficient of .77)



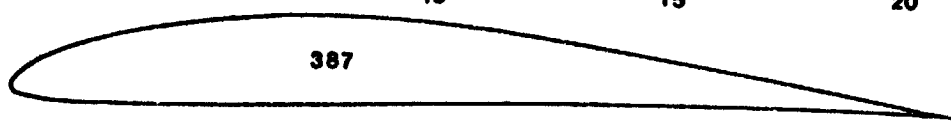
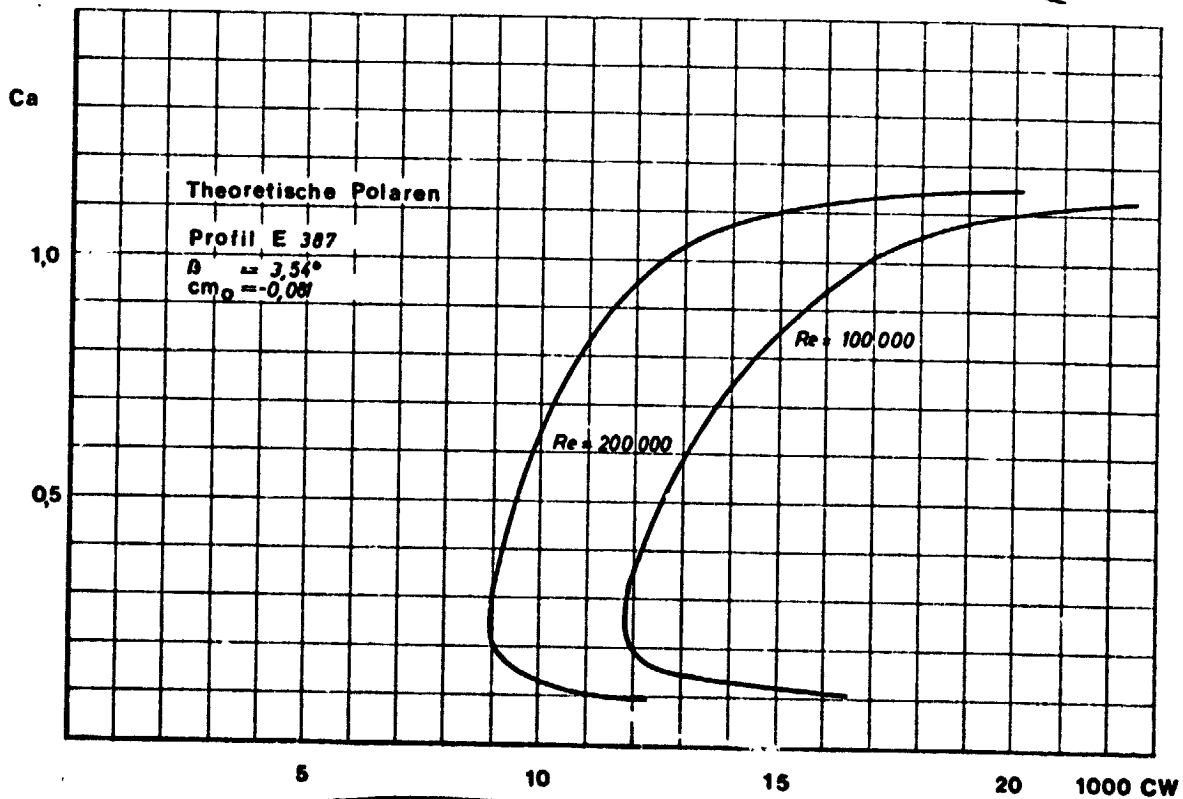
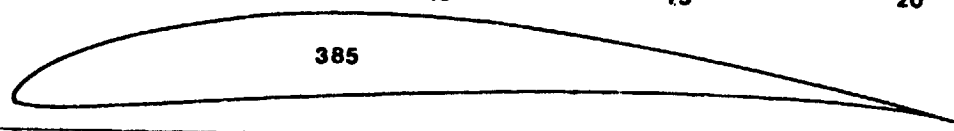
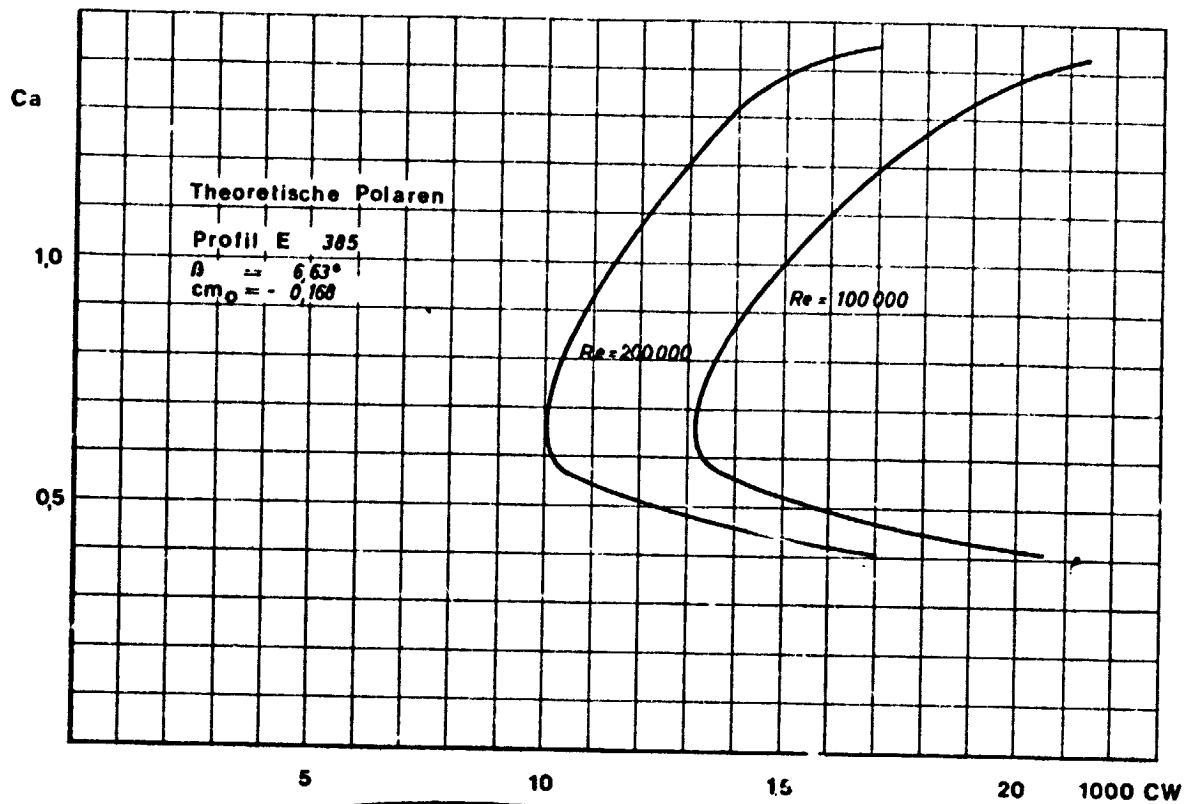


FIGURE (24b) THEORETICAL PERFORMANCE OF THE EPPLER 385 and 387 AIRFOILS

Figures 25 and 26 show the measured performance of the same airfoils. These are the results of a recent wind tunnel test by D. F. Volkers in the low-turbulence wind tunnel at Delft, Netherlands. The agreement with the calculated performance is reasonably good for Reynolds number of 2×10^5 but at 1×10^5 the measured performance is much lower and there are strong indications of early separation of the flow on the upper surface. The performance drops sharply below Reynolds number 1×10^5 and it is clear that these airfoils are too thick and may not offer the best performance possible at low Reynolds numbers.

Figure 27 shows the theoretical performance of two thin Eppler airfoils which are more suitable for the low Reynolds number use. No wind tunnel test results are available on these airfoils, but the vast experience accumulated with free flight model-aircraft prove that these 5.5% thick airfoils perform much better than the 8.5% - 9% thick 385 and 387 airfoils.

The design effort to maximize the wing area (minimize wing loading and cruise speed) was required mainly because of data rate limitations. But, at high altitude cruise (required to fly over high areas on Mars and for sounding flight for meteorology measurements) the Mach number increases to .5 (Figure 28). This may not seem to present a problem, but the combination of a cruise lift coefficient of 1 and a Mach number of .5 is not far from the transonic shock wave-boundary layer interaction problems. No existing low Reynolds number transonic test results is known to this study team. The difficulty in performing these tests and the little value they have for the industry make their existence improbable. It is felt that the present design will not present wing buffet problems. But, this problem is far more severe on the propeller blade (see section 3.2).

Figure 29 presents the best estimated lift/drag ratio of the Mars airplane. These estimates take into consideration both Reynolds number and Mach number effects, and they are based on the assumption that careful airfoil development program will advance

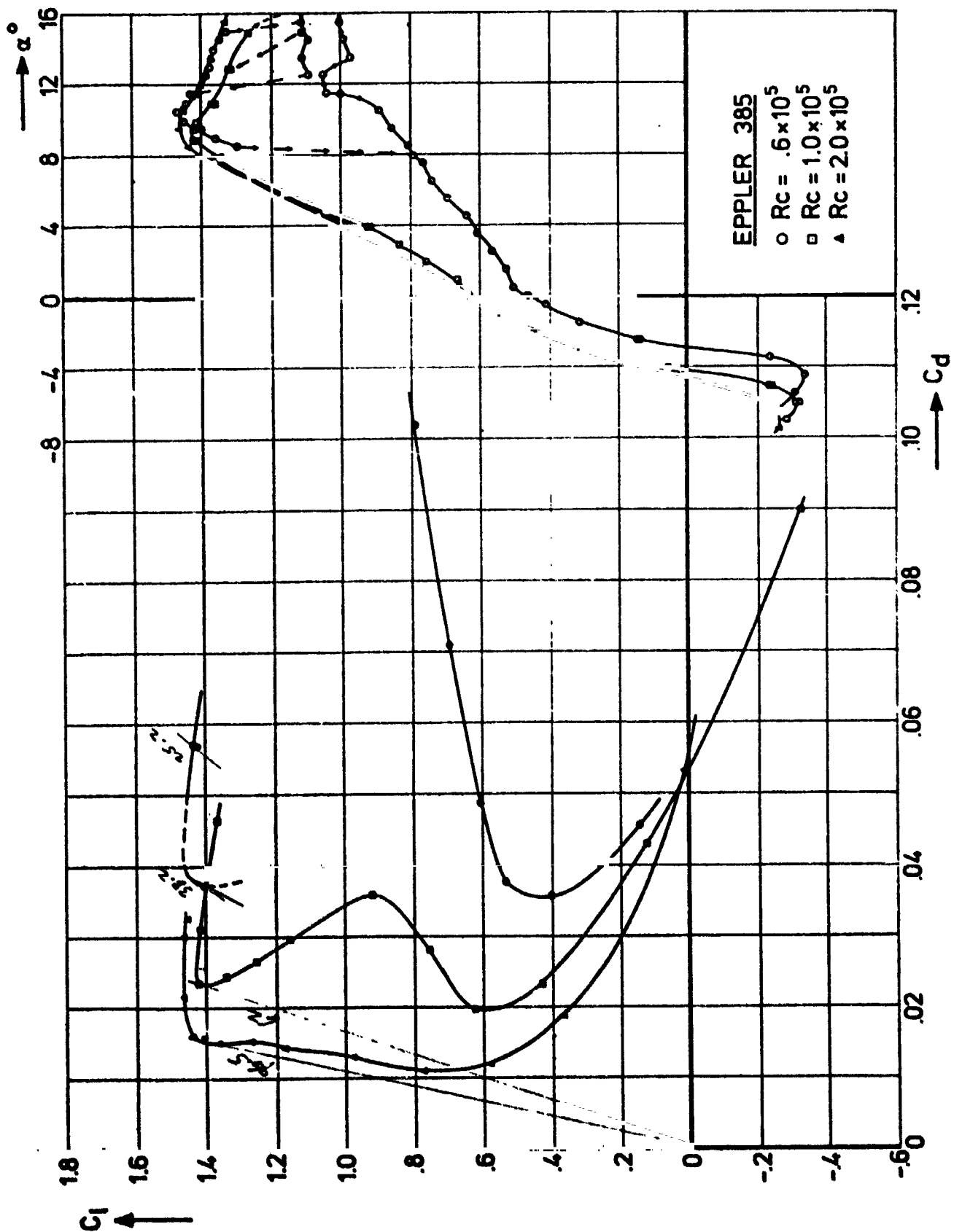


FIGURE (25) MEASURED PERFORMANCE OF THL EPPLER 385 AIRFOIL

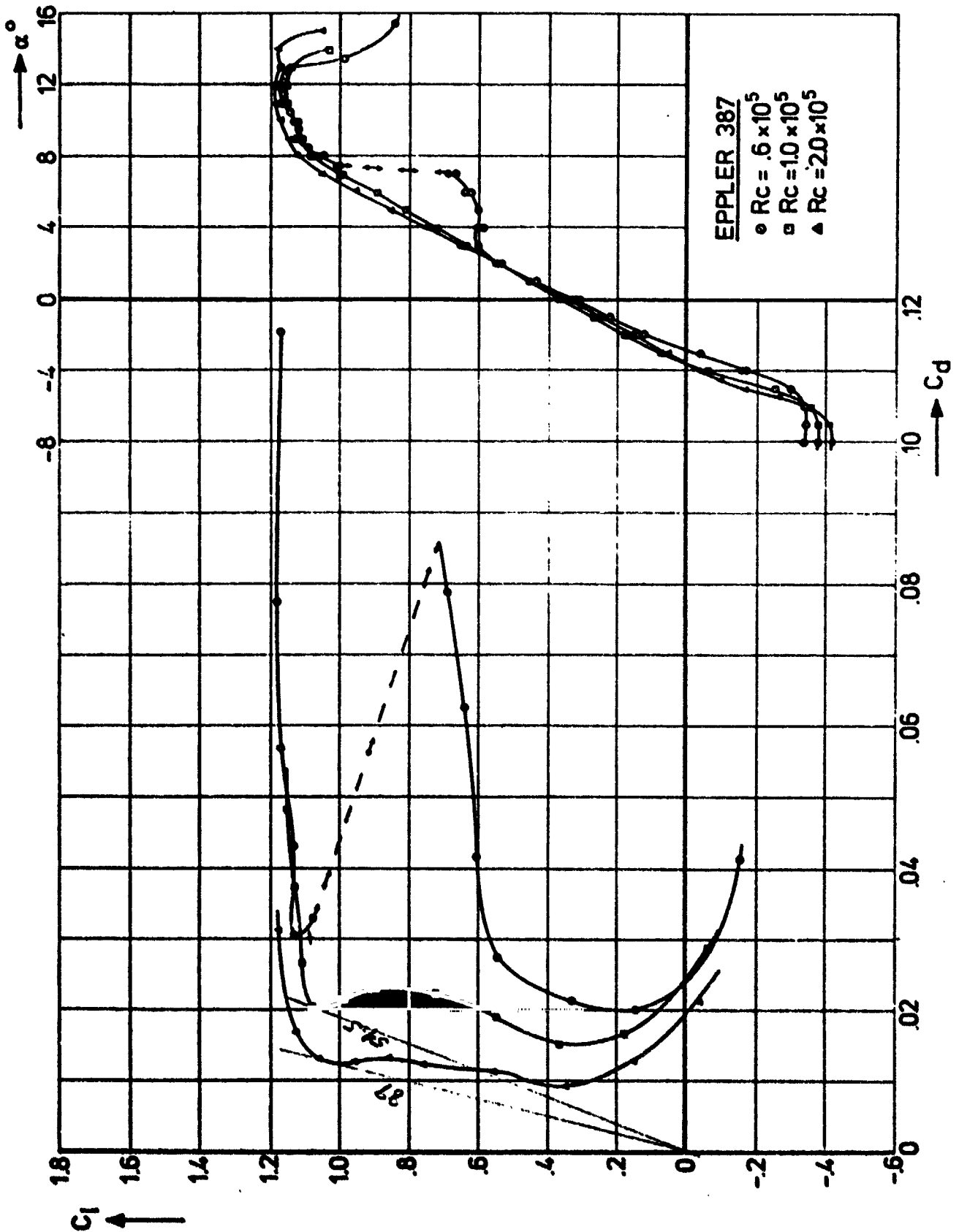


FIGURE (26) MEASURED PERFORMANCE OF THE EPPLER 387 AIRFOIL

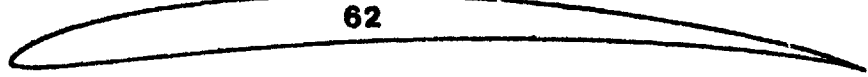
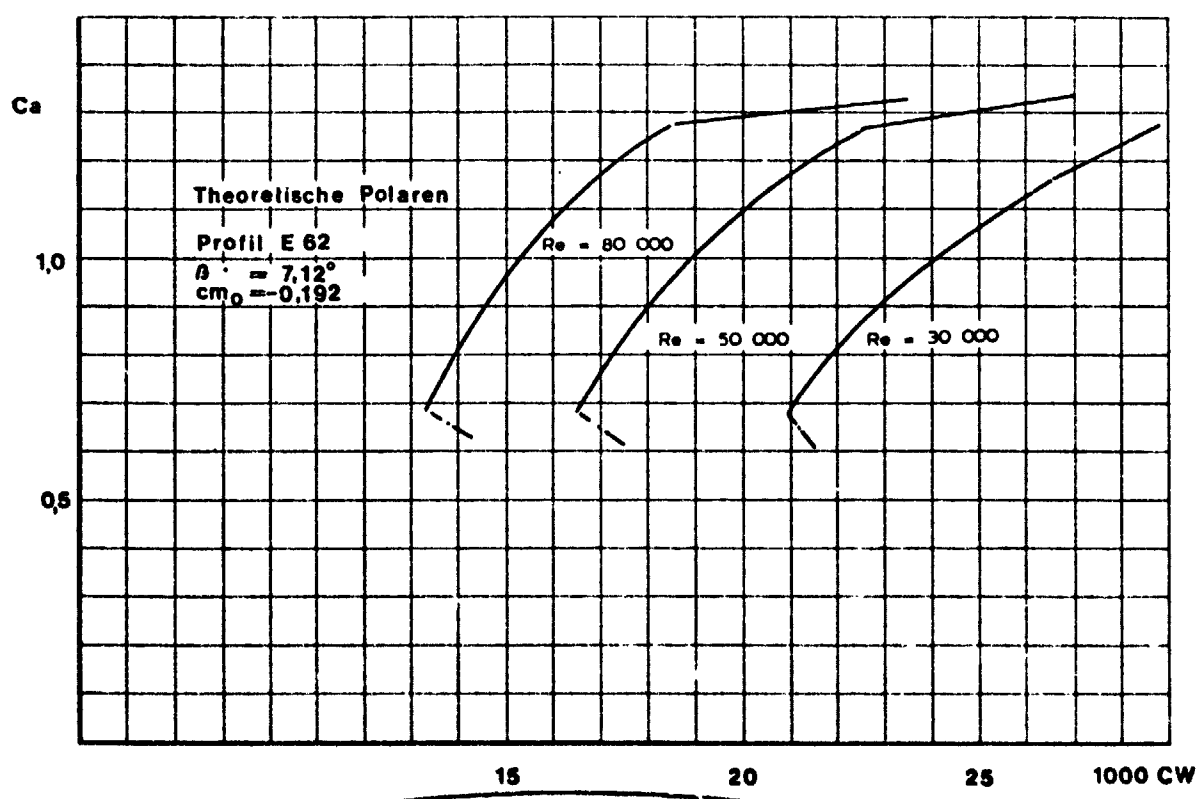
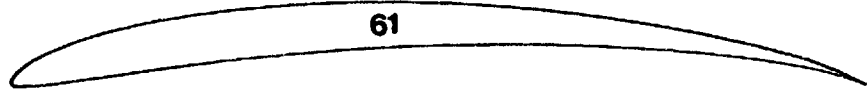
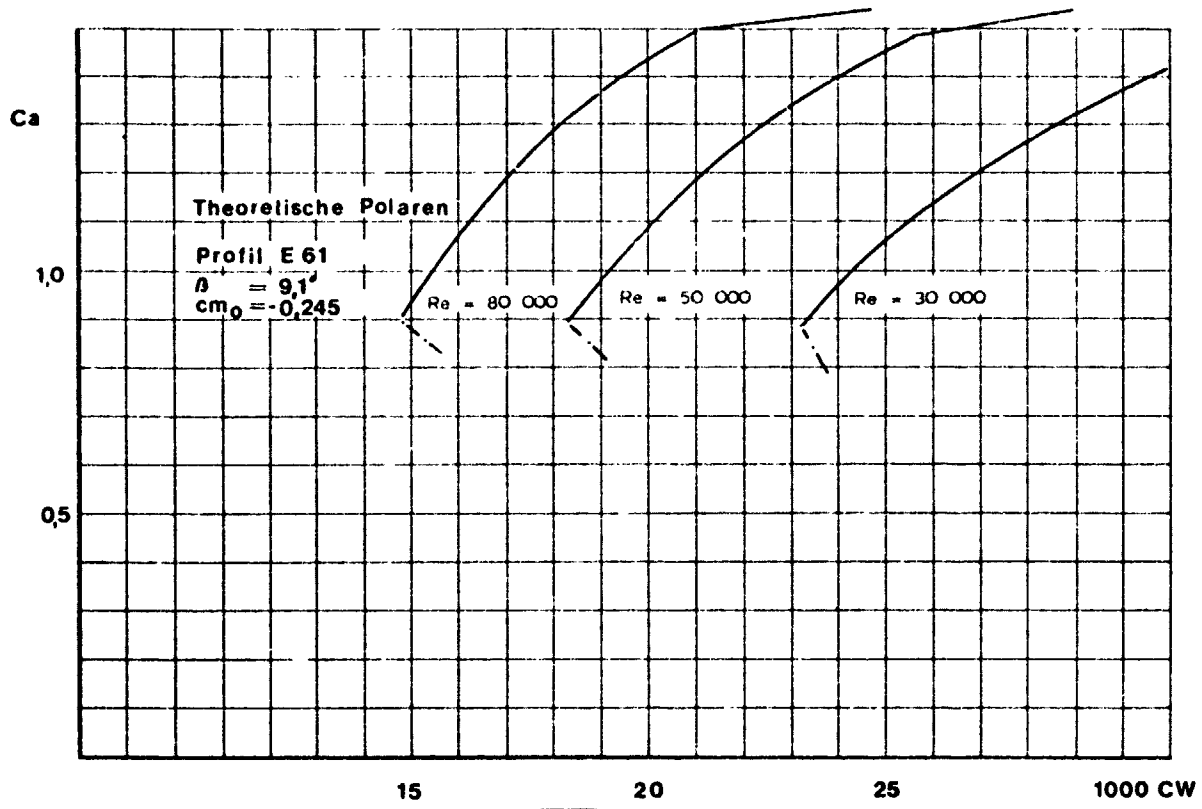


FIGURE (27) THEORETICAL PERFORMANCE OF THE EPPLER 61 and 62 AIRFOILS
- 47 -

FIGURE (28) CRUISE MACH NUMBER

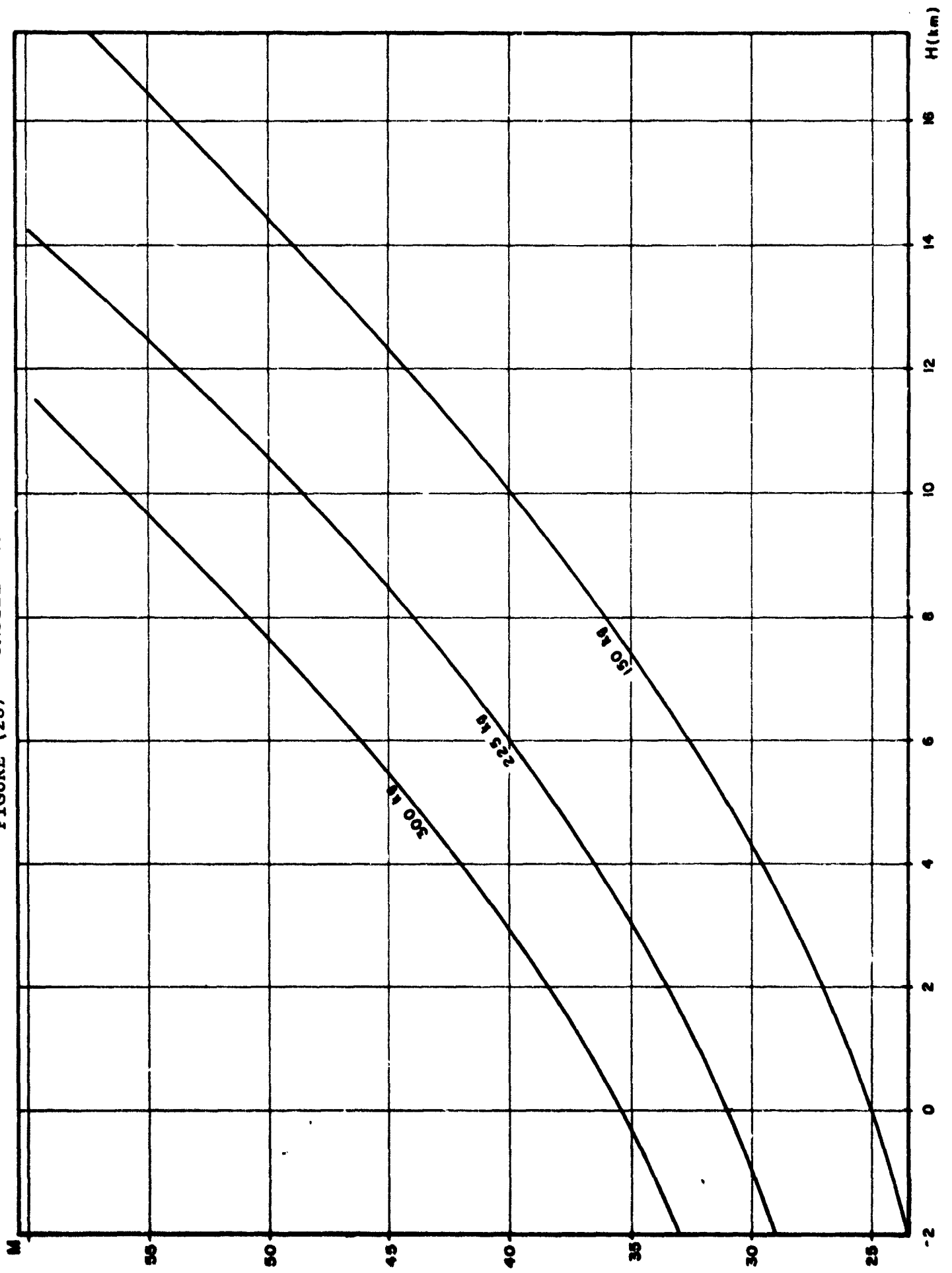
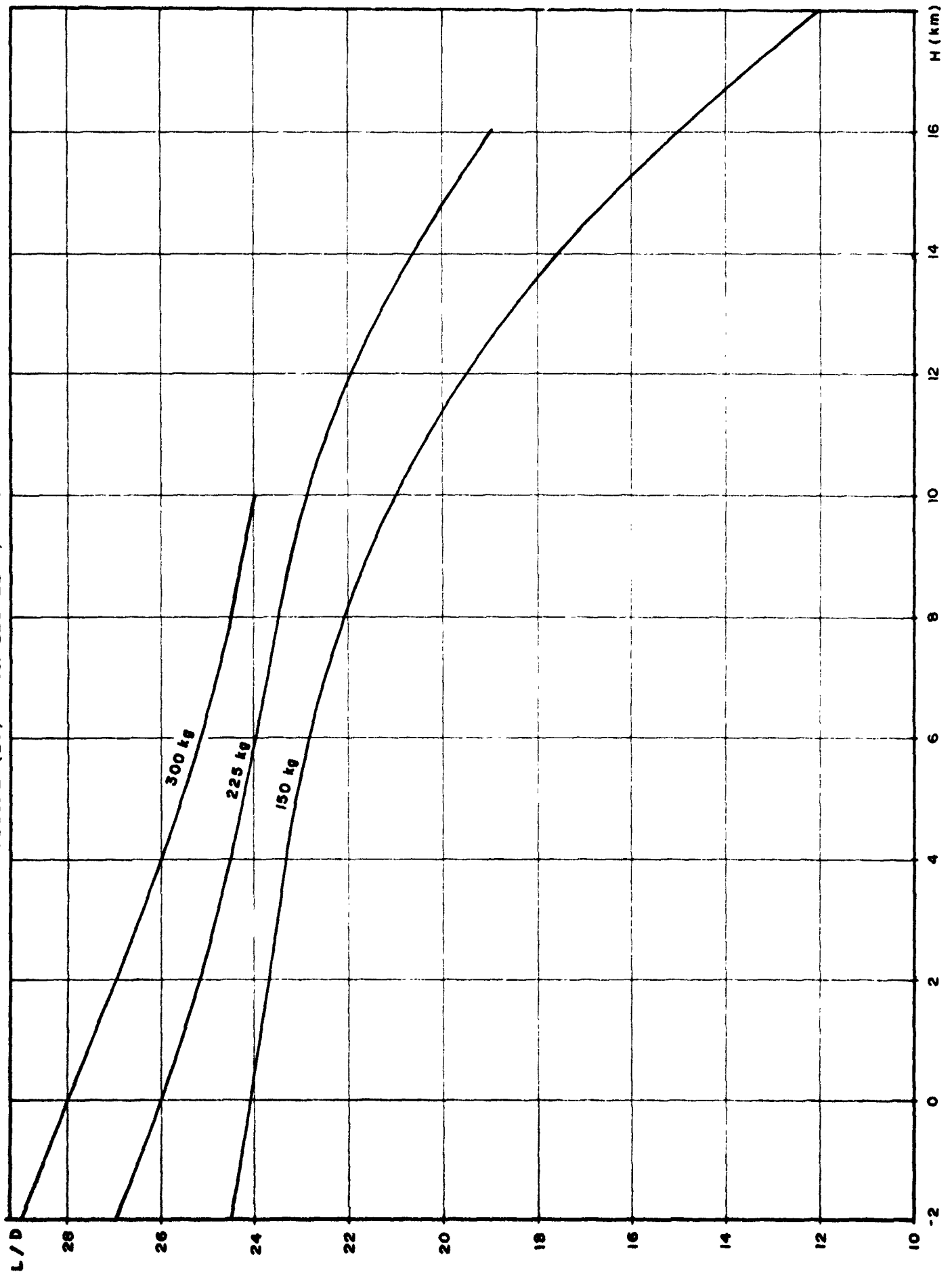


FIGURE (29) CRUISE LIFT/DRAG RATIO



low airfoil performance to what seems to be "easily" achievable (higher airplane performance will be achieved if the development proves more successful than was conservatively assumed in this study).

Scanning the existing knowledge and "tools" in the low Reynolds numbers regime it seems logical to combine three different steps in the development of an airfoil for the Mars Airplane wing:

1. Design of optimized airfoil for the required mission, using the Eppler computer program.
2. Testing of chosen airfoils in low-turbulence wind tunnels and experimenting with boundary layer tripping.
3. Verification of test results using free flight models and test techniques developed during the last two decades.

Even though this airfoil development program is strongly recommended, it is not required for a Mars airplane prototype, as the performance of existing airfoils is adequate for a prototype airplane.

3.2 Powerplant

Two cruise powerplants were considered in this study:

1. The Hydrazine engine developed by Jim Akkerman of NASA Houston powering the Mini-Sniffer RPV developed by Dale Reed of NASA Dryden.
2. Electric motor using Lithium primary batteries.

The Hydrazine engine is a reciprocating engine using the same Hydrazine monofuel and catalyst bed chambers used on space rockets. Figure 30 shows the engine installation and the 6 ft diameter variable pitch propeller on the Mini-Sniffer RPV. Engine details, testing and performance appear in a design report by

ORIGINAL PAGE IS
OF POOR QUALITY



FIGURE (30) THE HYDRAZINE ENGINE INSTALLATION IN THE MINI-SNIFFER

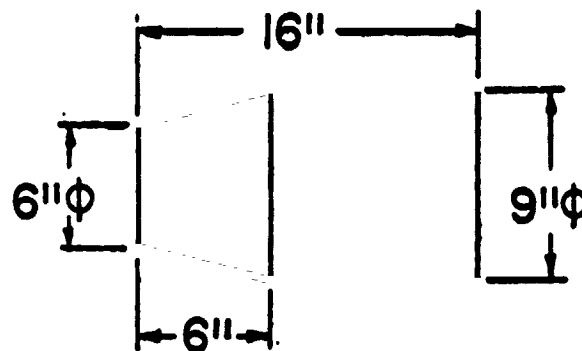
Akkerman and details of the installation in the Mini-Sniffer are given in NASA HOUSTON's drawing #SEE39113000.

The Hydrazine engine prototype has been tested in wind tunnel and flown on the Mini-Sniffer to an altitude of 20,000 ft. This same prototype is suitable for a first Mars Airplane prototype if the gear ratio is changed to accommodate the lower rpm required for the 13 ft. diameter propeller of the Mars Airplane at the design power of 15 HP (the Mini-Sniffer engine is designed for 30 HP and used at 20 HP). The Hydrazine engine for the development and the operational Mars Airplane would be a scaled-down version to give a maximum of 15 HP and weigh 15 lbs including gearbox.

The complete powerplant (engine, cooling and variable pitch propeller) and fuel system weight is estimated at 13 kg.

The best measured specific fuel consumption (to date) of the Hydrazine engine is 4.5 lb/HP h. The cruise sfc is somewhat higher, a mission average sfc of 4.85 lb/HP h is assumed for range calculations.

The electric motor is an integrated unit comprising a light-weight Samarium-Cobalt magnet rotor motor, solid state inverter, and planetary gearbox. The characteristics of the motor proposed by Sunstrand are:



OPERATING VOLTAGE	245 VOLT
RATED POWER	20HP (AT 20,000 R.P.M. MOTOR 850 R.P.M. PROP.)
EFFICIENCY AT RATED POWER	87 %
EFFICIENCY AT 6HP CRUISE	85 %
WEIGHT	13.5KG (30LBS)

The motor weight may be reduced to 9 kg (20 lbs) if a cruise efficiency of 79% could be tolerated. The cruiser airplane being a long cruise-high fuel fraction design, has longer range with the heavier higher efficiency motor; but the Lander, if configured with heavy payload and small battery, would have more range with the lighter engine (the extra 4.5 kg used for increased battery size).

A considerable decrease in motor volume and weight may be accomplished by an integrated motor-gearbox design; but, being of higher development cost and risk, it is not recommended by the study team (nor by Sunstrand).

The design of a propeller to efficiently operate in the thin Mars atmosphere is a challenge. The propeller blade operates at lower Reynolds numbers than the wing, the lift coefficient at high altitude flight is relatively high (up to 1.1) and the tip Mach number is well in the transonic regime. The preliminary design of the propeller was done by Peter Lissaman (designer of the Gossamer Condor) and Bart Hibbs of Aeroviroment, Inc., using the low Reynolds number aerodynamic data presented in section 3.1. The design process (using a computer program) included 5 iterations with the design gradually refined to a point that the calculated cruise efficiency of the propeller is 84 - 85%. This relatively high efficiency was achieved by an increase in blade size (to 4 m propeller diameter on the Hydrazine powered airplane) to affect an increase in Reynolds number and decrease in rpm and tip Mach number (tip Mach number is kept below .9 at the extreme operating conditions - high altitude climb).

As mentioned earlier, the propeller has variable pitch. This is required in order to operate efficiently within the very large operating regime (minimum cruise power of 2 HP to maximum climb power of 15 HP and altitude range from -2 km to 15 km on the Hydrazine powered airplane).

The propeller design and performance are presented in Appendix A.

3.3 Structure and Materials

The most important single goal in the Mars Airplane design is achieving an ultra lightweight vehicle with maximum weight allocated to mission-performance related system (e.g. payload, avionics, and fuel/battery). Cutting the structural weight of the airplane to the practical minimum consistent with the structural integrity and deployment requirements was a major design effort.

The big advance in composite structure technology in the past decade (especially with carbon fibers and Kevlar 49) made possible a structural weight fraction of 17% and wing structural weight of 1.5 kg/m² on a deployable 5.5% thick wing of 22 aspect ratio. This weight estimate is based on DSI's experience with the production of lightweight military RPVs.

Several design iterations led to the preliminary structural design presented in this section. The main design criteria were:

1. Ultimate strength load factor of 6 Mars g's.
2. Structural rigidity and shear center-center of gravity locations to achieve flutter free dynamic pressure of 200 N/m² (cruise dynamic pressure is 55 N/m² and deployment recovery pull-up is performed at a maximum of 117 N/m²).
3. Wing bending and torsional rigidity high enough to keep the cruise deflections within acceptable limits for flight stability and control (wing tip bending deflection is .3 m in cruise and .9 m in a 3 g deployment pull-up maneuver).

The structure is all-composite. The high temperature sterilization requirement (30 hrs soak at 112°C) implies that the structure is cured at high temperature (175°C curing temperature is specified). Most of the structure is a high strength Thoronel 300 carbon-fiber and epoxy composite. The wing spar caps are designed to rigidity requirements and made of high modulus GY-70 carbon fibers. The wing outer panel and the tail surface are very lightly loaded, so that the use of the thinnest gauge Kevlar 49 achieves minimum weight on these parts.

Figure 31 shows typical wing structure, the combination of honeycomb sandwich skin and closely spaced ribs in the forward part and full depth honeycomb construction in the aft part present the best structural design arrived at during this study. The higher skin thickness near the leading edge moves the shear center forward to be near the average center of pressure location and so minimizing the wing warping under load (a serious problem of a lightweight thin wing of high aspect ratio).

3.4 Deployment and Descent System Interface

The descent system is briefly described in section 1.1 and detailed in Martin Marietta report No. MCR-78-570. The folded airplane is brought to a 60 m/sec descent at 7.5 km above Mars. The aeroshell is detached and falls-off. The airplane is suspended under the base-cover and parachute by a riser attached to the top of the fuselage near the center of gravity.

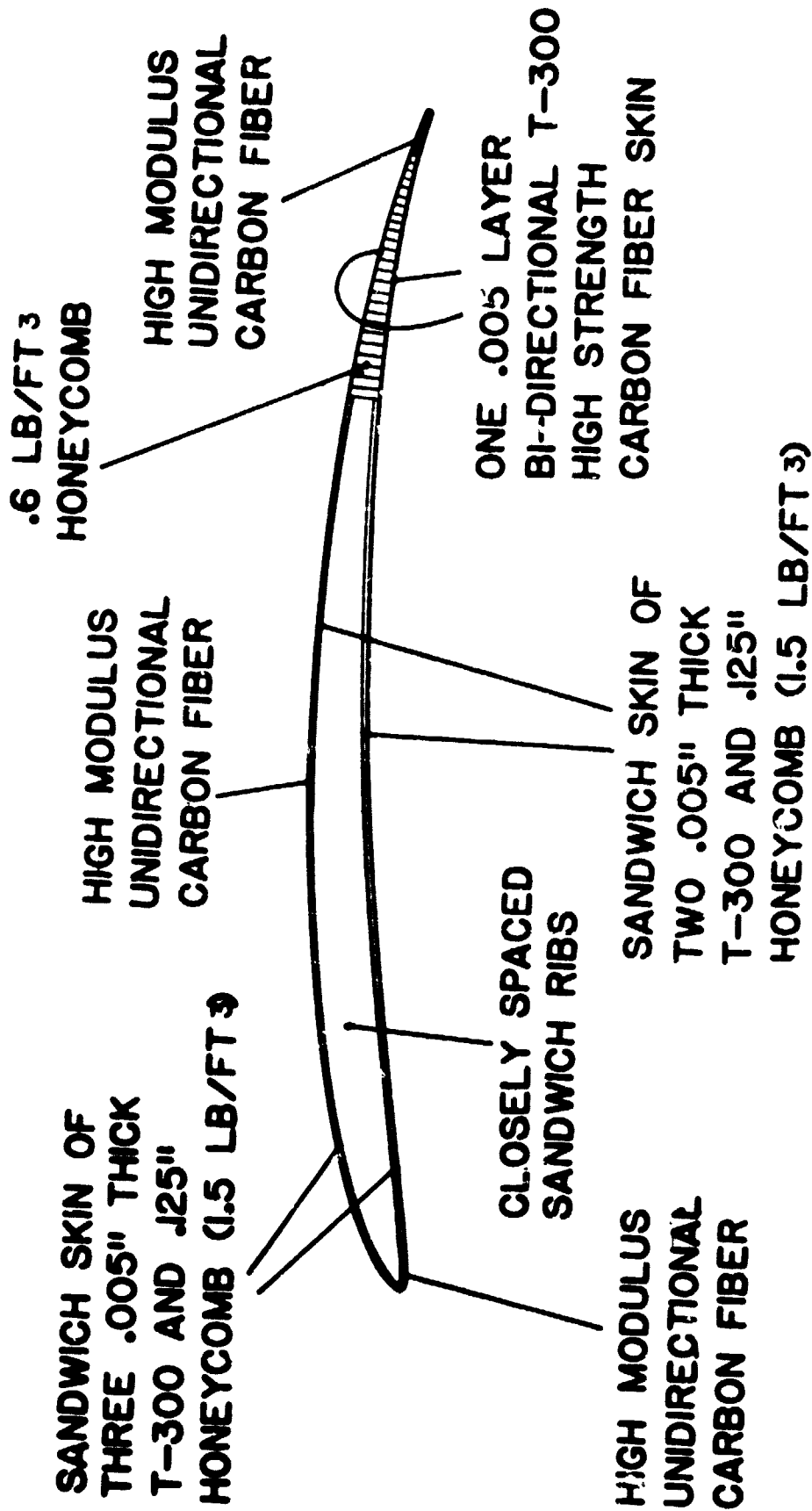
The low descent speed at the very low density at 7.5 km altitude (dynamic pressure 15 N/m^2) make the forces on the airplane very small during deployment (approximately 30% of their values in a 1 g cruise). This fact is important if lightweight deployment system and docile airplane movement during deployment are to be achieved (the stowed geometry creates asymmetric loads during deployment resulting in a slow rotation of the airplane which is damped before the airplane is released from the descent parachute.

Deployment of all airplane segments is almost simultaneous (some sequencing is required for clearance considerations), the propeller is deployed and locked at a minimum pitch angle to create maximum drag during the dive recovery maneuver. The airplane is released after a complete "lock-in-deployed position" signal is received from all 11 structural breaks.

Figure 32 shows the parameters of the recovery maneuver. The airplane dives vertically at maneuver initiation and pull-up is a constant lift coefficient ($C_L = 1.4$) maneuver. The maximum

TYPICAL WING STRUCTURE

FIGURE (31)



WING WEIGHS 70 % OF TOTAL STRUCTURAL WEIGHT

ORIGINAL PAGE IS
OF POOR QUALITY

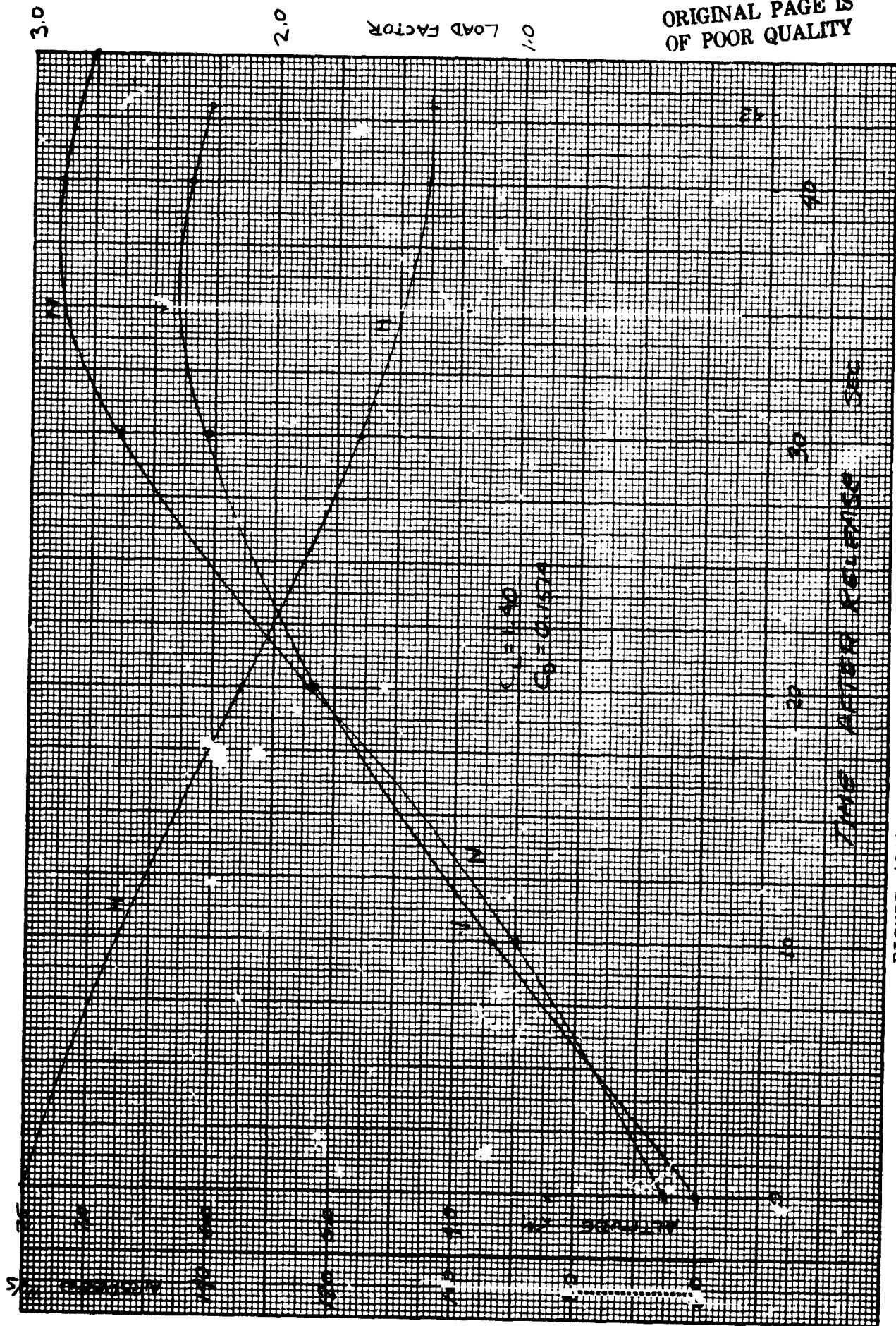


FIGURE (32) DIVE RECOVERY FROM 7.5 KM DEPLOYMENT

load factor is 2.9 and the maximum speed is 146 m/sec at 4.4 km (dynamic pressure of 117 N/m^2). The minimum altitude during the maneuver is 4.25 km but the airplane overspeed may be used to carry it to 5.7 km at cruise speed of 105 m/sec.

If mission requirement calls for deployment over surface higher than the 4 km minimum recovery altitude, the deployment of the airplane may be performed at higher altitude (assuming the same parachute size and same deployment dynamic pressure but parachute deployment speed may have to be changed). Figure 33 shows the parameters of the recovery in an 11 km 70 m/sec deployment, the minimum altitude being 6.8 km.

In this study of the descent system, Martin Marietta recommended the attachment of the airplane to the basecover as being an overall superior concept to the support on the aeroshell. The latter being potentially lighter, it is DSI's strong recommendation to pursue the concept of the aeroshell supported airplane unless the design problems cannot be satisfactorily solved and become development risks.

As mentioned in section 1.1, the descent system includes a small number of system components (rocket system, communication antenna and radar altimeter antenna). All other system functions needed for the descent phase (flight control, communication, computer, power supply, etc.) are provided by the airplane itself. This concept results in a significant reduction in weight and cost (relative to a fully furnished aeroshell).

3.5 Payload

Section 1.3 describes some of the scientific payloads proposed for the Mars Airplane. DSI's report 14134 is a preliminary specification of the Airplane-Payload interface. Section 3.12 shows the payload/range capability of different airplane versions. Sections 3.7 - 3.10 describe payload related airplane systems (power supply, environmental control, flight control, navigation and communication). All of these systems are con-

ORIGINAL PAGE IS
OF POOR QUALITY

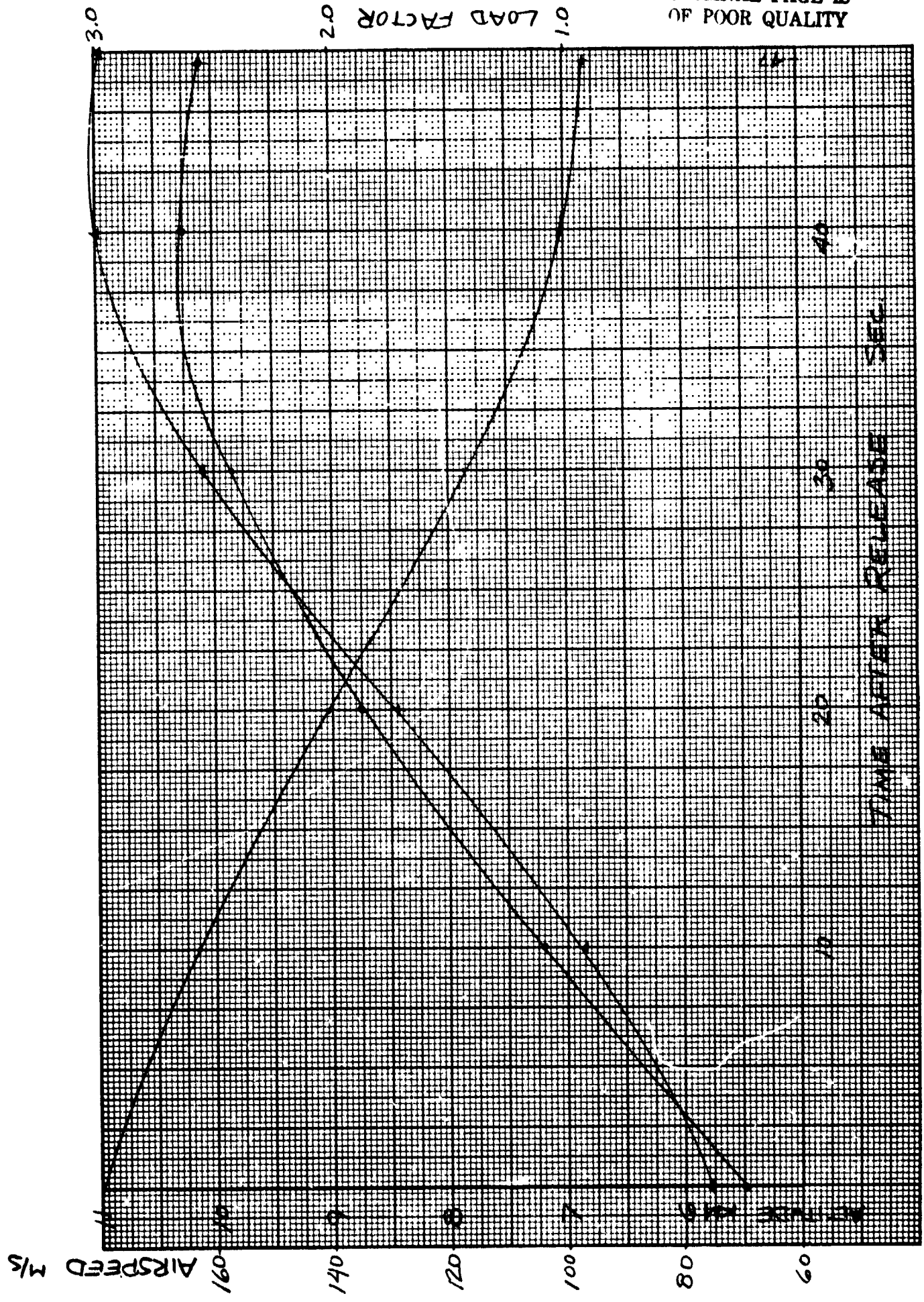


FIGURE (33) DIVE RECOVERY FROM 11 KM DEPLOYMENT

sidered as airplane systems (in weight and volume). But, any special payload requirements (power conditioning, environmental control of deployed payload, etc.) are considered as payload systems. The imaging system weight is added to the payload package weight, but the imaging system is considered an airplane system, it will be installed on all airplane versions (even though it is not essential for operating or navigating the airplane).

3.6 Lander Version

The Lander version of the Mars Airplane is basically a cruiser with added systems:

1. Rocket system for take-off and landing (see section 2.4).
2. Landing gear (see section 2.4)
3. Landing site selection capability.
4. Retractable propeller.
5. Solar-electric power system (see section 3.7).
6. Improved environmental control system (see section 3.8).

The communication delay makes it impossible to use man-in-the-loop real time landing site selection. The Lander site selection includes 2 modes:

1. Straight-in mode
2. Fly-back mode

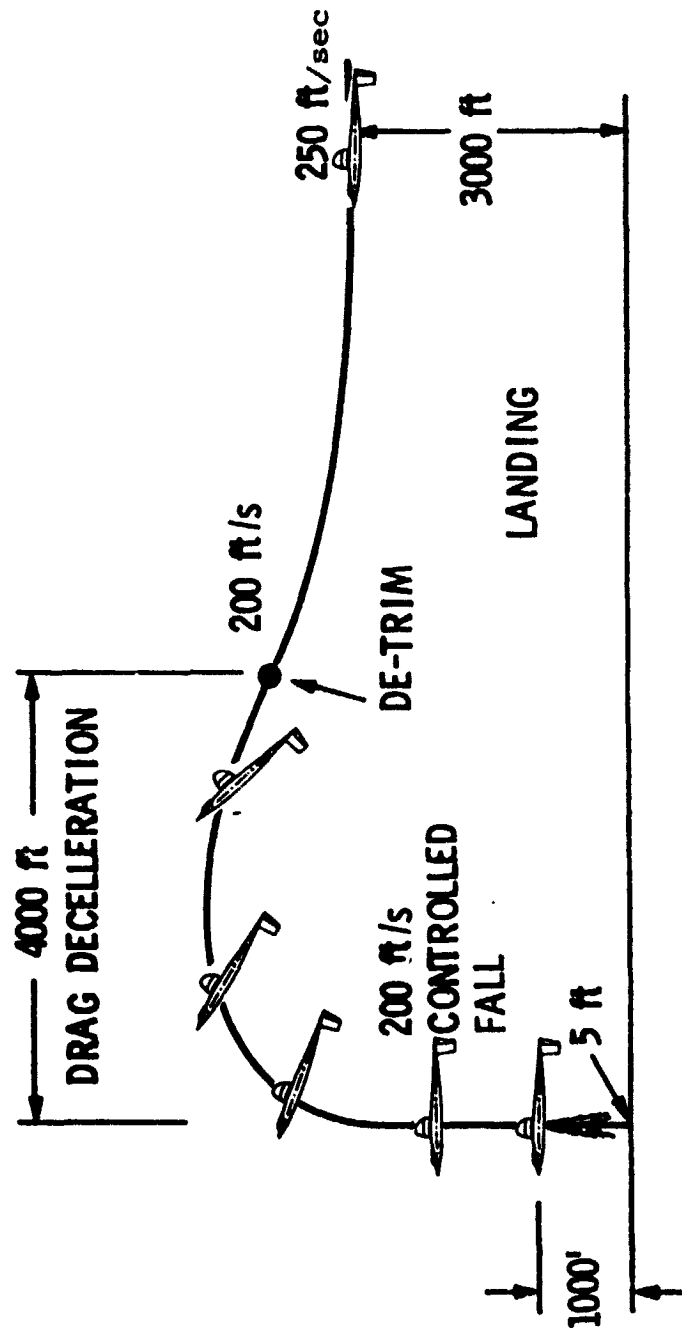
Both modes use the automatic site selection capability of the Lander. This system uses the imaging system and an added image processing capability to navigate the Lander to the point of minimum contrast in a given area. This system was proposed by Martin-Marietta for the Viking Lander. It was demonstrated by simulation to repeatedly choose the flattest point on photographs of different terrain.

In the straight-in mode, the Lander is commanded to land on a given site. This command is based on previous surveillance data (either orbiter or other airplane missions). The command includes site location and maximum distance authority. The Lander navigates accurately to the site (see section 3.10). Flying at 1 km altitude above terrain and using the required focal length on its imaging system zoom lens (the format covers the required search area consistent with the maximum distance authority), the site selection system chooses the landing point. The stabilized imaging system is locked on the chosen point and the Lander is automatically flown on a path to overfly this point. At a distance of 1.5 km from the landing point the Lander performs a power-off pull-up to reduce speed (Figure 34) and then detrim to a deep stall condition that brings the Lander to a vertical descent over the selected point at an average speed of 60 m/sec (depends on landing weight). The flight control system uses data from the radar altimeter and radar doppler to control the rocket system to bring the Lander to a landing at chosen point at 1-2 m/sec vertical speed and negligible ground speed.

The deep stall flying mode is shown to be very stable on configurations like this of the Mars airplane, it was used for the last 3 decades as the standard mode of retrieval-descent of free flight model in updraft currents. NASA Langley has recently investigated the deep stall mode as a way of descent to safety of light airplanes in emergency situations (engine cut, complete disorientation in zero visibility, etc.). Using radio controlled scale models of light aircraft, it has proven the deep stall mode to be a very stable descent in all control combinations.

In the vertical rocket controlled descent, the aerodynamics of Lander have very little significance and the landing is from all aspects identical to the landing of a spacecraft in the way it was performed on previous landers.

In the fly-back mode the Airplane is earth commanded to fly-back and land on a point it overflew 7-15 minutes prior to the com-



VERTICAL LANDING

FIGURE (34)

mand. The Airplane uses the site-selection system to land at the "smoothest" point near the target (within the specified maximum deviation authority).

Figure 35 shows the take-off maneuver. The airplane lifts vertically to 1 km altitude. During this phase the speed is kept to 30 m/sec (very low aerodynamic forces). The airplane then dives for speed and performs a gentle pull-out maneuver. The flight control system accurately controls the flight path throughout the maneuver and the airplane flies at 300 m at cruise speed.

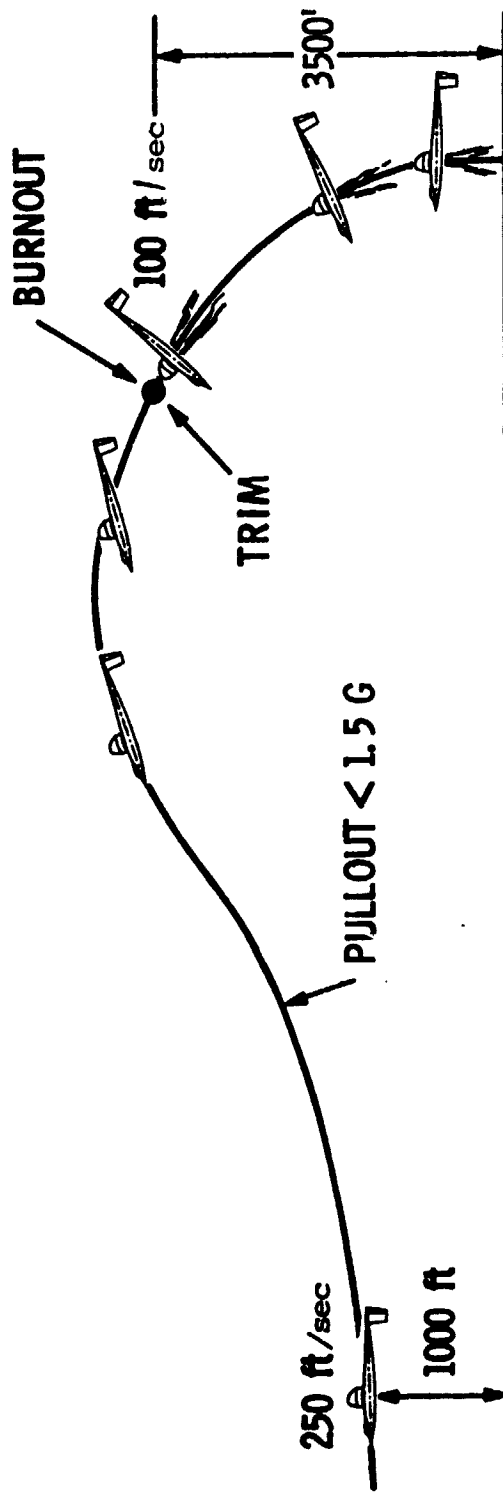
The propeller on the Lander version is stopped at the horizontal position and the blades are retracted along the fuselage to avoid limitation of the field of view of the imaging system.

Peter Lissaman of Aerovironment, Inc. performed the calculations of the Lander blow-over by surface winds. His findings are that with the landing gear configuration described (see section 2.4) the blow-over speed (from any direction) is very near cruise speed (approximately 60 m/sec for the minimum weight Hydrazine powered Lander, and 80 m/sec for the electric powered Lander. These are relatively high values and to Viking findings are not expected to occur on the surface of Mars. Figure 36 shows the surface wind speed for blow-over of a 150 kg Lander (minimum weight of a Hydrazine powered Lander).

3.7 Secondary Power

Inflight, the electrical power is supplied by an engine driven alternator on the Hydrazine powered cruiser and either by a separate 28 volt primary battery or by the main primary battery on the electrical powered cruiser.

The Lander version uses a solar cell array and a Lithium rechargeable battery to power the payload, communication and environmental control systems. The solar cell array covers the two wing panels just outboard of the center section, the 5 m² area gives a peak power of 300 W and an estimated daily average of 100 W. This power is adequate for the operation of the payload and for several hours of data transmission daily. But, it is too low for payload



VERTICAL TAKEOFF

FIGURE (35)

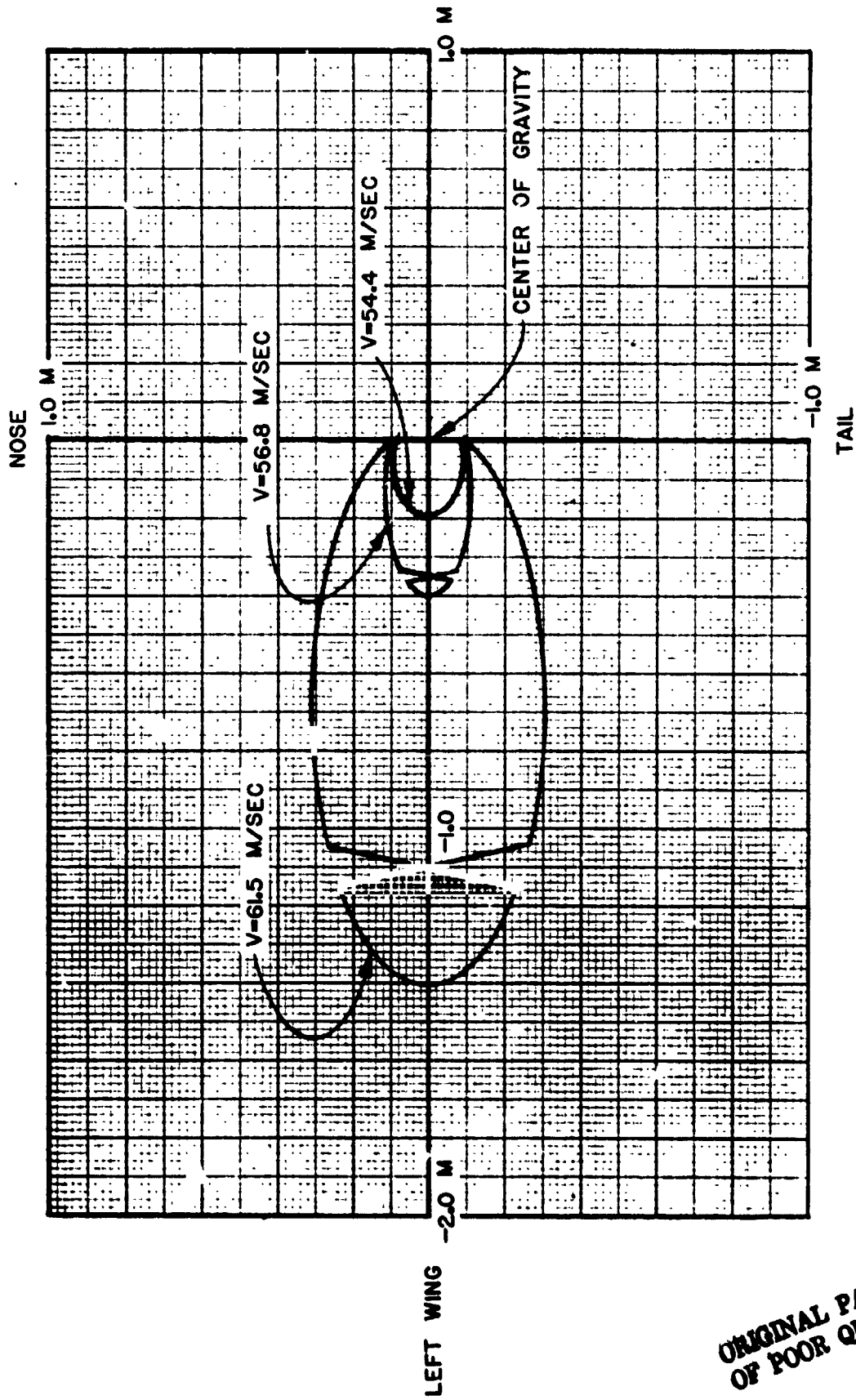


FIGURE (36) SURFACE WIND SPEED FOR BLOW OVER OF 150 KG LANDER

ORIGINAL PAGE IS
OF POOR QUALITY

temperature control unless good thermal insulation and heating during the day are carefully used (see section 3.8).

The power supply will be a basic 28 V (varies between 26-30 V). Any power conditioning required for the payload will be considered as payload (in volume and weight).

Some important factors in determining the secondary battery weight are the required life, the requirement (if any) for data transmission during the night and the temperature limits of the payload. Some additional study is required before a payload interface for landed experiment is defined.

3.8 Thermal Control

Atmospheric temperature near the surface of Mars ranges from 150°K to 270°K depending on location, season and time of day. These temperatures pose little problem for the cruiser as the low temperatures will ease its main thermal control problem, powerplant cooling. In the Hydrazine powered airplane, engine oil is cooled by a Hydrazine and "air" heat exchangers. Through variation of the amount of oil flowing through the Hydrazine heat exchanger, the Hydrazine temperature is kept within working limits (Hydrazine freezes at 2°C). The electrical powerplant is forced "aircooled". The flow cools the solid state inverter first, then the motor and the gearbox is cooled last.

Payload thermal control during cruise has not been defined as it is determined by payload temperature limits which are still to be determined. On the cruiser, efficient thermal insulation (2.5 cm thick foam in the sandwich construction payload bay walls), controlled aircooling and the payload power (200 - 300 W) are used to keep the temperature within the required limits (say $\pm 5^\circ\text{C}$).

A more demanding problem is the thermal control of the Lander, for long periods, on the surface of Mars. This problem will be studied as part of the integration of the science landed experiments. It is envisioned that efficient insulation and payload power (estimated at 100 W average daily) will be adequate to keep the temperature above the minimum level through the night.

Forced aircooling will be used to cool the payload during the day (especially during data transmission). Payload deployed to the surface should be either qualified to operate in the full temperature range on Mars or insulated so that available power would keep it within its operating temperature range. The big payload bay door (more than .5 x 1 m in the existing design) will be normally closed save of short periods of payload deployment, sample collection or other operations (drilling, etc.).

3.9 Navigation, Guidance and Control

The study of the navigation, guidance and control of the airplane was performed by Lear Siegler, Astronics Division as a sub-contract to DSI. The study was headed by Richard Lewis.

The complete study report appears in Appendix B. The Mars airplane mission presents some challenges in this area which are different than operating a remotely piloted airplane on earth (navigation on Mars with no magnetic field, over-fly and land accurately on pin-point scientific targets whose positions are known within ± 5 km accuracy, etc.).

The proposed system does not require an advance in the state-of-the-art to achieve the required performance (see Appendix B for details).

3.10 Communications

The principal means of communication from the airplane to Earth is via the Comsat, which is in a 1 sol (24 hr 37 min), 28° inclined, circular synchronous orbit. A system block diagram for the airplane-Comsat link is shown in Figure 37. The airplane carries a NASA standard S-Band transponder which drives a 20 W solid state transmitter. Airplane transmission frequency is in the 2290-2300 Mhz band and receive frequency is in the 2110-2120 Mhz band. The transmitter outputs to a 26 db electronically steerable planar array imbedded in the top of the central wing panel. A microcomputer programs an acquisition sequence which varies the peak reception

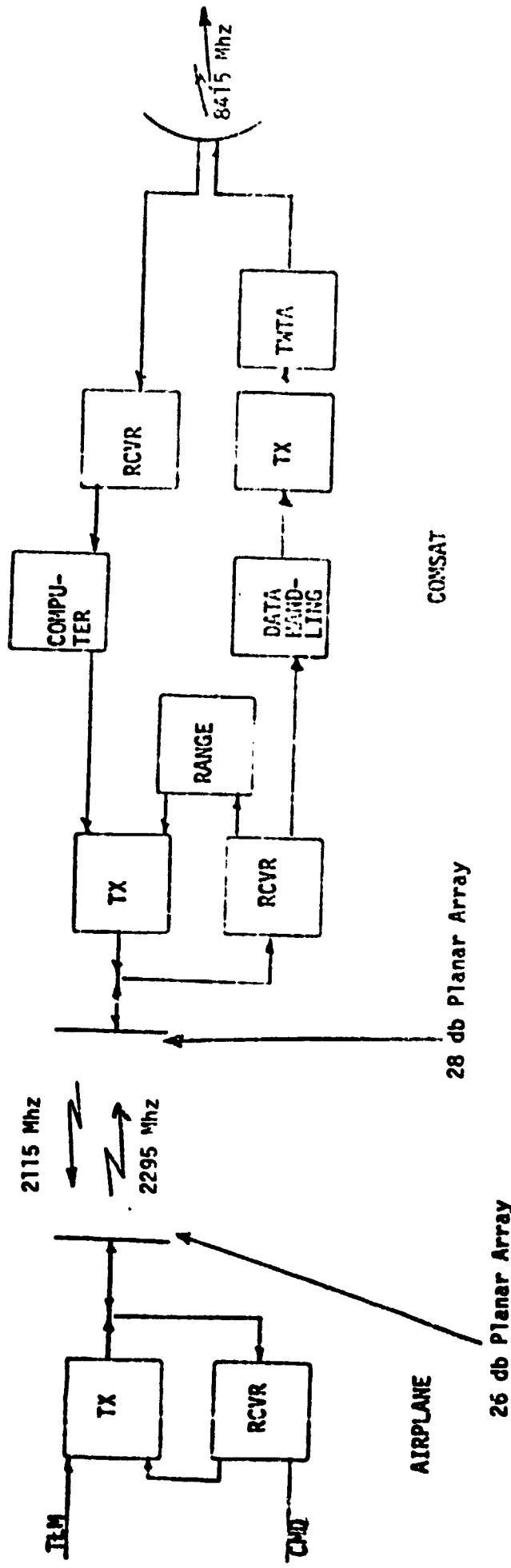


FIGURE (37) AIRPLANE/COMSAT COMMUNICATION SYSTEM BLOCK DIAGRAM

ORIGINAL PAGE IS
OF POOR QUALITY

direction of the array until the downlink signal from the Comsat is acquired. The airplane coherently retransmits the received signal until two-way lock is achieved. As the airplane moves or changes attitude orientation, signals from the airplane's inertial navigation system are fed to the antenna steering microcomputer to maintain peak gain. Once in two-way lock, ranging pulses are transmitted to the plane, returned to Comsat, and measured in a range machine aboard the Comsat. Doppler, a measure of plane-Comsat line-of-sight speed, is also measured.

The Comsat receives the airplane's S-band signal on a 28 db planar array mounted so that its peak broadside gain direction is along the nadir. The plane will always be within $\pm 10^\circ$ of the nadir direction. The Comsat transmits S-band to the plane via a 14 db horn as was flown on Mariner 9. Maximum data rate from plane to Comsat is 5.12×10^6 bps. Downlink data rate for command is 125 bps. Data received from the plane is immediately retransmitted to Earth via a 16 foot furlable X-band antenna powered by a 42 watt TWTA. When the Comsat is occulted by Mars from the Earth for 80 minutes each sol, transmission from plane to Comsat is limited to 20 kbps and the data is recorded on one of two NASA standard 4.5×10^8 bit tape recorders aboard the Comsat for later replay.

The airplane may also transmit directly to Earth via its S-band transmitter, but data rate is drastically reduced to about 20 kbps. The airplane also carries a UHF receiver and transmitter for relay communications during entry. Transmission is via a 42 cm x 42 cm planar element mounted atop the central wing section, or via a UHF omni antenna mounted on the entry capsule. UHF communication is only possible between airplane and Comsat. Total mass of all communication elements are given in Table I for the airplane.

TABLE I
AIRPLANE COMMUNICATION MASS

<u>ITEM</u>	<u>MASS (kg)</u>
S-band transponder	2.9

20 W S-band Transmitter	2.2
2 Telemetry Modulation Units	4.4
UHF Receiver	2.0
20 W UHF Transmitter	2.2
UHF Command Detector	0.5
UHF Antenna	1.0
S-band Low Gain Antenna	0.5
S-band High Gain Antenna	2.0
S-band Diplexer	0.5
Cabling	<u>1.0</u>
Total	19.2

3.11 Weight and Center of Gravity

Figure 38 shows the weight breakdown of the airplane in its four versions. The airframe weight is based on the preliminary design of the wing and tail structure and the measured weight of fuselage main section (fabricated of Kevlar 49 instead of carbon fibers in the operational airplane). The Hydrazine powerplant weight is based on the estimate of Dale Reed of NASA Dryden for the 15 HP version of the engine. The weight of the electrical powerplant is based on Sunstrand's estimates of their proposed powerplant. Propeller and engine cooling weights are based on the preliminary design of these systems. The avionics system weight is based on the Lear Siegler study (see section 3.8), and the weight of the communication system is based on the system described in section 3.10.

The weight estimates are the best we can state at this stage. A substantial weight saving is possible if advanced structural materials are used for the packaging of the avionics and the payload. But, a more indepth study is required before a realistic figure of weight saving could be stated and it is better if this potential weight allocation is credited towards a required contingency weight.

The efficient design of the airplane makes it a high payload/fuel weight fraction. This gives it a good payload/range

FIGURE (38)

WEIGHT BREAKDOWN (KG)

	<u>CRUISER</u>		<u>LANDER</u>	
	<u>HYDRAZ ENGINE</u>	<u>ELECTRIC ENGINE</u>	<u>HYDRAZ ENGINE</u>	<u>ELECTRIC ENGINE</u>
AIRFRAME	50	50	50	50
POWERPLANT AND FUEL SYSTEM	13	20	13	20
SOLAR CELLS AND RECHARGEABLE BATTERY	0	0	8	8
LANDING SYSTEM	0	0	27	27
NAVIGATION, GUIDANCE, MISSION COMPUTER AND FLIGHT CONTROL	30	30	30	30
MISCELLANEOUS SYSTEMS (COMMUNICATION, ANTENNA, ENVIROMENTAL CONTROL, ETC.)	20	20	20	20
	<hr/>	<hr/>	<hr/>	<hr/>
SUBTOTAL	113	120	148	155
PAYLOAD	40-100	40-100	40-100	40-100
	<hr/>	<hr/>	<hr/>	<hr/>
DRY WEIGHT	153-213	160-220	188-248	195-255
FUEL	147-87	0	112-52	50-20
BATTERIES	0	140-80	0	85-25
	<hr/>	<hr/>	<hr/>	<hr/>
ALL UP WEIGHT	300	300	300	300

capability, but may raise severe center of gravity problems if this is not carefully solved in the configuration definition phase. The concept adopted in the airplane design is that both payload center of gravity and fuel (or battery) center of gravity are very close to the total airplane center of gravity, so that all combinations of payload and fuel (within weight limitations) may be adopted with no changes in system installations. The powerplant and avionics "balance" the weight of the tail so that the empty airplane's center of gravity is in the range required for stability and control (at approximately 50% of wing chord).

3.12 Performance

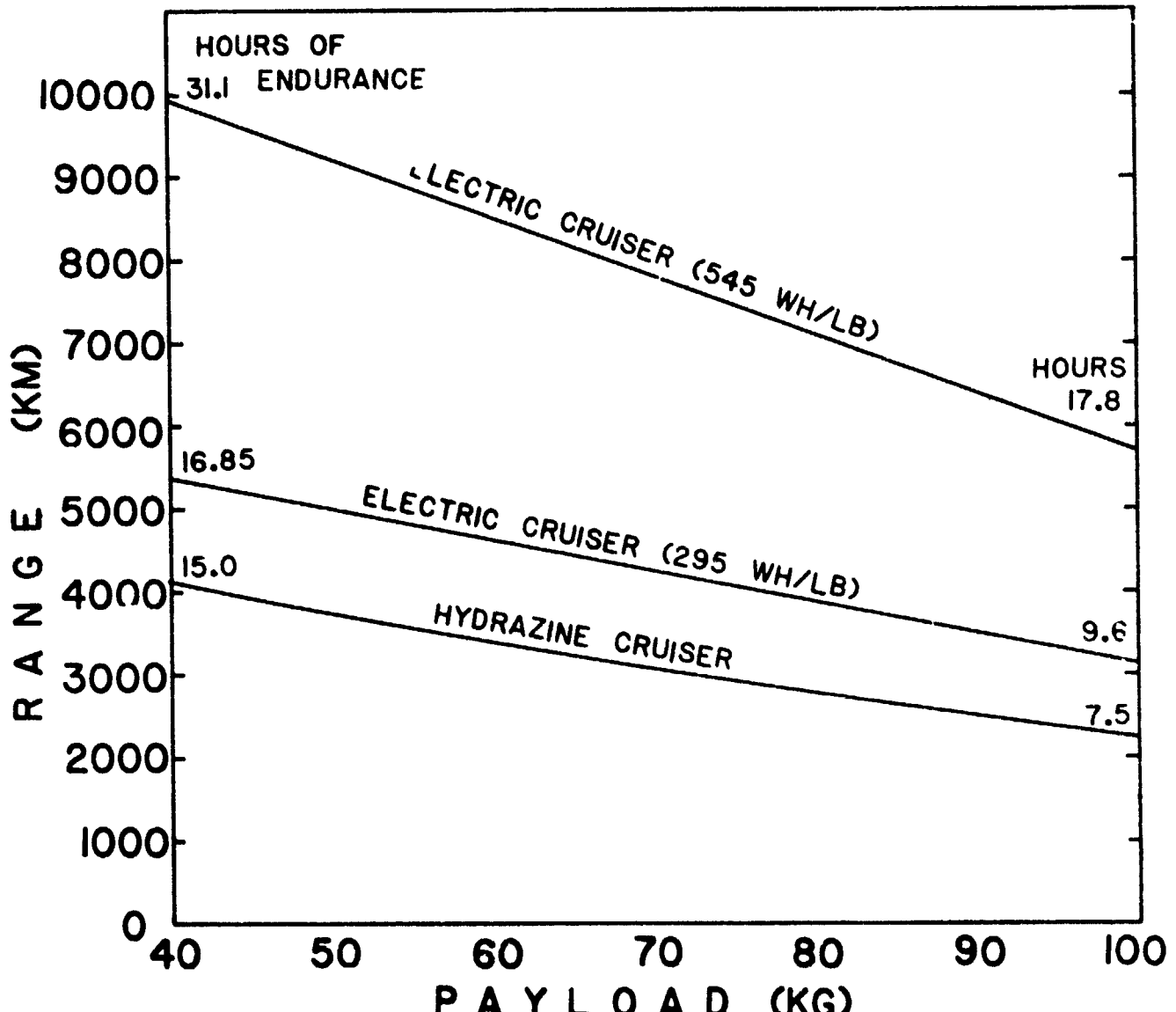
Figure 39 shows the cruise range and endurance of the cruiser in three versions (Hydrazine powered and electric powered with two battery energy densities). Range and endurance of the Lander are reduced with number of landings. For example, the electrical powered cruiser with 545 Wh/lb battery and 40 kg payload has 10,000 km range and 31 hours endurance, the range of the Lander in similar conditions is 6000 km for one soft landing and 4000 km for one intermediate stop and one final soft landing (the endurance is reduced to 19 hours and 12.5 hours respectively).

Figure 40 shows the climb performance of the Hydrazine powered airplane. The maximum rate of climb is 2500 ft/min (similar to that of turboprop powered airplanes on earth). The high altitude capability is good, ceiling is 10-15 km depending on weight, this performance is impressive if we remember that the density at 15 km above Mars is similar to the air density at 130,000 ft on earth.

Even though the rate of climb of the airplane is adequate for high altitude sounding (for meteorological measurements, climb out of a canyon, etc.), the angle of climb and angle of glide may prove too shallow for good terrain following flight (required for optimal altitude above terrain for best sensor resolution and area coverage). The average lift/drag ratio of 25 gives a glide angle of 2.3° and the climb angle at 225 kg at 2 km is 5.7° .

FIGURE (39)

CRUISE PERFORMANCE



AUW	300 KG	PROP EFFICIENCY	.85
WING SPAN	21 M	HYDRAZINE ENGINE	
WING AREA	20 M ²	CRUISE SFC	4.85
CRUISE ALTITUDE	1 KM	ELEC. MOTOR EFFICIENCY	.85
LIFT/DRAG AT 300 KG	27.75	AUX. POWER CONSUMPTION	.4 KW

ORIGINAL PAGE IS
OF POOR QUALITY

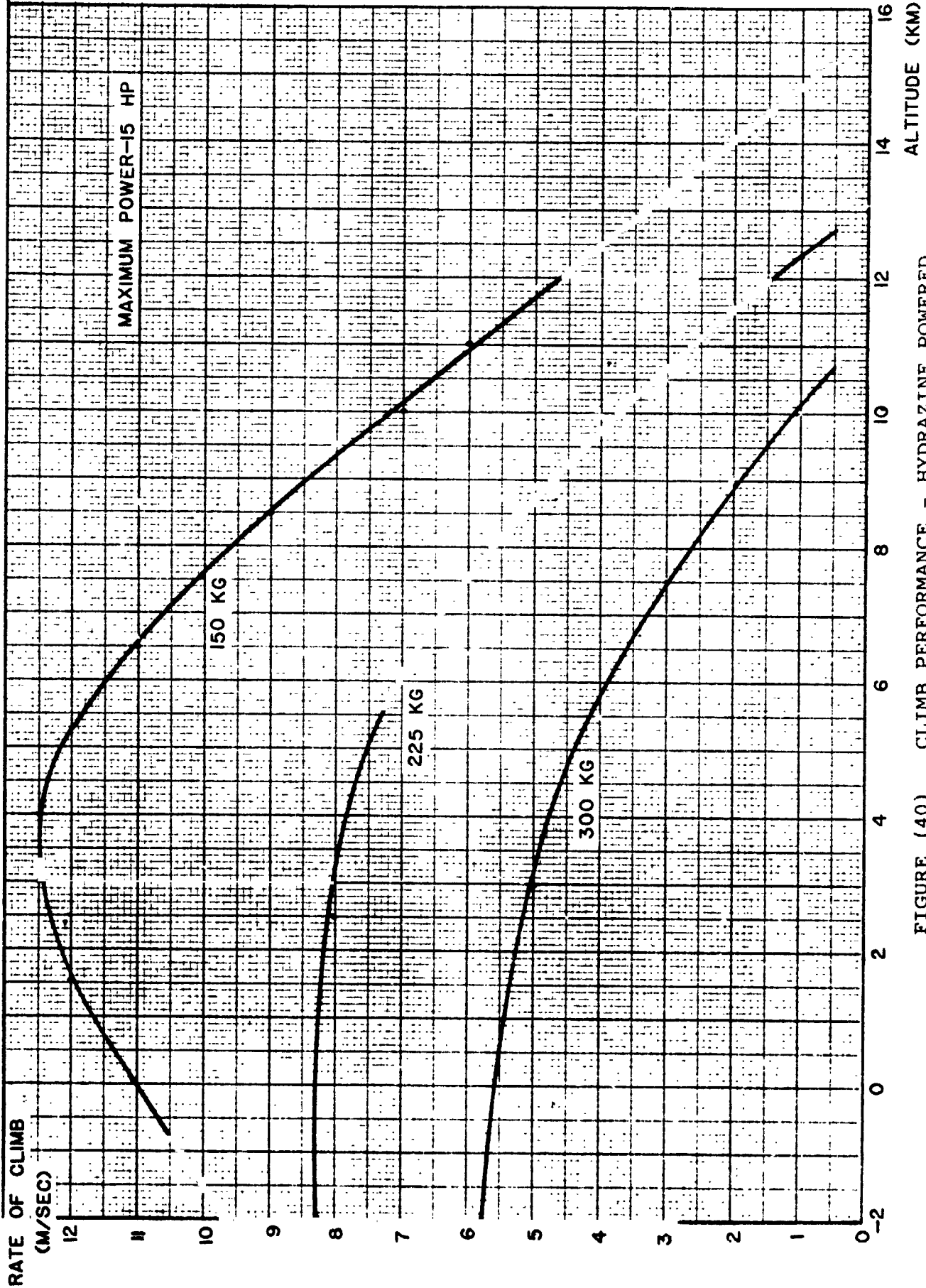


FIGURE (40) CLIMB PERFORMANCE - HYDRAZINE POWERED

Terrain following was carefully studied as it is felt that it is important for good payload performance. A good terrain following performance is obtained through "Energy Management" (e.g. increase of flying speed during steep glide and decrease of speed in steep climb), the combination of low density, low gravity and good aerodynamics of the airplane make this method an attractive one. The airplane cruises at 95 m/sec at 300 kg at 3 km altitude (nominal cruise lift coefficient $C_L = 1$) using energy management it has a 1.5 km "total altitude authority" by changing the flight speed between 83 m/sec and 134 m/sec (lift coefficient of 1.3 and .5 respectively). This 1.5 km capability covers most terrain following requirements with only small range penalty. Any higher altitude change required in a steep angle may be obtained by bigger change in speed (acceleration to a higher speed prior to a climb or during a dive) or by spiral sounding flight resulting in a bigger range penalty.

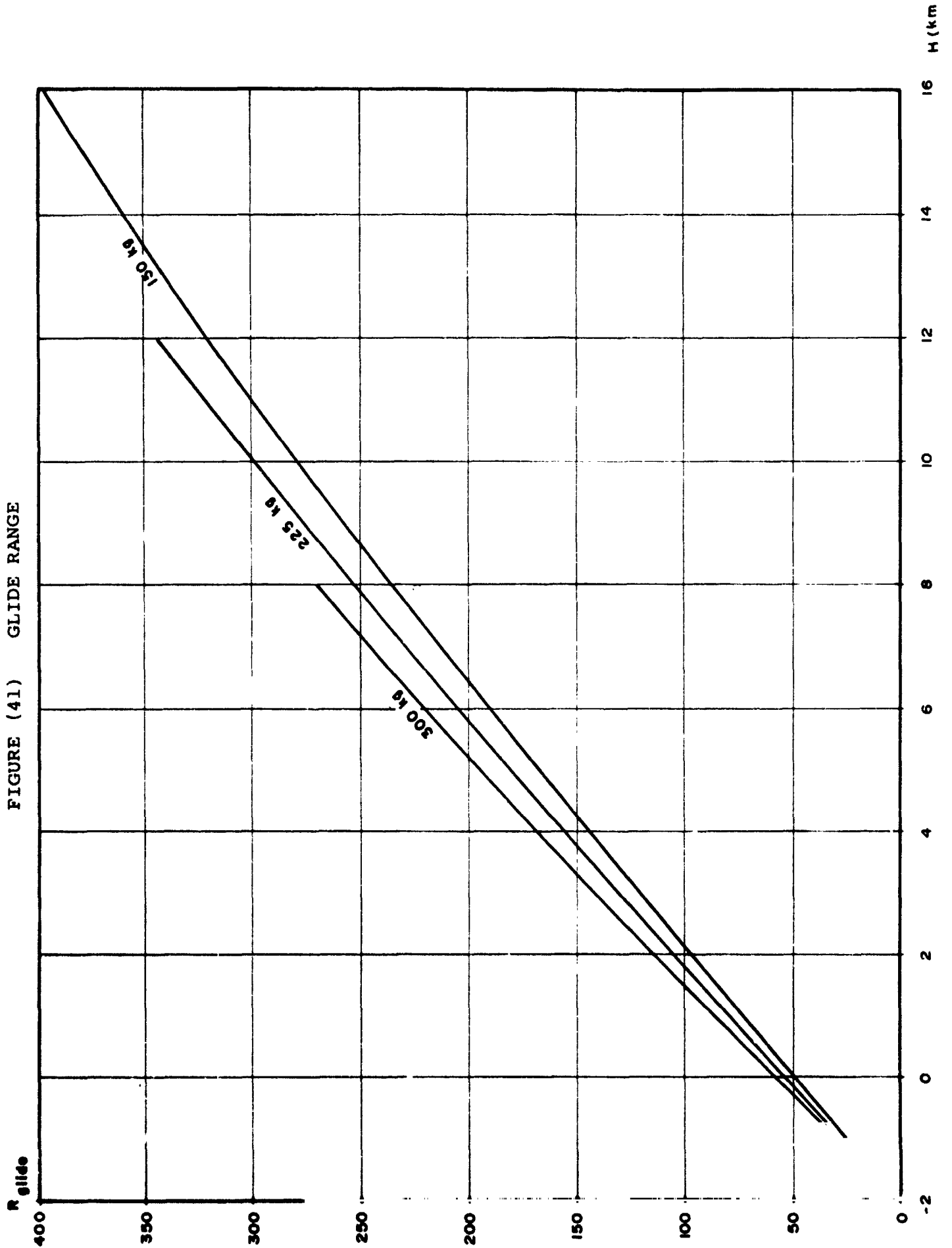
Figure 41 shows the glide range of the airplane. The nominal deployment of the airplane (300 kg at 7.5 km attaining cruise speed at 5.7 km) gives a 100-150 km glide range and 17-26 minutes endurance for cruise altitudes of 0-2 km.

3.13 Flight Testing

The Mars Airplane will be tested extensively in flight on earth. This test capability is very important for increasing the reliability of the airplane system at a reasonable cost. Development flight testing is the phase when most of the system malfunctions are discovered and corrected, final adjustment to the flight control system and optimization of propeller pitch angles are made, accurate performance figures are obtained, etc.

To simulate the flight on Mars (gravity only 37.7% of its value on earth) the airplane will be flown with decreased fuel (or battery) weight, payload weight (imaging system only) and avionics (lightweight communication system) for a total weight of 113 kg (simulating a 300 kg constant weight of an electric powered Mars Airplane).

FIGURE (41) GLIDE RANGE



The air densities at 103,000 - 130,000 ft is the same as at -2 km to + 15 km altitude on Mars. This gives the same dynamic pressure and practically the same Reynolds numbers as on Mars. The Mach numbers will not be accurately simulated because of the lower speed of sound on Mars. The use of higher propeller tip speed and higher cruise speeds may be used to check the airplane performance at the exact Mach numbers it will encounter on Mars.

The test sequence will include a balloon drop from high altitude, parachute descent, deployment, parachute release, dive, recovery, perform flight test (cruise, climb, dive, etc.), and descent for landing. The descent from cruise altitude to landing will be mostly in the deep-stall mode (see section 3.4) in order to speed the descent. A glide descent at maximum diving speed (200 N/m² dynamic pressure) from 105,000 ft will take 2 hours and 40 minutes, a deep stall descent will endure only 25 minutes and the dynamic pressure will be only 35 N/m², so that the deep stall mode appears to be a safer descent mode. The Airplane will be commanded to recover from the deep-stall mode at adequate altitude to make a conventional landing on the planned landing strip. The landing speed being 8 m/sec (15.5 kts) at sea level and the high glide ratio of the Airplane make a soft and safe landing possible.

The Airplane flight testing is to be performed at the NASA Dryden flight research center and the balloon drop system will be pretested with a Mini-Sniffer high altitude RPV.

4. RECOMMENDED CONFIGURATION

The recommended configuration for the Mars Airplane is the electric powered Cruiser/Lander. This recommendation is based on the following considerations:

- a. The superior performance of the electric powered Airplane (section 3.12).
- b. The higher expected reliability and lower development and qualification costs of the electric powerplant.
- c. The configuration design is such that the Lander version has very high commonality with the Cruiser version, so that a single Airplane will . . . developed with a relatively small separate development effort of an add-on Lander related system to be either incorporated in the proposed 1984 mission or more probably for use in sample collection role in a later MSR (1988 - 90).

APPENDIX A

AV FR8090

Final Report

**PROPELLER DESIGN AND
BLOWOVER CALCULATIONS FOR
THE MARS AIRPLANE**

Prepared for

Developmental Sciences Inc.
15747 East Valley Boulevard
City of Industry, California 91744

By

P.B.S. Lissaman and B. Hibbs

AeroVironment Inc.
145 Vista Avenue
Pasadena, California 91107

9 June 1978

TABLE OF CONTENTS

	<u>Page</u>
1. SUMMARY	1
2. PROPELLER DESIGNS	4
3. BLOWOVER FOOTPRINT CALCULATION	11

1. SUMMARY

The attached is an informal engineering report defining the propeller design, the performance characteristics, and blowover footprint for the Mars Airplane.

Propeller Design: The propeller layout was determined using a propeller design program developed at AeroVironment. This method uses standard blade element theory, incorporating both axial and tangential interference flows and the tip correction. The chord, twist and section aerodynamic properties are arbitrarily defined at five equidistant stations on the blade span. The program then prints out power coefficient and propeller efficiency for a range of advance ratios and pitch angle settings (β); from which power and efficiency curves may be plotted as a function of advance ratio for various pitch angles. In addition, local operating lift coefficients are printed out at each condition. These can be used to determine whether the stall limits of the section have been exceeded.

The propeller airfoil operates at a low Reynolds number ($\sim 50,000$) and the flight speed corresponds to a Mach Number of about 0.5 to 0.9 in the worst case. Thus conventional airfoils will not be suitable. A study of existing low Reynolds number airfoils was made. It is believed that a suitable airfoil will be thin (5.5%), of relatively large camber (5%), and will probably require artificially induced transition. For the final design, a representative performance was assumed, corresponding to an airfoil operating between the conditions of $C_L=0.5$, $C_D=.02$ and $C_L=1.1$, $C_D=.0265$. This appears to be an achievable performance compared with theoretical predictions of the Eppler 61 and 62 and airfoils actually tested by the designer. It is believed that while no existing airfoil has exactly these characteristics, one can be designed which will meet them.

Five propeller planforms were designed, constituting an iterative process directed towards tailoring the propeller for the given airframe, engine and atmosphere. Propeller V appears to be very well matched to the

task. It has a diameter of 4 m, tip chord of 0.5 m and twist of 25° . It is intended that this should be a variable pitch propeller, and a β range of 20° is required to meet design conditions. The propeller operates between 340 and 950 RPM, and has an efficiency of about 80% over the major operating range. Maximum power requirement is 11.55 KW (15 HP).

It is noted that the propeller performance is limited by a number of configurational and aerodynamic constraints. Diameter and blade number are restricted by requirements that the propeller blades fold, while the properties of the Martian atmosphere cause the airfoil to operate at high Mach Number and low Reynolds number.

Performance Characteristics: The aircraft performance curves at three different masses (150, 225, 300 kg) and at altitudes between -2 and 15 km are presented. A table showing performance limiting factors in various flight ranges is also provided. Characteristic performance for the aircraft with propeller V is as follows:

Aircraft Mass	Cruise Power at 4 km		Ceiling km	Max. Climb Rate m/s
	KW	HP		
Light (150 kg)	2.5	3.25	15.5	12.5
Heavy (300 kg)	5	6.5	11	5.0

Blowover Footprint: A study of the blowover characteristics of the aircraft was made. This involved calculating the aerodynamic forces for a horizontal wind of any orientation relative to the airframe. The intersection with the ground plane of the resultant of the aerodynamic force and the gravitational force was then computed, yielding a closed curve on the ground (called the blowover footprint) for each assumed wind dynamic pressure. This analysis does not require specification of the landing gear geometry, which the designer can arbitrarily select. Providing the envelope enclosing the landing gear contact points falls outside the blowover footprint, the aircraft will not be upset by horizontal winds. Blowover footprints were plotted for the aircraft horizontal case and also for the wings tilted at 3° to the horizontal.

It is found that, for the proposed landing gear configuration, for the horizontal case, blowover will not occur until wind speeds comparable to the flight speed are achieved. However, for the wing tilted 3° , blowover occurs at a q of about 19 N/m^2 , when the wind is blowing 45 degrees off the nose.

The general result of the blowover analysis is that if there is a small degree of tilt the aircraft is sensitive to quartering winds (blowing at 45° off the nose). However, stability up to a q of about 19 N/m^2 is obtained from an arrangement of landing gear with the lateral pads located in line with, or ahead of, the c.g. and about 2 meters either side of the vertical plane of symmetry and a pair of rear supports about the same distance apart and 1 meter or more behind the c.g. The above is not a proposed landing gear layout, only a description of a layout which would be suitable from blowover considerations. Obviously, the landing gear must meet other more important requirements. The footprint shown in this report will aid the designer for the blowover case.

C. 2

2. PROPELLER DESIGNS

Propeller design I was a false start that was made using improper assumptions. No more needs to be said of it.

Design II was made using a radius for the prop of 1.25 meters. The resulting propeller had such a large chord that it did not appear practical. This large chord was needed to produce sufficient thrust without having the blade tip become supersonic.

For propeller design III, radius 1.75 meters, the design parameters were chosen as follows. The tip Mach Number must never exceed 0.9, and for the aircraft at 300 kg and at an altitude of 7 km the propeller must be able to absorb all the output power of the engine without stalling or exceeding the tip Mach Number limitation. These requirements gave a first iteration chord and twist distribution for the prop, when constant loading was assumed. The chord for the inner sections of the prop was modified to provide for a transition to the hub, and the twist distribution was modified to counteract tip loss effects. The resulting propeller was found to be good for cruise, but not so good for climb. The main problem was that the prop would stall at a low thrust level. This level became lower as the plane flew slower, resulting in the paradox that the plane would climb slower when it was light than when it was heavy. The propeller was incapable of absorbing all of the engine output at these low flight speeds without stalling.

To overcome this problem, it was decided to analyze the prop at different collective pitch angles, and to see what the performance was like after the prop had stalled. From the results of this analysis, the best settings for the prop were found for both cruise and climb, while still staying below the tip Mach limit. The resulting performance was found to be more reasonable with the lighter plane having a greater rate of climb than the heavy one.

In an effort to improve the climb and cruise performance of the prop, another design was tried with a larger radius, but with the same absolute chord distribution and twist distribution. This prop showed climb and cruise performance superior to design III. The increase in performance is attributable to two effects. First, the larger prop has more area, and hence is less prone to stalling at any given thrust level. Second, the larger prop has lower axial and radial interference terms, which tend to increase the efficiency of the prop at any one operating point.

Up to this point a rather conservative estimate had been made as to the drag of the airfoil section to be used on the prop. The drag of the airfoil was assumed to increase rapidly as the lift coefficient varied from an optimum value. Although this does occur with low Reynolds number airfoils, it was found that this effect had been greatly overestimated. If all drag is removed, the total aerodynamic losses are cut in half or better. This gives up to 91% efficiency for the prop. Because of this it was decided to use the lift - drag polar of an Eppler section. The low Reynolds number Eppler sections can all have their polars approximated by a parabola. The magnitude of the drag increase with lift coefficient is about the same for all the Eppler sections, with the only difference being in the location of the minimum drag point and the angle of attack range for unstalled flow. For airfoils similar to the Eppler 62 and 63 sections, these parameters are determined by the airfoil camber and Reynolds number. The polar used for design V, is shown in Figure 2-1. Note that only C_L values between 0.5 and 1.1 are considered in the analysis.

The planform for design V was different from those used previously, in that the chord at the tip was increased and the chord at the inner areas was decreased. The resulting propeller data and planform are shown in Figure 2-2. The performance of this prop is shown in Figure 2-3. Note that the efficiency is almost always greater than 80% when the C_L is between 0.5 and 1.1. The climb and cruise performance of the prop is shown in Figure 2-4. The shape of the climb curve for the 150 kg aircraft is due to the inability of the propeller to absorb all the output power of the engine at low altitude. The propeller collective pitch angles and J's are shown in Tables 2-1 and 2-2, along with other data of interest.

ORIGINAL PAGE IS
OF POOR QUALITY

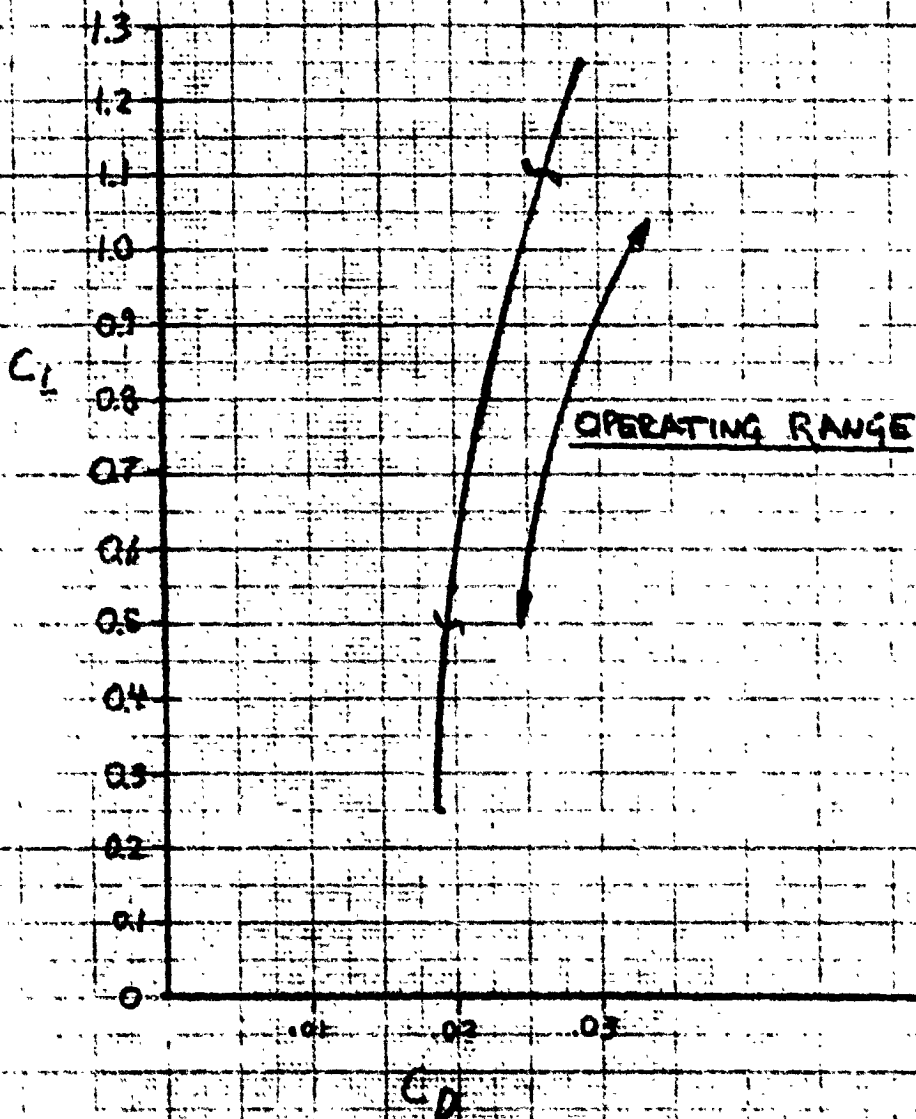


FIGURE 2-1

AIRFOIL POLAR: PROP V

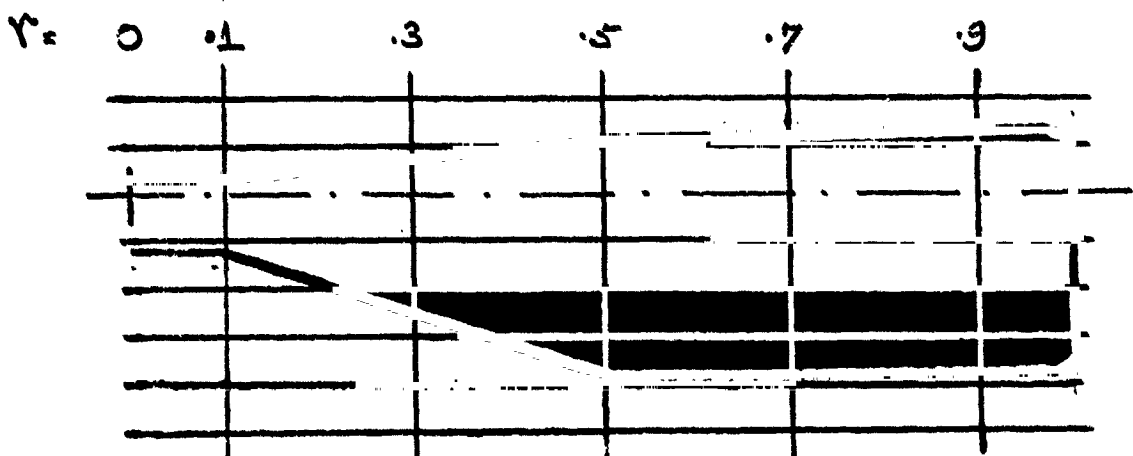
PROPELLER NO V DIAM. 4.0 M.

γ	c/R	β	α_0	C_{d0}	γ_{d0}	C_{D}	$\Delta C_{m_{ax}}$
.1	.08	82	0	.05	.01	0	0.85
.3	.17	72	-3	.03	.01	.15	0.85
.5	.25	63	-5	.019	.01	.25	0.85
.7	.25	57	-5	.017	.01	.25	0.85
.9	.25	57	-5	.019	.01	.25	0.85

DRAQ RISE MACH NO 0.9

CHORD R_c at 0.7R 50,000

NO OF BLADES 2



BLADE PLANFORM

FIGURE 2-2

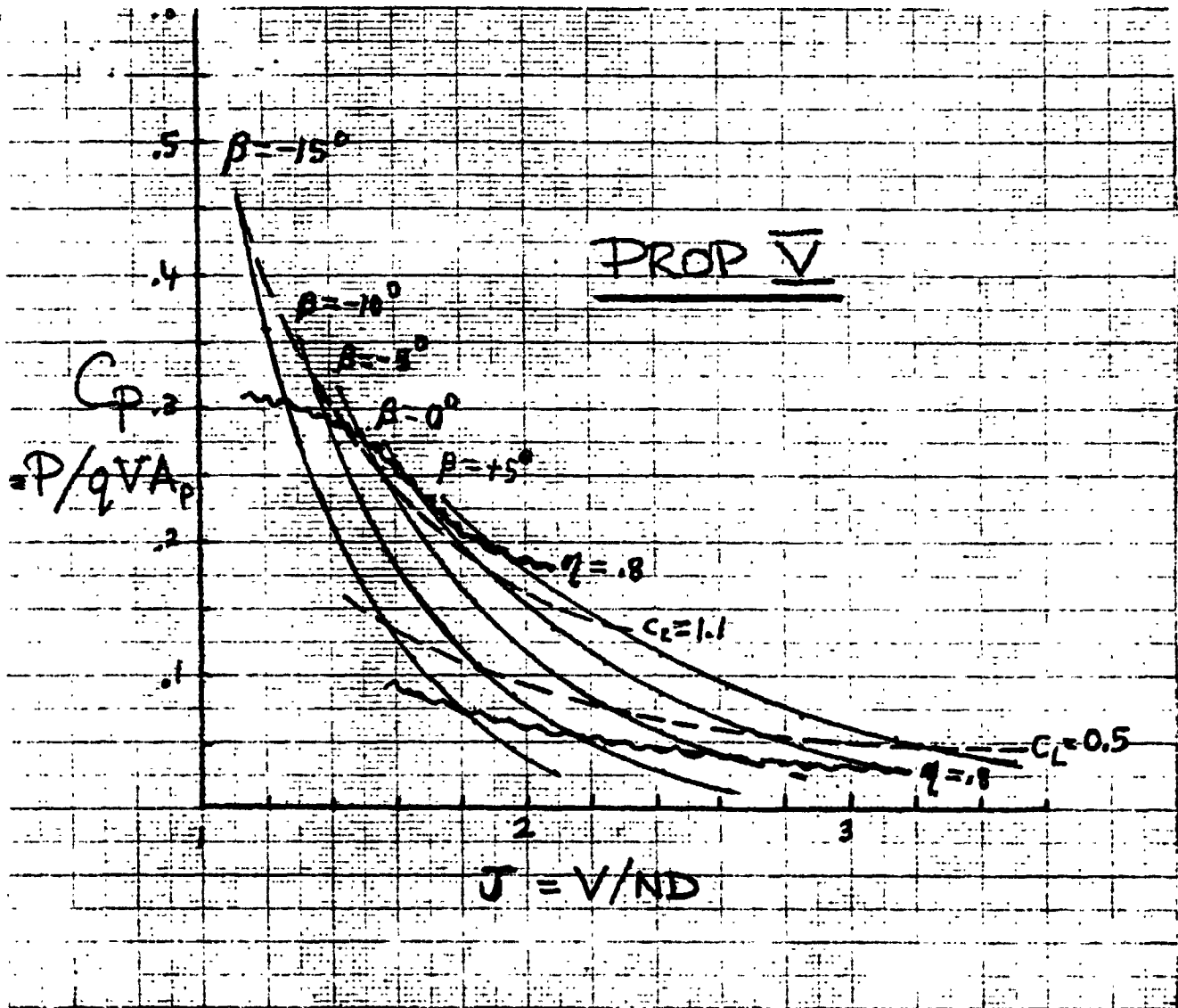


FIGURE 2-3
PROPELLER PERFORMANCE

ORIGINAL PAGE IS
OF POOR QUALITY

PROP V

ORIGINAL PAGE IS
OF POOR QUALITY

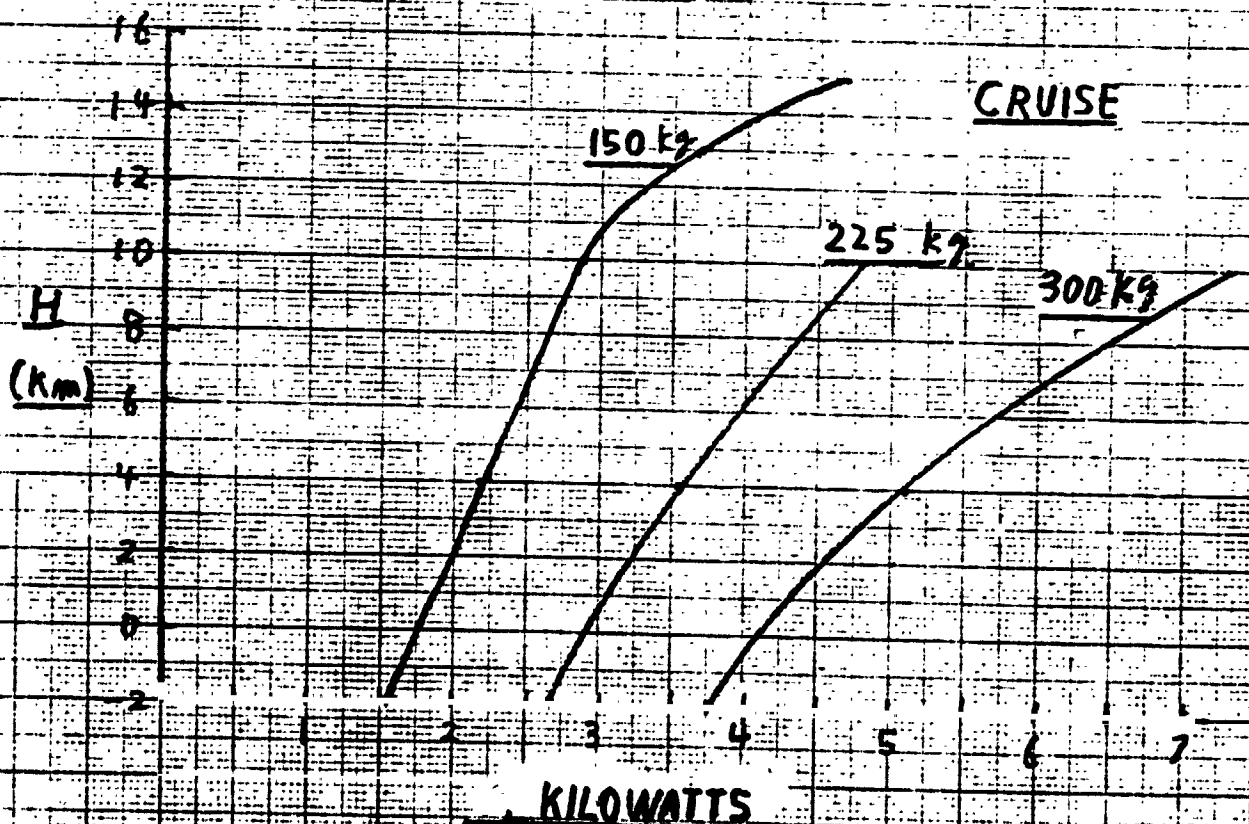
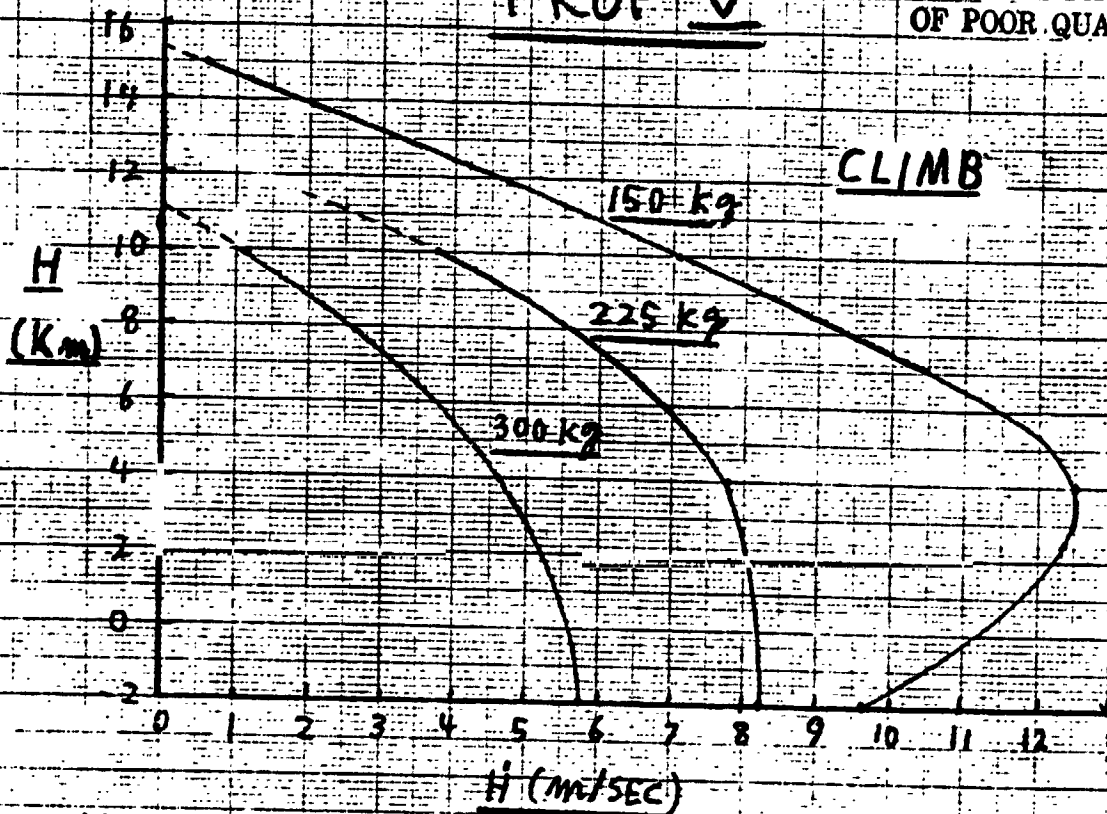


FIGURE 2-4

Design V

Table 2-1. Propeller settings and parameters for climb.

W(kg)	H (km)	β	J	Limit	C_p	C_T	η	$\dot{H}(m/s)$
300	-2	-15°	1.4	POWER	.2096	.175	.835	5.73
	4	-10°	1.78	POWER	.1744	.143	.806	4.60
	10	$+5^\circ$	2.54	C_L+MACH	.102	.0825	.805	1.30
	15	—	—	—	—	—	—	—
225	-2	-15°	1.26	POWER	.3116	.248	.796	8.22
	4	-10°	1.43	POWER	.2673	.222	.831	7.77
	10	0°	1.99	C_L+MACH	.153	.128	.837	3.73
	15	—	—	—	—	—	—	—
150	-2	-15°	1.12	C_L	.46	.352	.765	9.63
	4	-15°	1.19	POWER	.389	.300	.771	12.49
	10	-5°	1.56	C_L+MACH	.25	.210	.840	7.11
	15	$+5^\circ$	2.28	C_L+MACH	.135	.108	.800	0.59

TABLE 2-2. Propeller settings and parameters for cruise.

W(kg)	H(km)	β	J	C_p	C_T	η	P(watts)
300	-2	0	2.6	.068	.0573	.842	3747
	4	0	2.51	.077	.0644	.836	5100
	10	+5	2.74	.081	.0663	.819	7365
	15	—	—	—	—	—	—
225	-2	0	2.56	.071	.0601	.846	2634
	4	0	2.46	.082	.0695	.848	3544
	10	0	2.44	.085	.0716	.842	4772
	15	—	—	—	—	—	—
150	-2	0	2.47	.082	.0685	.835	1574
	4	0	2.54	.074	.0621	.839	2197
	10	0	2.38	.093	.0784	.843	2842
	15	0	2.20	.118	.0996	.844	4687

3. BLOWOVER FOOTPRINT CALCULATION

The forces acting on the aircraft when it is sitting on the ground are gravity and aerodynamic forces from the wind, as well as support reactions. Aerodynamic forces come from three main items: the wings, tail, and fuselage. For each of these items, there are six components: three forces and three moments. It can easily be shown that the moment about the vertical axis (the yawing moment) can be ignored for the blowover problem. Of the five remaining components, only a few are of sufficient magnitude to be of interest. These are the fuselage and tail side force, the wing lift, drag, and moment. Each of these forces or moments acts on or about a certain point in space. These forces and moments can be transformed to components about a common point, which was arbitrarily taken to be the c.g. of the aircraft. The resultant of the gravitational and aero forces and moments about the aircraft may now be found. The interaction of this resultant with the ground plane represents the point of application of the ground reaction. The locus of such points is made by varying the sideslip angle, β , at constant dynamic pressure. This gives the blowover footprint for the aircraft. If the footprint lies entirely within a polygon defined by the landing gear, the aircraft will not blow over.

The blowover footprint for the aircraft in a normal attitude is shown in Figure 3-1. Positive X is in the forward direction for the aircraft and the origin is directly below the c.g. Note that a q of 26.4 N/m^2 will not overturn the aircraft, even though the aircraft would be airborne if q reaches 28.3 N/m^2 .

The second footprint, Figure 3-2, shows what would happen if the aircraft landed with the wings tilted 3 degrees off of horizontal. In this attitude, a q of about 19.6 N/m^2 is needed for overturning.

ORIGINAL PAGE IS
OF POOR QUALITY

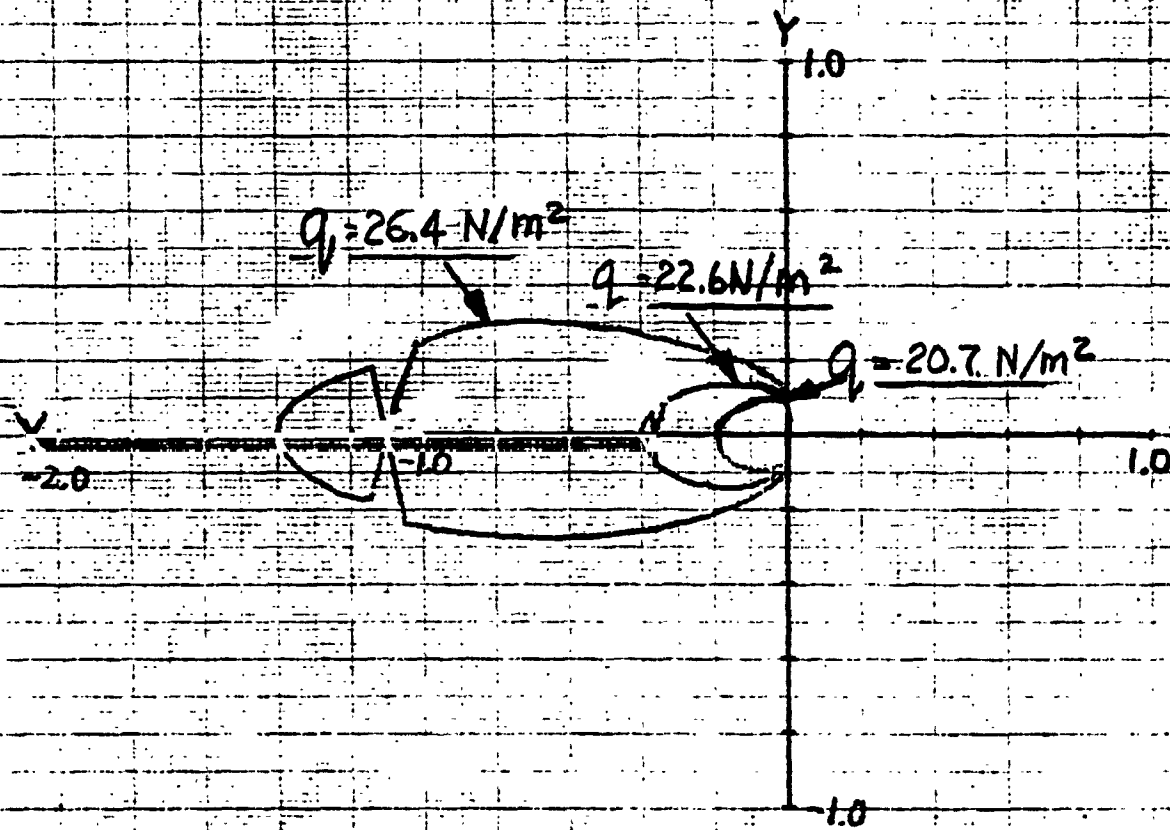
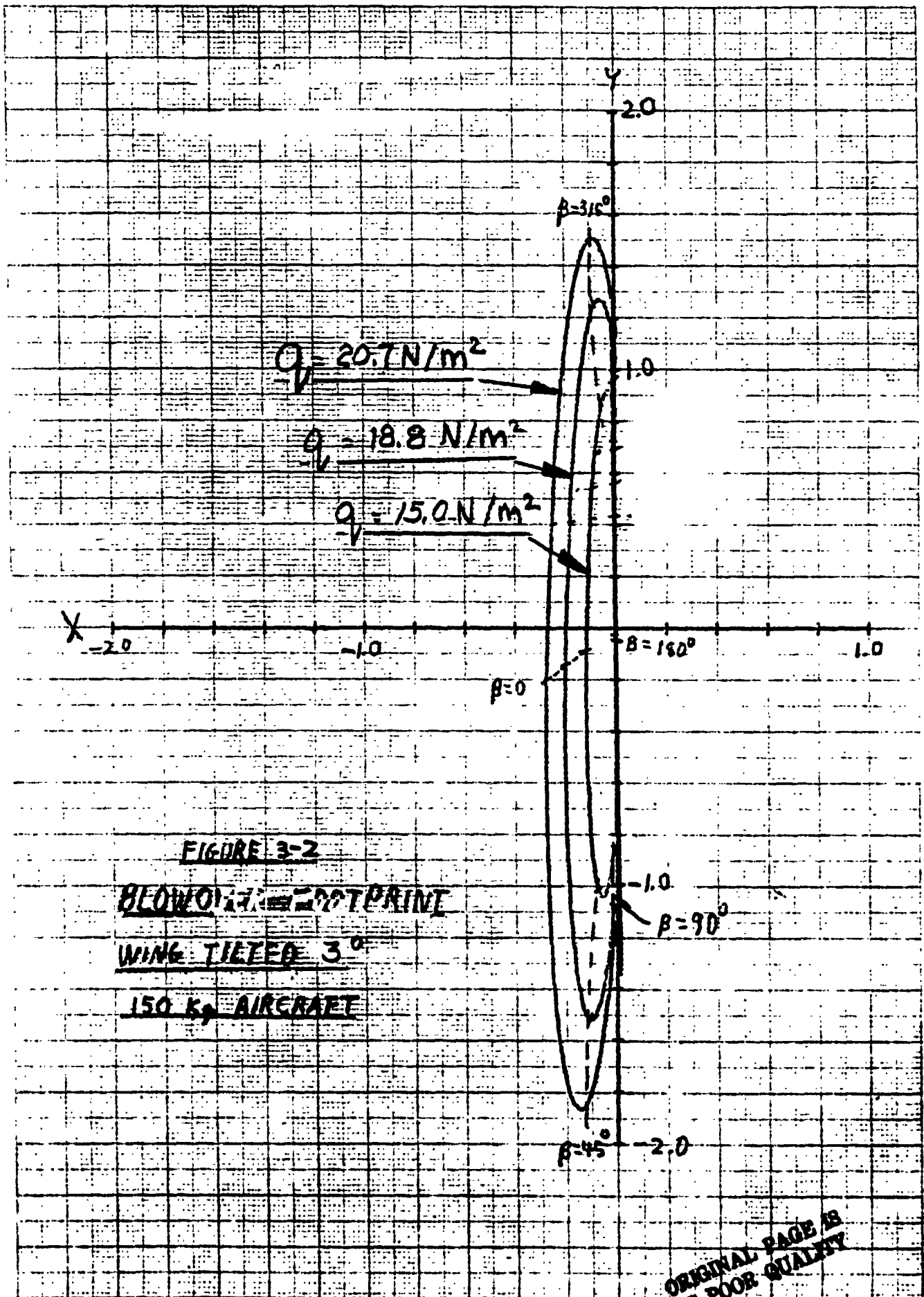


FIGURE 3-1
BLOWOVER FOOTPRINT
NORMAL ALTITUDE
150 K AIRCRAFT



ORIGINAL PAGE IS
OF POOR QUALITY

The drooped wing case was not fully analyzed for several reasons: (1) It does not seem to be necessary. The aircraft is not very easily overturned in its normal configuration. (2) It would appear that the drooped wings may be counter-productive. This configuration creates a rolling moment into the wind sufficiently powerful to cause overturning.

An approximate calculation of the into the wind overturning moment is as follows. The horizontal section of the wing is assumed to have a lift coefficient of one. Assume that the wind is coming about 30° to 45° off of the nose. Then it is easy to see that the drooped tips will be stalled and thus generating a force coefficient equal to one in a direction normal to their surfaces. The windward tip will be forced down, the leeward tip forced up, thus causing an overturning moment into the wind. From this moment, and from the total vertical force on the aircraft it is now possible to compute the half width of the blowover footprint Y^* due to this effect alone. This varies with q as follows:

Lateral Footprint Semi-width due to droop tips alone	
q (N/m^2)	Y^* (m)
15	2.4
17.5	4.3
20	5.9
22.5	8.5
25	13.8

As can be seen, the aircraft will be overturned in any wind of about $q = 23 N/m^2$ or more, compared to a q over $26.5 N/m^2$ without drooped tips. In the case of the 3° tilted wing the problem is more complicated. The wings may not be drooped the same amount, or one tip might not touch the ground. However, the best that could be hoped for is a small improvement in the overturning moment. This improvement is less than the degradation in the zero tilt case.

It should be noted that the values Y^* given are the lateral semi-width of the footprint due to the droop tip alone, ignoring all other aerodynamic forces. As an indication of the combined effect, a full calculation was made at $q = 22.5 \text{ N/m}^2$ and a yaw angle of 30° . For the wings level and 3° tilted case, with droop tips, the new Y^* value is shown below.

Lateral Footprint Semi-width		
Droop tip alone	Droop tips plus other aero terms (0°)	Droop tips plus other aero terms (3°)
m	m	m
8.5	8.4	7.0

APPENDIX B



**LEAR SIEGLER, INC.
ASTRONICS DIVISION**

Prepared for:
Developmental Sciences, Inc.
P.O./Contract No. 3566/JPL 955012

**INITIAL CONCEPT STUDY
NAVIGATION, GUIDANCE AND CONTROL FOR THE
MARS AIRPLANE**

ADR-823

15 June 1978

**3171 SOUTH BUNDY DRIVE
SANTA MONICA, CA. 90408
AREA CODE 213 391-7211**

TABLE OF CONTENTS

- 1. ABSTRACT**
- 2. REPORT ORGANIZATION**
- 3. MISSION DESCRIPTION AND REQUIREMENTS**
 - 3.1 Pre-launch Checkout and Flight to Mars Orbit**
 - 3.2 Separation from Carrier in Mars Orbit**
 - 3.3 Deorbit Maneuver**
 - 3.4 Atmospheric Entry**
 - 3.5 Aeroshell Chute Deployment**
 - 3.6 Airplane Deployment**
 - 3.7 Mars Airplane Free Flight**
 - 3.8 Airplane Landing (Optional Configuration)**
 - 3.9 Airplane Vertical Takeoff (Optional Configuration)**
- 4. NAVIGATION, GUIDANCE AND CONTROL FUNCTIONS, AND HARDWARE IMPLEMENTATION**
 - 4.1 Strapdown Inertial**
 - 4.2 Comsat Range**
 - 4.3 Altitude Above Ground**
 - 4.4 Barometric Altitude and Airspeed**
 - 4.5 Doppler Velocity**
 - 4.6 Terrain Avoidance**
 - 4.7 Flight Control**
 - 4.8 Aircraft Controls**
 - 4.9 Terminal Site Selection System**
- 5. COMPUTER REQUIREMENTS**
 - 5.1 Computer Hardware**
 - 5.2 Computer Software**
- 6. ENVIRONMENTAL REQUIREMENTS**
- 7. RELIABILITY**

LIST OF ILLUSTRATIONS

- Figure 1 Mars Airplane Avionics Scenario**
- Figure 2 Navigation, Guidance & Control Software Block Diagram**
- Figure 3 Signal Interconnection Drawing**
- Figure 4 Airplane Control Laws**

- Table I Preliminary Avionics Characteristics**
- Table II NG&C Computer Timing and Memory Requirements**
- Table III Preliminary NG&C Reliability for 20 Hour Mission**

1. ABSTRACT

Proposed scientific experiments for Mars planetary exploration will require a certain level of performance from the Mars airplane. Requirements based upon this level of performance were used in this report for the preliminary design of the aircraft navigation, guidance, and control equipment and associated software.

A mission scenario is developed to determine the functions and sequencing of each item of equipment. Choices are critical because of the extreme need to minimize weight. Based on current technology, equipment has been selected or estimated to fulfill the performance requirements. Special effort was given to navigating on Mars, which has no magnetic field reference, after a long journey through space. Avoiding collision with the as-yet inaccurately mapped terrain, and soft vertical landing after a long flight, are other areas which contributed to equipment selection.

3. MISSION DESCRIPTION AND REQUIREMENTS

3.1 Pre-Launch Checkout and Flight to Mars Orbit

A typical Mars Airplane can be equipped with a number of scientific payloads. Airplanes with a particular configuration of payloads will be released on Mars as required.

There is enough similarity between the aircraft performance requirements for all of the payloads, however, so that only one design aircraft with one design navigation, guidance, and control avionics will be built for all the missions.

Four aircraft in their individual aeroshells will be mounted together onto a deployment fixture in a space vehicle called a carrier. The navigation, guidance, and control avionics (hereafter called "avionics") will have been completely checked out prior to this installation. Each aircraft is electrically connected through its aeroshell to the carrier, so that additional testing or last minute program changes can be made from the launch area. After launch, checkouts can be conducted periodically upon earth command via radio link to the carrier. Except for these inflight checks, there is no requirement for avionics operation until Mars orbit is reached, and so the equipment will remain off nearly all of the time after earth launch.

The carrier will obtain a highly elliptical orbit around Mars after final maneuvering commands from earth. The carrier will remain in this orbit to deploy the airplane aeroshells as required.

PRECEDING PAGE BLANK NOT FILL

3.2 Separation from Carrier in Mars Orbit

The carrier remains under control from earth as to when each airplane/aeroshell is deployed. The aeroshells can be released in any order, or together, at any time, up to the storage life of the equipment. Since most of the equipment will be derived from currently available hardware, the storage life is presently specified as five years. Longer spans can be provided if necessary.

At least thirty minutes prior to aeroshell separation time, the airplane must be "turned on" from earth. This time is exclusive of the communication delay time between Mars and Earth. As listed in Figure 1, this time is used to perform the final airplane pre-separation functions. Final checkout prior to separation is followed by alignment of the strapdown inertial system to the carrier coordinates. Mission programming changes, if any, can be entered into the airplane computer at this time. The equipment is brought up to operating temperature and the strapdown computations are monitored against the carrier reference to correct any inertial sensor biases which are present.

The status of each of the operations will be available to the carrier to transmit down the radio link to earth. The last step will be to transfer the primary power source from the carrier batteries to the airplane batteries, and again assess operation of the avionics on "internal power". When each of these steps has been completed, the separation command will be issued from the carrier and all mechanical and direct electrical connections will be broken. The airplane

RECEIVED FOR THE DIRECTOR
 1968 JUN 15 10 45 AM '68

CARRIER ORBIT
 10000 km

DEPOSIT MANEUVER

Final SMC Test
 Inertial Alignment
 Heat Abatement
 Internal Power Transfer
 Program Changes
 Begin navigation; correct
 for biases using carrier
 reference

AV's comp starts
 Shut Timer
 Autonomous Navigation
 Returns Mode Handling

Control RCS Requests
 Navigation - compute position
 maintain attitude reference
 Count down to entry time
 Turn on Radar Altimeter
 Begin Communication Link
 Status monitoring - failure mode
 handling
 Compute gravity field

h = 240 km
 V = 2.5 g
 r = 4600 mps = 200 kts
 Compute gravity offset

h = 7 km = 200 ft
 V = 2000 kts = 1000 mps
 r = 4600 mps = 100 kts
 a = 2.5 g

ROUTE DELIVERY
 Begin optical position
 Count down time to Aeroball injection
 Radio position update
 Compute position, maintain heading
 Status monitoring
 Radar altitude
 Radar RCS results
 Status monitoring, failure handling

Radio position for update (carrier)
 Doppler velocity
 Radar altitude
 Radar altitude, corrected
 Inertial navigation
 Status monitoring
 Status monitoring, failure handling
 Status change
 System status, sequencing

SURFACE
 LANDING

ORIGINAL PAGE IS
 OF POOR QUALITY

FIGURE 1
 MARS AIRPLANE
 AVIONICS SCENARIO



3.2 (Continued)

avionics will continue to sense inertial inputs and will maintain and compute airplane attitude and position for the remainder of the flight. Communication with the carrier or in-view comsat(s) will now begin via the airplane's data link, using the aeroshell link antenna.

3.3 Deorbit Maneuver

The Mars Airplane strapdown inertial system now provides attitude data which causes the control system rockets to orient the aeroshell prior to the deorbit maneuver. When the correct attitude and time is reached, the aeroshell will be accelerated towards Mars by the Reaction Control System (RCS) under control of the avionics. The direction of the acceleration vector will be commanded with reference to the aeroshell. In order to achieve the desired entry orbit, aeroshell attitude must be known to an accuracy of TBD degrees. This accuracy is expected to be well within the airplane's capability, which is designed to handle the greater task of providing an inertial reference from carrier separation until atmospheric flight. Thus we can expect an attitude accuracy of better than 0.08 degrees if the deorbit maneuver occurs within five minutes of carrier separation.

3.4 Atmospheric Entry

The deorbit maneuver starts several internal timers in the avionics computer. One of these will be used to predict the time of atmospheric entry. Others serve various roles such as sequencing communications and other equipment and estimating times for other phases of the mission.

3.4 (Continued)

As the time approaches for entry, the aeroshell is travelling in an environment free from measurable external torques and accelerations. G-sensitive drift components and biases of the inertial sensors will not degrade accuracy, allowing for a better inertial performance than will be possible during atmospheric flight. All of the non-used scientific and avionics payloads will be turned off during this phase to conserve battery power. The avionics control system and RCS continue to maintain aeroshell stability against any minor disturbances.

One of the interval timers will predict when the aeroshell is at 12 km altitude. The radar altimeter will then be turned on in preparation for reading the 9 km chute deployment altitude. The 12 km precedes the 9 km altitude by three to four minutes time.

3.5 Aeroshell Chute Deployment

The avionics computer provides the chute deploy command to the aeroshell chute system when it passes through 9 km. At this time a number of additional navigation and control sensors are turned on to provide computer inputs during the 20 second parachute fall. These sensors include barometric altitude and airspeed, doppler radar, and Comsat ranging. At this time, the strapdown computations are resolved into Mars surface rather than inertial space coordinates. The fall time is used to advantage to verify the vertical reference which will have drifted slightly from the inertial reference system

3.5 (Continued)

coordinate equivalent last fixed at carrier separation. Both pitch and roll attitude will, therefore, be improved. Azimuth angle will remain with the accuracy left from carrier separation, while azimuth rate will be maintained by the RCS rockets and the control avionics. The aeroshell will be oriented towards the desired initial flight heading and the cover will be ejected towards the end of the fall sequence.

3.6 Airplane Deployment

Two and a half kilometers and 20 seconds after the chute has deployed, the airplane will unfold while attached to the then-coverless aeroshell and be released for flight. An aircraft flight angle accuracy of better than ten degrees is required with respect to the x-y plane. It is expected that this angle will be known to better than three degrees at the time of airplane release. The strapdown system, acting in part as a "vertical gyro", will continue to improve its estimates of pitch and roll angle as the mission proceeds. During the period immediately following release, the airplane will climb (or dive) on an indicated airspeed schedule to an initial reference altitude in order to enter the free flight mission stage with maximum probability of success. The initial condition elevator and wings-level afteron trim conditions will be blended out as the airplane achieves stability.

3.7 Mars Airplane Free Flight

The airplane turns and begins to fly at the altitude and in the direction contained in its stored profile program. Scientific payloads will now be activated according to the preprogrammed sequence or on command from the Comsat uplink. The Comsat will transmit range pulses to the airplane along with the uplink command data. These pulses will be transponded back to the Comsats, which will then transmit computed range back to the airplane. A position accuracy of 1 km in the Mars x-y plane is desirable. The airplane will be capable of achieving twice that accuracy in the x-y plane, along with an accuracy of four percent of altitude, while in flight.

Guidance, in general, will be with respect to the stored flight profile in the avionics computer. Earth control can change this profile whenever desired. During flight in canyons and over hazardous or less-well-mapped terrain, guidance to the flight profile will operate in conjunction with real-time terrain avoidance. Maintaining clearance to vertical and horizontal obstacles will provide the primary inputs to the control system while the aircraft otherwise follows the planned profile as closely as possible. Collision avoidance does not degrade navigation accuracy, however. Even though the aircraft may be temporarily self-guided "off course", it will always maintain its estimate of its actual position.

Long term roll and pitch angle references are derived from the direction of the gravity vector using the strapdown accelerometers.

3.7 (Continued)

There is no such easily accessible heading reference on Mars, however. Gyrocompassing while in flight would be subject to the only slightly known turbulence characteristics of the atmosphere, and would require inertial instruments better than those required to perform the navigation. Celestial navigation is uncertain due to possible atmospheric obscurity and difficulty of acquisition. Position fixes from the Comsat, however, will provide for an improving estimate of airplane heading as the mission proceeds. Heading accuracy is expected to improve from an initial 3° accuracy to 1° accuracy within 30 minutes time after start of atmospheric flight.

An actual mission leg will proceed under either normal or terrain-avoidance-augmented guidance between two points. Two other modes will be available for special parts of the mission. When the objective will be primarily to travel from one point to another, a minimum energy profile will be computed to conserve fuel and prolong mission time. When aircraft stability has increased importance, such as during certain measurements, flight control loops will be tightened at the expense of a small loss in guidance accuracy during these measurements. This will be used, for example, during high resolution photo imaging, or during certain gravity gradiometer measurements where body axis rates must be either kept to, or known to, a precision of 3×10^{-5} rad/sec.

3.8 Airplane Landing (Optional Configuration)

A landing site will have been selected prior to the landing operation. The site will be programmed into the computer from earth launch, and will be modified if necessary anytime prior to the landing. The airplane will navigate to the landing site and proceed to a smooth landing, augmented by the Terminal Site Selection System (TSSS). The TSSS provides fine corrections in the landing sequence for object avoidance.

As forward speed is reduced and the airplane pitches up, control surface effectiveness decreases. The flight control system transfers control from the elevator, aileron and engine thrust to a controlled altitude rate descent using the forward and aft vertical thrusters and the left and right roll thrusters. Altitude rate command is flared to a nominal value (e.g., 1.5 m/s v_y) for touchdown. Landing strut switches signal the computer to cut all engines. Airplane power remains on, to measure present position using the Comsat, and present heading by sensing planetary rotation.

3.9 Airplane Vertical Takeoff (Optional Configuration)

The avionics system is powered up at least thirty minutes prior to takeoff, exclusive of Mars to Earth communication delay time. This allows for a self-test to assure success of the next mission leg. Following the self-test, the airplane's three axes are "aligned" in the strapdown computer using the gravity vector and planet rotation for pitch, roll, and heading angles.

3.9 (Continued)

The aircraft will be able to lift off vertically by the four thrusters, with stability maintained by the control avionics. At 1,000 meters altitude, the airplane engine is turned on and control is blended into the aerodynamic control surfaces as forward airspeed increases. After approximately one minute of thruster burn time, the thrusters are able to be turned off as the aircraft achieves stable forward flight towards the next programmed experiment.

4. NAVIGATION, GUIDANCE AND CONTROL FUNCTIONS, AND HARDWARE IMPLEMENTATION

The Navigation, Guidance and Control (NG&C) Avionics (previously designated as "avionics" for this report) can be considered as a system which requires certain inputs, performs the NG&C function, and provides certain outputs. Figure 2, which is a block diagram of the NG&C computer software modules, is introduced here because it doubles well as a functional block diagram from which to derive the hardware requirements and implementation. Figure 3 is a block diagram of the proposed hardware implementation. Table I shows the specifications and performance of some possible sample equipment.

4.1 Strapdown Inertial

With respect to Figure 2, the "Navigation" function requires aircraft attitude, attitude rates, position, and position rates in order to perform the complex filtering necessary to estimate the actual vehicle attitude and position state vectors. Attitude, attitude rates, and position rates are derived primarily from the strapdown function. Strapdown inertial was chosen over gimbal inertial because of the lower weight, and the high performance which has now become possible with microcircuits to perform the algorithms formerly carried out mechanically by rotating gimbals. Attitudes and attitude rates are also used in the flight control function which provides the output drives to the aircraft controls. Flight control is included in Figure 2 in the five most right-hand blocks.

MISS AIRPLANE NAVIGATION GUIDANCE & CONTROL SOFTWARE

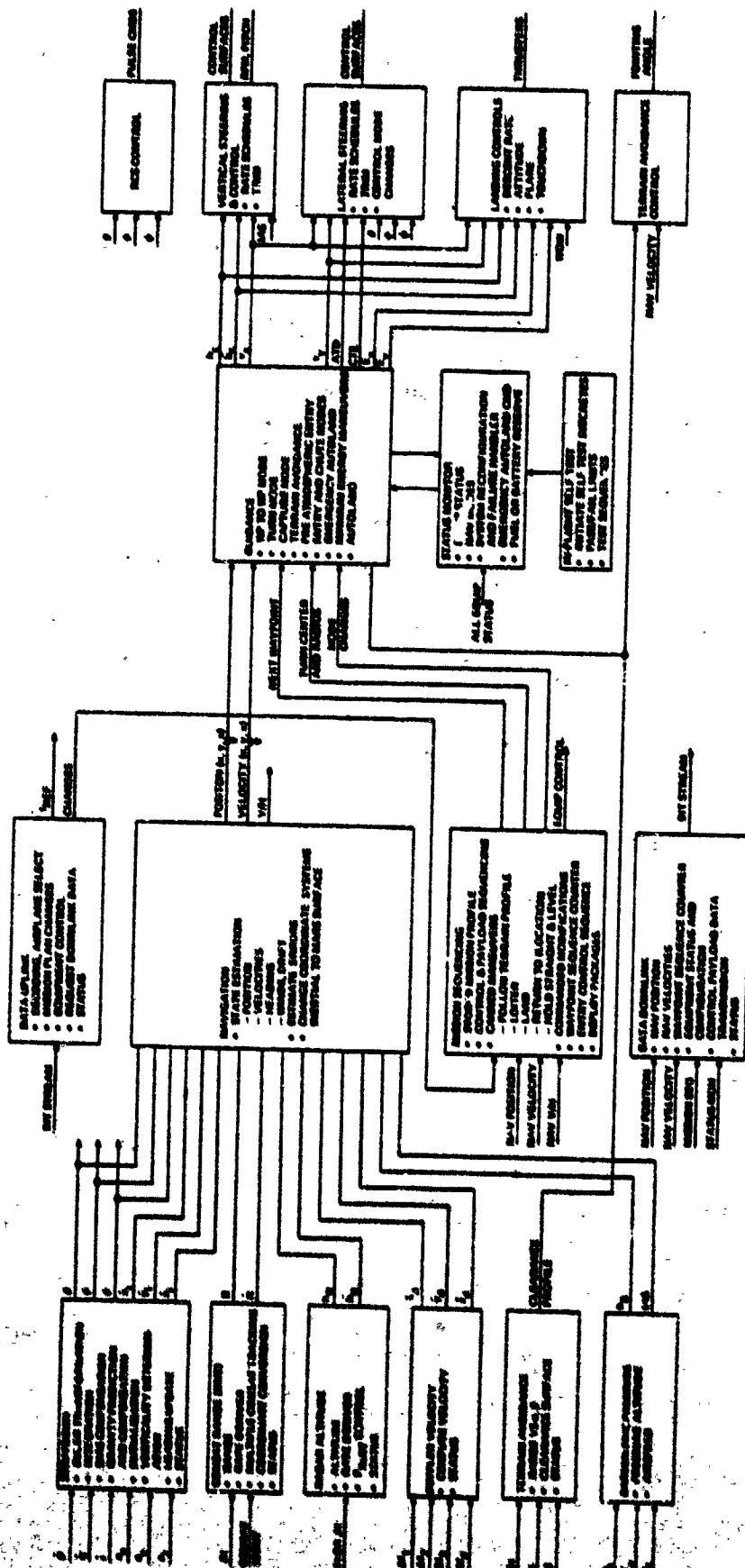


Figure 2

ORIGINAL PAGE IS
OF POOR QUALITY

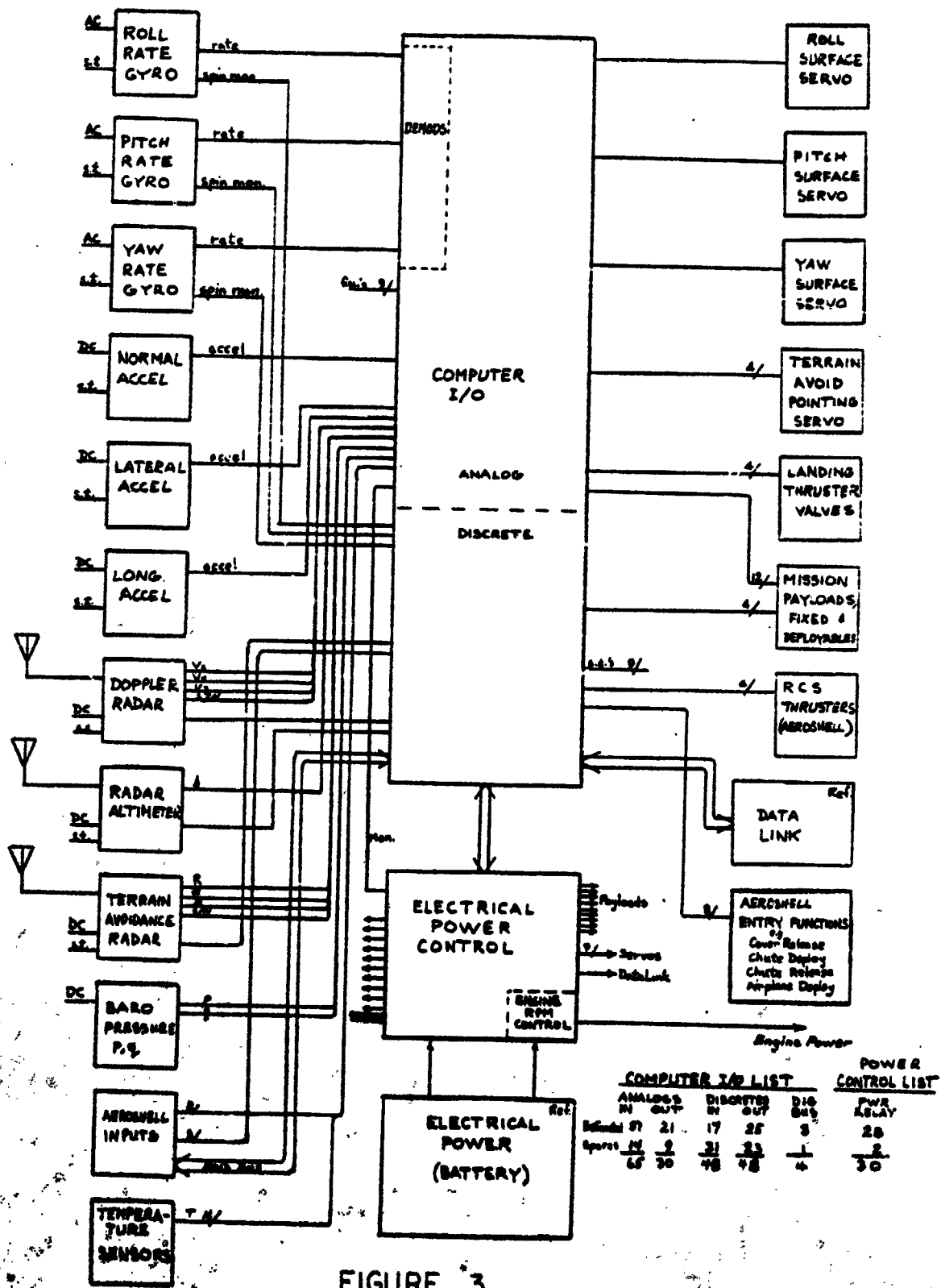


FIGURE 3
MARS AIRPLANE
SIGNAL INTERCONNECTION DRAWING



TABLE I

MARS AIRPLANE PRELIMINARY AVIONICS CHARACTERISTICS

FLY CONTROL
HORIZ NAV
VERT NAV
GUIDANCE
TERRAIN AVOID
TERRAIN AVOID
TERRAIN AVOID
MISSION SEQUENCING

EQUIPMENT NAME	PERFORMANCE	SIZE	MASS, Kg		POWER REQ.
			PRESENT	PROJECTED	
ACCELEROMETER - NORMAL LATERAL LONGITUDINAL	1 mg (earth) 1 mg (earth) 1 mg (earth)	1" x 1" x 2" 1" x 1" x 2" 1" x 1" x 2"	0.1 0.1 0.1	0.1 0.1 0.1	0.8W 0.8W 0.8W
RATE GYRO - PITCH ROLL AZIMUTH	0.1 DEG/HR 0.1 DEG/HR 0.1 DEG/HR	1" DIA x 2.4" 1" DIA x 2.4" 1" DIA x 2.4"	0.2 0.2 0.2	0.2 0.2 0.2	2.5W 2.5W 2.5W
RADAR ALTIMETER	4% 0 TO 12 KM	3.2" x 3.8" x 7.1"	3.2	3.2	35.0W
DOPPLER RADAR	0.2%V + 0.2KT	15" x 15" x 3.5"	9.1	6.9	50.0W
TERRAIN AVOIDANCE RADAR	5KM RANGE	10" DIA x 6" (2 UNITS)	11.3	9.6	75.0W
COMPUTER	2.5MSEC. ADD 20KROM. 4KRAM 0 TO 0.1 PSIA	6.8" x 9" x 7"	6.8	4.5	70.0W
ATMOSPHERIC PRESSURE - STATIC	0.06% ACCURACY	3" DIA x 3"	0.4	0.3	2.0W
TEMPERATURE - PITOT	0.7 PSI, 0.1% ACCURACY	3" DIA x 3"	0.4	0.3	2.0W
TEMPERATURE - OUTSIDE AIR	0.1°K	0	0	0	0
INTERNAL MONITORS	0.5°K	0	0	0	0
SERVO ACTUATOR - RCS	TBD				
- ELEVATOR SURFACE	360 IN.-LB: 40 DEG/SEC	1.5" x 2" x 3"	0.8	0.8	34.0W
- AILERON SURFACE	120 IN.-LB: 40 DEG/SEC	1.5" x 2" x 3"	0.8	0.8	17.0W
- THRUSTLE	INCLUDED ABOVE				
- RADAR ANTENNA	TBD				
- VTOL ROCKETS					
ELECTRICAL POWER CONTROL	HI/LO CURRENT: 30 LOADS	4.3" x 3.3" x 14.7"	1.4	1.2	
TOTAL			33.7KG	28.5KG	285W

4.1 (Continued)

The attitudes and their rates are further used as data to be transmitted on the downlink for aircraft flight evaluation as well as in scientific experiment data reduction. They are available on the aircraft for the scientific payloads, for adjusting pointing angles or providing compensations.

Body angular rates are measured by the three integrating rate gyros which are aligned to the airframe axes. A three axis inertial-grade accelerometer package mounted near the center of gravity of the aircraft provides the three components of acceleration. Quantitative specifications for the inertial sensors chosen are listed in Table I. Computer performance is reported separately in Section 5.

4.2 Comsat Range

Although the navigation function can compute attitude and position by transforming and integrating the inertial rates and accelerations, errors in computation increase with time. The most reliable method for bounding these errors will be to fix the position of the aircraft at regular intervals (say every minute (time)) by radio from the Comsat. Range and range rate will be obtained with respect to two or more Comsats for determining position and flight path angle. A degraded accuracy will be available with only one Comsat in view.

The RF transponder receives and retransmits a time marker whose round trip time is measured in the Comsat. This function is expected to be performed in the data up-down link hardware.

4.2 (Continued)

Derived rate or doppler techniques will provide the range rate information which will be used with present position to provide an accurate heading reference.

4.3 Altitude Above Ground

Two altitudes are required for the NG&C--altitude with respect to the terrain and altitude with respect to the center of the planet. The former will be obtained from a radar altimeter. The latter is discussed in Section 4.4.

The radar altimeter will have a wide beamwidth antenna and will measure range to the closest object in the beam. This provides the NG&C with altitude above the local terrain with little loss in accuracy during turns or other attitude maneuvers. The radar altimeter will operate from 12 km altitude, using the aeroshell antenna, down to zero meters (for landing), using the two airplane antennas. Radar altitude data will be used to determine RPV deployment time from the aeroshell, to fly at prescribed altitudes above the terrain, and to calibrate the barometric altitude sensor when flying over terrain whose elevation is accurately known.

4.4 Barometric Altitude and Airspeed

Altitude from barometric pressures will be subject to errors in instrument inaccuracy, variations in local temperature, time of sol, and season (due to sublimation of the ice cap). The diurnal

4.4 (Continued)

and seasonal variations can be predicted in advance to some extent at least, and outside temperature can be measured. Resulting accuracy in determining altitude will, therefore, be in the order of 10 meters accuracy near the surface. This could be improved to better than 5 meters by calibration with the radar altimeter as noted in Section 4.3.

The absolute pressure transducer and temperature sensor, which provide altitude data, are accompanied by a differential pressure transducer which measures pitot less static pressure for computing indicated airspeed (IAS). IAS is used in flight control and during the landing and takeoff maneuvers.

4.5 Doppler Velocity

Standard aerospace doppler radar techniques will be used to measure doppler shifts induced by the three axes of aircraft motion. A four beam doppler will be used to provide minimum sensitivity to aircraft attitude. The resulting velocities will be resolved into heading velocity, drift velocity, and vertical velocity.

4.6 Terrain Avoidance

A terrain avoidance radar will be used to establish both horizontal and vertical clearance planes so that the aircraft can avoid vertical obstacles and sidewalls. It is not intended for the aircraft to fly open loop through random terrain, guided only by the terrain avoidance system. Rather, the flight path will be planned to avoid

4.6 (Continued)

obstacles within the accuracies of the Mars maps and of the aircraft navigation system. It is the deficiencies in the maps and the navigation which will be corrected by the terrain avoidance radar.

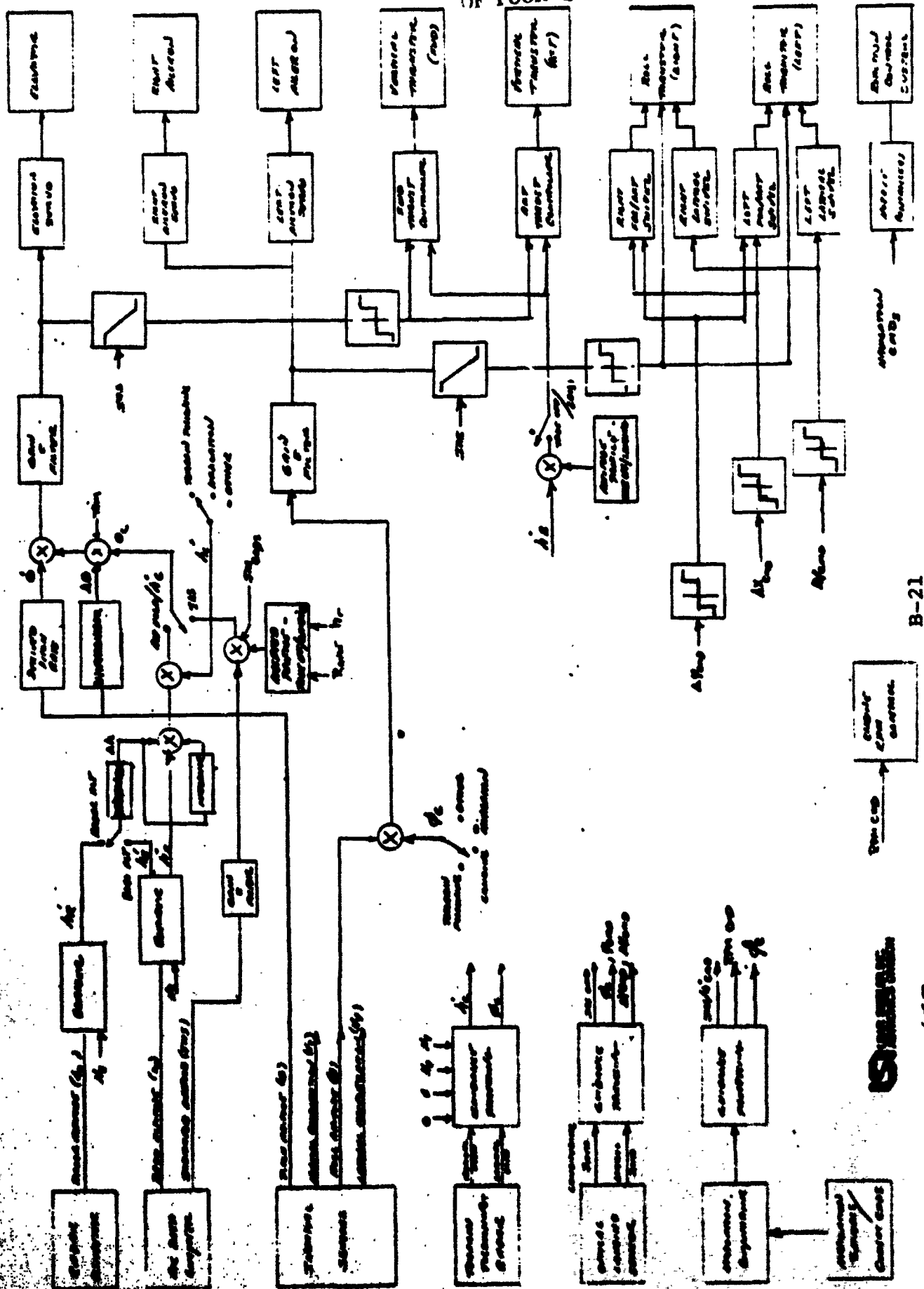
The radar sensor, using its monopulse narrow beam, provides range, azimuth, and elevation angle to the surrounding terrain. This is coupled with the aircraft altitude, groundspeed, and aerodynamic capability in the avionics computer to program a climb or turn as necessary to avoid the obstacle.

4.7 Flight Control

In most aircraft, the flight control computations are performed by a dedicated analog, or more recently, digital computer. In the Mars airplane, the flight control computations will be performed in the NG&C computer. A separate block diagram of the flight control computations is given in Figure 4. There it can be seen that the inertial sensors provide the basic pitch and roll stability. The radar and barometric altimeters provide altitude, derived altitude rate, and each can be synchronized to fly an altitude-hold mode. An airspeed control mode is provided for takeoff and landing, and will be used for steep climbs or dives. Control signals are provided to the appropriate thruster or aerodynamic control surface.

ORIGINAL PAGE IS OF POOR QUALITY

MAR'S AIRLINE CONTROL LANS
FIGURE 4



AR SIEGLER, INC. / ASTRONICS DIVISION

4.8 Aircraft Controls

During deorbit, descent, and parachute flight, "on-off" thrusters which are part of the aeroshell are used to control stability, under command of the aircraft flight control. After the airplane is released from the aeroshell and parachute, atmospheric flight is controlled by the ailerons and elevator. The surfaces are driven by electromechanical actuators which will provide 360 in-lbs of stall torque with a 40 degree/sec no-load speed. These actuators will provide proportional control of the surfaces and will supply position and rate follow-up signals to the computer for loop closure. For the landing and optional takeoff phase, control will be by "on-off" thrusters mounted on the aircraft fuselage. They will provide the necessary attitude stability and descent rate control.

4.9 Terminal Site Selection System (TSSS)

The TSSS will provide corrections into the guidance system in much the same way as the terrain avoidance function. The aircraft will autonomously navigate to the landing area. The TSSR will identify the presence of anomalies--boulders, crevices, and small craters-- and steer the airplane to the smoothest area within its total field of view. This type of system was proposed for the Viking missions, and is planned now for the Mars airplane.

5. COMPUTER REQUIREMENTS

5.1 Computer Hardware

The airplane computer performs the following general functions:

- flight control
- navigation
- guidance
- mission sequencing
- vehicle management
- input/output
- self-test

As is evident from this list, the computer will be what is often termed a "general purpose" machine, in that it will require a large instruction set and a lot of I/O capability. Each of these functions has a very close parallel in certain remotely piloted vehicles flying today. Estimates for computer speed and memory requirements have been based on current remotely piloted aircraft and are shown in Table II. The figures are based on a computer with the following instruction times: add - 2.5 usec multiply - 9.0 usec.

The computer will have double precision arithmetic which will be necessary for some of the navigation computations. The memory is estimated to be composed of 20K of 16 bit word semiconductor read-only-memory (ROM) for the permanent program and 4K of plated wire or shielded core for the read-write memory.

5.1 (Continued)

The interfaces to the computer have been shown in Figure 3. Most of the computer I/O will be Direct Memory Access (DMA) to handle the large number and frequent cycling of the inputs and outputs.

5.2 Computer Software

Figure 1 has already shown a breakdown of the Mars airplane computer software. The program is arranged in modules to allow flexibility for changes during the design cycle and verification during system testing. Each of the modules has been sized for processing time and memory based on the remotely piloted airplane computer of Section 5.1. Table II shows this information, resulting in a 48% processing duty cycle and some extra memory to assure a conservative estimate.

EAR SIEGLER, INC.

ASTRONICS DIVISION

TABLE II

NG&C COMPUTER TIMING & MEMORY REQUIREMENTS

<u>MODULE</u>	<u>TIME (μs)</u>	<u>ITERATION RATE</u>	<u>TOTAL TIME/SEC</u>	<u>MEMORY</u>
Strapdown	3000	50	150,000	2000
Comsat Ranging	1000	10	10,000	2000
Radar Altitude	50	10	500	30
Doppler Velocity	1000	10	10,000	350
Terrain Following	3000	20	60,000	600
Air Data Computations	150	10	1,500	50
Data Link	900	10	9,000	200
Navigation	2800	10	28,000	600
Mission Sequencing	1100	10	11,000	500
Guidance	2900	10	29,000	400
Status Monitor	500	10	5,000	300
In-Flight Self Test	100	10	1,000	1200
Flight Control	3000	50	150,000	2000
Landing	500	10	5,000	300
Misc.	1000	10	<u>10,000</u>	<u>4000</u>
TOTALS:			480,000 usec	14530 words

6. ENVIRONMENTAL REQUIREMENTS

The two Mars airplane environments of particular interest are temperature and pressure. Mechanical and electromagnetic environments will be specified, however these are not expected to be greatly different than required for present earth equipment. Since one objective of this airplane is that it be low cost, the use of existing lightweight and rugged military and other government equipment will be maximized. If shielding or shock mounts are required, they would need to be traded off against equipment design changes. However, these type of changes are not expected except for some temperature or pressure sensitive components.

Most of the avionics equipment being considered is designed to operate within the specifications of MIL-E-5400. This allows for ambient temperatures from -54°C up to $+125^{\circ}\text{C}$. Altitudes are specified from 0 feet (earth) to 100,000 feet (earth). A thermal analysis of the aircraft equipment bay must be performed to determine whether the equipment temperature limitations may be exceeded. If so, some redesign will be necessary, or some type of temperature control will be required.

The altitude limits, which reflect the equipment ambient pressure allowed, will be greater than the 100,000 feet of MIL-E-5400. The equipment will be investigated to determine which components are the pressure sensitive ones (such as capacitors) and these will be replaced by equivalent space-program approved types.

7. RELIABILITY

Table III shows preliminary estimates for failure rates of the avionics equipment. The total probability of successful operation of the avionics for a 20 hour mission is 95.5%.

For the probability of success of the entire mission, failure contributions for the payloads and airframe must be added. For example, if the failure rate of the payload is equal to the avionics and the airframe has half that failure rate, the total mission probability of success would be 89%.

TABLE III

PRELIMINARY MARS AIRPLANE NG&C RELIABILITY FOR 20 HOUR MISSION

<u>SUBSYSTEM</u>	<u>FAILURE RATE</u>	<u>QUANTITY PER AIRPLANE</u>	<u>PROBABILITY OF FAILURE</u>
Accelerometer	30×10^{-6}	3	1800×10^{-6}
Rate Gyro	85×10^{-6}	3	5100×10^{-6}
Comsat Radio Range	300×10^{-6}	1	6000×10^{-6}
Radar Altimeter	135×10^{-6}	1	2700×10^{-6}
Doppler Radar	400×10^{-6}	1	8000×10^{-6}
Terrain Avoidance	500×10^{-6}	1	$10,000 \times 10^{-6}$
Air Data Sensor	25×10^{-6}	2	1000×10^{-6}
Computer I/O	100×10^{-6}	1	2000×10^{-6}
Processor + Memory	240×10^{-6}	1	4800×10^{-6}
Control Surface Actuators	100×10^{-6}	2	4000×10^{-6}

20-hour mission probability of failure: $45,400 \times 10^{-6}$

20-hour mission probability of success: 95.5%